UNIVERSITÄT ZU LÜBECK

From the Research Center Borstel
Leibniz Lung Center
CEO: Prof. Dr. Ulrich E. Schaible
Priority Research Area Infections
Research Group: Bioanalytical Chemistry
Head: PD Dr. habil. Dominik Schwudke

Lipidomic and Structural Characterization of the Cell Wall of *Streptococcus pneumoniae*

Dissertation
for Fulfillment of Requirements
for the Doctoral Degree
of the University of Lübeck

from the Department of Natural Sciences

Submitted by

Belal Alshaar

From Hama, Syria

Lübeck 2025

==========

First referee: PD Dr. Dominik Schwudke

Second referee: Prof. Dr. Lars Redecke

Date of oral examination: 11.04.2025

Approved for printing.: Lübeck, 13.05.2025

Declaration

Hereby I declare that I have written this dissertation completely on my own. Furthermore, I confirm that no other sources have been used than those specified in the dissertation itself. This dissertation, in the same or similar form, has not been submitted to any other doctoral degree committee.

Belal Alshaar

Hamburg, 14.05.2025

Table of contents

List of abbreviations and symbols

AATGal: 2-acetamido-4-amino-2,4,6-trideoxygalactose
BCA: bicinchoninic acid
BHT: butylated hydroxy toluene
CBPs: choline binding proteins
CFU: colony forming units
CL: cardiolipin
CPS: capsule polysaccharide
DAG: diacylglycerol
FESEM: field emission scanning electron microscopy
FA: fatty acids
GalGlcDAG: galactosylglucosyldiacylglycerol
GLs: glycerolipids
GPs: glycerophospholipids
Glc: glucose
GlcDAG: glucosyldiacylglycerol
GlcNAc: *N*-acetylglucosamine
HF: hydrofluoric acid
HIC: hydrophobic interaction chromatography
HILIC: hydrophilic interaction chromatography
HR-MS: high-resolution mass spectrometry
IS: internal standard
LC-MS: liquid chromatography coupled to mass spectrometry
MAG: monoacylglycerol
MFQL: molecular fragmentation query language
min: minute
mol%: mol percent
m/*z*: mass-to-charge ratio
MurNAc: *N*-acetylmuramic acid
NMR: nuclear magnetic resonance
P-Cho: phosphorylcholine
PA: phosphatidic acid
PC: phosphatidylcholine
PE: phosphatidylethanolamine
PG: phosphatidylglycerol
PGN: peptidoglycan
PI: phosphatidylinositol
PS: phosphatidylserine
QC: quality control

Rha: rhamnose
RPLC: reverse-phase liquid chromatography
RUs: repeating units
SDS: sodium dodecyl sulfate
s: seconds
SPs: sphingolipids
STs: sterol lipids
TacL: teichoic acid ligase
TA: teichoic acid
TAG: triacylglycerol
TFA: trifluoroacetic acid
TLC: thin layer chromatography
Wt: wild type
WTA: wall teichoic acid

Summary

Streptococcus pneumoniae (*Spn*) is a Gram-positive bacterium that naturally colonizes various niches within the human body, but can also lead to infections with varying degrees of symptoms. Despite the availability of vaccines, *Spn* infections remain a significant health concern, exacerbated by the rising threat of antibiotic resistance. This growing challenge underscores the urgent need to explore new drug targets that are common across different strains. A particularly promising target is the pneumococcal cell wall, which has become a central point of structure-focused research. The cellular membrane, a key component of this wall, plays a crucial role in host-pathogen interactions. Nevertheless, the precise quantities of its components are still not well understood.

This thesis presents a first-of-its-kind quantitative analysis of the pneumococcal lipidome, conducted in close collaboration with the group of Prof. Dr. Sven Hammerschmidt from the University of Greifswald. The implementation of a standardized pipeline applicable for in-depth microbial lipidomics on pneumococcal samples is described. Further, I examined how the knockout of selected genes influenced the membrane lipid composition. As a proof of concept, the wild-type serotype 2 strain *S. pneumoniae* D39 was compared to three mutant strains with single gene knockouts. The targeted mutant strains investigated here are: 1) Δ*tacL*: TacL is responsible for the attachment of the polymeric teichoic acid chain on the glycolipid anchor, thus forming the lipoteichoic acid (LTA); 2) Δ*lgt*: Lgt (diacylglyceryl transferase) catalyzes the diacylation of preprolipoproteins via a thioester bond by transferring a diacylglycerol moiety from a phosphatidylglycerol (PG) precursor; 3) Δ*cps*: enzymes of the *cps* cluster are responsible for capsule polysaccharide formation. To date, such quantitative lipidome studies have not been performed for *Spn*.

Methodically, shotgun lipidomics was employed and the development of a customized mix of internal standards ensured accurate quantitative analysis. The analysis allowed quantification of more than 100 lipids across the following six classes: diacylglycerol, glucosyldiacylglycerol (GlcDAG), galactosylglucosyldiacylglycerol (GalGlcDAG), cardiolipin, phosphatidylcholine and PG, with GlcDAG and GalGlcDAG being the predominant classes. Gas Chromatography-Mass Spectrometry (GC-MS) and Thin Layer Chromatography in conjunction with high-resolution tandem mass spectrometry were further utilized for the validation of identified lipid species. The lipid composition of Δ*tacL* and Δ*lgt* strains showed no significant changes compared to the wild type, while the non-encapsulated strain exhibited significant adaptations.

Another aim of this thesis was to optimize a GC-MS method for the accurate quantification of pneumococcal wall glycopolymers, particularly wall teichoic acid and lipoteichoic acid. This is a challenging task for researchers in the field since decades. This quantification technique is anticipated to provide a basis for studying enzymes that affect teichoic acid

levels without using radioactive materials in cultures and may also be used for capsule polysaccharide quantification, advancing our understanding of pneumococcal cell wall regulation. Preliminary results from this optimized method have already provided insights into how LytR, which plays an essential role in attaching the wall teichoic acid to the peptidoglycan, influences the teichoic acids ratio.

In summary, a robust quantitative method for lipidome analysis has been established, along with a developed method which delivered the first successful proof of concept for teichoic acids quantification in *Spn*. These approaches enable future investigations into membrane homeostasis and biosynthesis regulation in other mutants or under various growth conditions.

Zusammenfassung

Streptococcus pneumoniae (*Spn*) ist ein Gram-positives Bakterium, das natürlicherweise verschiedene Bereiche des menschlichen Körpers besiedelt, aber auch Infektionen mit unterschiedlichen Symptomen verursachen kann. Trotz der Verfügbarkeit von Impfstoffen stellen *Spn*-Infektionen nach wie vor ein erhebliches Gesundheitsproblem dar, das durch das zunehmende Risiko einer Antibiotikaresistenzen verschärft wird. Diese wachsende Herausforderung unterstreicht die dringende Notwendigkeit, neue Wirkstoffziele zu erforschen, die bei verschiedenen Stämmen gleich sind. Ein besonders viel versprechendes Ziel ist die Pneumokokken-Zellwand, die zu einem Schwerpunkt der strukturorientierten Forschung geworden ist. Die Zellmembran, eine Hauptkomponente dieser Zellwand, ist für die Interaktion zwischen Wirt und Erreger von entscheidender Bedeutung. Über die Zusammensetzung der Zellmembran ist jedoch im Hinblick auf die Menge der verschiedenen Moleküle noch wenig bekannt.

Diese Arbeit beschreibt die erste quantitative Analyse des Pneumokokken-Lipidoms, die in enger Zusammenarbeit mit der Gruppe von Prof. Dr. Sven Hammerschmidt von der Universität Greifswald durchgeführt wurde. Die Implementierung einer standardisierten Methode für umfassende mikrobielle Lipidom-Analysen an Pneumokokken-Proben wird dargelegt. Außerdem habe ich untersucht, wie der Knock-out ausgewählter Gene die Zusammensetzung der Membranlipide beeinflusst. Zur Überprüfung des Konzepts wurde der Serotyp 2-Wildtyp-Stamm *S. pneumoniae* D39 mit drei genetisch modifizierten Stämme, in denen jeweils ein Gen gezielt deletiert wurde, verglichen. Die hier untersuchten genetisch modifizierten Stämme sind: 1) Δ*tacL*: TacL ist verantwortlich für die Anheftung der polymeren Teichonsäurekette an den Glykolipidanker und bildet somit die endgültige Li-poteichonsäure (LTA); 2) Δ*lgt*: Lgt (Diacylglyceryltransferase) katalysiert die Diacylierung von Preprolipoproteinen über eine Thioesterbindung durch Übertragen eines Diacylglycerols von einem Phosphatidylglycerol (PG) als Ausgangsmolekül;

3) Δ*cps*: Enzyme des *cps*-Clusters sind für die Bildung der Kapsel-Polysaccharide verantwortlich. Bisher sind derartige quantitative Lipidomics-Studien an *Spn* nicht durchgeführt worden.

Als Methode wurde Shotgun Lipidomics eingesetzt, und durch Entwicklung eines maßgeschneiderten Mixes interner Standards konnte eine präzise quantitative Analyse durchgeführt werden. Die Analyse ermöglichte die Quantifizierung von mehr als 100 Lipiden aus den folgenden sechs Klassen: Diacylglycerol, Glukosyldiacylglycerol (GlcDAG), Galaktosylglucosyldiacylglycerol (GalGlcDAG), Cardiolipin, Phosphatidylcholin und PG, wobei GlcDAG und GalGlcDAG die hauptsächlich vorkommenden Molekülklassen sind. Gas Chromatographie-Massenspektrometrie (GC-MS) und Dünnschichtchromatographie in Verbindung mit hochauflösender Tandem-Massenspektrometrie wurden darüber hinaus zur Validierung der identifizierten Lipid-Spezies verwendet. Die

Lipidzusammensetzung der Δ*tac*L- und Δ*lgt*-Stämme zeigte im Vergleich zum Wildtyp keine signifikanten Veränderungen, während der kapsellose Stamm deutliche Anpassungen aufwies.
Ein weiteres Ziel dieser Arbeit war die Optimierung einer GC/MS-basierten Methode für die genaue Quantifizierung von Pneumokokken-Wandglycopolymeren, insbesondere von Wandteichonsäure und Lipoteichonsäure. Dies stellt seit Jahrzehnten eine Herausforderung für die Forschung auf diesem Gebiet dar. Die entwickelte Quantifizierungstechnik soll zukünftig als Grundlage für die Untersuchung von Enzymen dienen, die den Teichonsäuregehalt beeinflussen, ohne dabei radioaktive Materialien in den Kulturen verwenden zu müssen. Darüber hinaus ist sie möglicherweise auch für die Quantifizierung von Kapselpolysacchariden einsetzbar, was unser Verständnis der Regulierung der Pneumokokken-Zellwand voranbringen könnte. Vorläufige Ergebnisse dieser optimierten Methode haben bereits Einblicke gegeben, wie das Enzym LytR, welches eine entscheidende Rolle bei der Bindung der Wandteichosäure an das Peptidoglykan spielt, das Teichosäureverhältnis beeinflusst.
Zusammengefasst wurde ein robustes quantitatives Verfahren für die Lipidomanalyse etabliert, zusammen mit einer entwickelten Methode, die den ersten erfolgreichen Proof-of-Concept für die Quantifizierung von Teichonsäure in *Spn* geliefert hat. Diese Methoden ermöglichen künftige Untersuchungen der Membranhomöostase und der Regulation der Biosynthese in anderen Mutanten oder unter verschiedenen Wachstumsbedingungen.

1) Introduction

1.1 Cell wall architecture in Gram-positive bacteria

Bacterial cell walls serve as a protective layer against external influences and osmotic stress. Bacteria can be classified into two groups, namely Gram-negative and Gram-positive. This classification was determined based on their staining characteristics, as observed in Gram's research back in 1841[1].

Gram-negative bacteria have a cytoplasmic membrane surrounded by a thin layer of peptidoglycan and an outer membrane containing lipopolysaccharides. On the other hand, Gram-positive bacteria lack an outer membrane but have a thick, multi-peptidoglycan layer. Both types of bacteria rely on their cell walls for protection and preservation of cellular integrity[2]. This work is focused on studying the cell wall of the Gram-positive pathogen *Streptococcus pneumoniae*.

The innermost layer of Gram-positive cell wall is the cytoplasmic membrane, which separates the intracellular components from the extracellular space and consists mainly of lipids and proteins. The following peptidoglycan layer serves as an attachment site for various other cell wall polymers, including capsular polysaccharides and teichoic acids[3,4]. When all these cell wall components are considered together, it becomes evident that the cell wall plays a crucial role in bacterial shape, pathogenicity, and survival. This makes the cell wall an ideal target for antibiotic interventions.

1.2 *Streptococcus pneumoniae*

1.2.1 Background about *S. pneumoniae*

The Gram-positive bacterium *S. pneumoniae* was discovered in 1881 by Georg Miller Sternberg and Louis Pasteur. It is characterized by its double-sphere appearance, hence the original name “Diplococcus”[5].

Pneumococci continue to be a significant reason of illness and death worldwide. They can lead to a range of illnesses, starting from relatively mild local infections like ear and sinus infections, all the way to more severe conditions like pneumonia, sepsis, and meningitis (**Figure 1**). *Spn* possesses various factors that contribute to its virulence, including different types of choline-binding proteins (CBPs) and capsule polysaccharides (CPS). Due to that, *Spn* is considered an important threat, especially to susceptible populations such as young, elderly and individuals with weakened immune system[6].

Vaccines can be used to prevent pneumococcal infections, while antibiotics can be utilized for their treatment. The vaccines that are currently used target specific CPS present in pneumococcus. It's worth mentioning that the 104 known pneumococcal different serotypes are differentiated by their CPS and geographical origin[7,8,9]. This is of importance because the existing vaccines cover high-risk serotypes (for example: serotype 3 and 19A)

while ignoring others. Therefore, the reduction in invasive pneumococcal infections can be explained as a result of vaccines, but at the same time, it might also lead to an increase in infections caused by non-vaccine serotypes, which could be linked to this limited coverage of used vaccines[10].

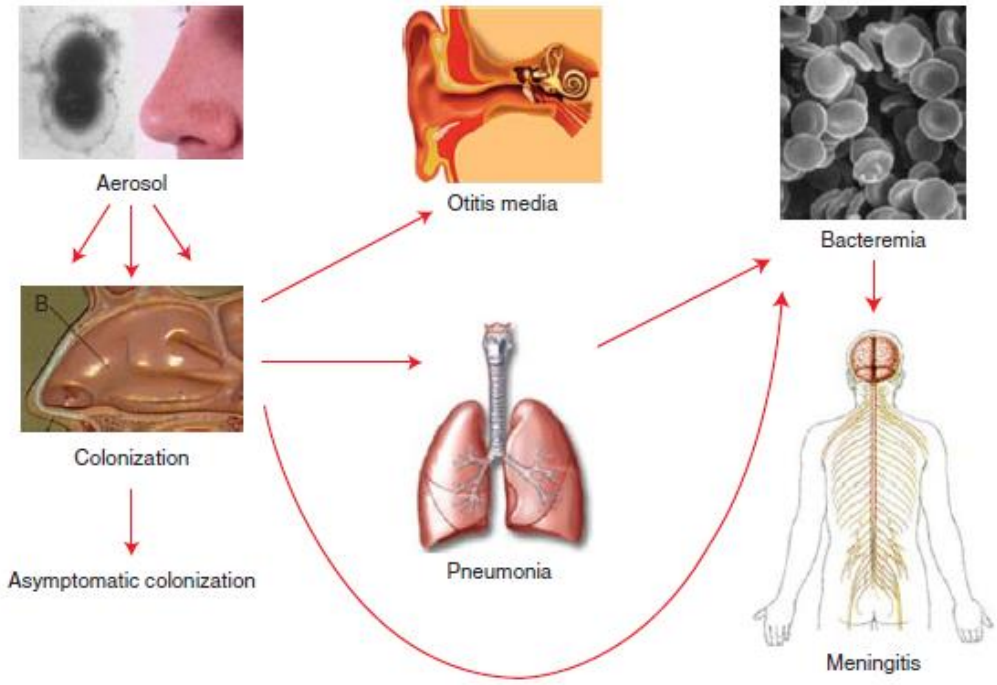

Figure 1: Illustration of the progression of pneumococcal disease. Pneumococci are transmitted through aerosols and colonize the nasopharynx. Ear infections (Otitis media) are a common disease in children. In more severe cases, the bacteria invade the lungs and bloodstream, leading to a systemic disease, with meningitis being the most severe outcome. This figure is taken from ref (6).

Regarding antibiotics, the first choices of antibiotics for pneumococcal infection have been penicillin, macrolides, and fluoroquinolones. While penicillin interacts with target sites at penicillin binding proteins, macrolides inhibit protein synthesis by binding to ribosomal sites, whereas fluoroquinolones inhibit DNA synthesis. Each of the mentioned antibiotic class has its own mechanism of action, benefits, limitations and distinct resistance mechanisms. In the last few years, the number of antibiotic-resistant pneumococcal strains has dramatically accelerated due to widespread antibiotics usage. The misuse of antibiotics (for example, in the case of inappropriate antibiotic selection or incorrect dosage) contributes also to the emergence of microbial resistance as well as accelerating the decline in the effectiveness of specific antibiotics over time[11]. This underscores the necessity of identifying new drug targets for tackling pneumococcal infections, particularly targets that are common across all pneumococcal serotypes.

1.2.2 The structure of the pneumococcal cell wall

The following paragraph highlights the main components in the pneumococcal cell wall, which includes surface proteins, CPS, peptidoglycan (PGN), wall teichoic acid (WTA), and lipoteichoic acid (LTA), each of which is briefly explained in the following.

1.2.2.1 Surface proteins

One of key players in the virulence process of *Spn* are surface proteins which maintain viability and participate in various stages of infection. Four classes of surface proteins (**Figure 2**) are known and differentiated based on their anchoring mechanism: (a) choline-binding proteins that attach non-covalently to the cell wall phosphocholine (*P*-Cho), (b) proteins with an LPxTG motif that can be covalently incorporated into the PGN polymer through a sortase-dependent process, (c) nonclassical surface proteins, also known as moonlighting proteins, which are associated with the surface but lack classical secretion and anchoring motifs, and (d) lipoproteins that are covalently bound to the cytoplasmic membrane through the actions of lipoprotein diacylglyceryl transferase (Lgt) and lipoprotein signal peptidase II (Lsp II)[12].

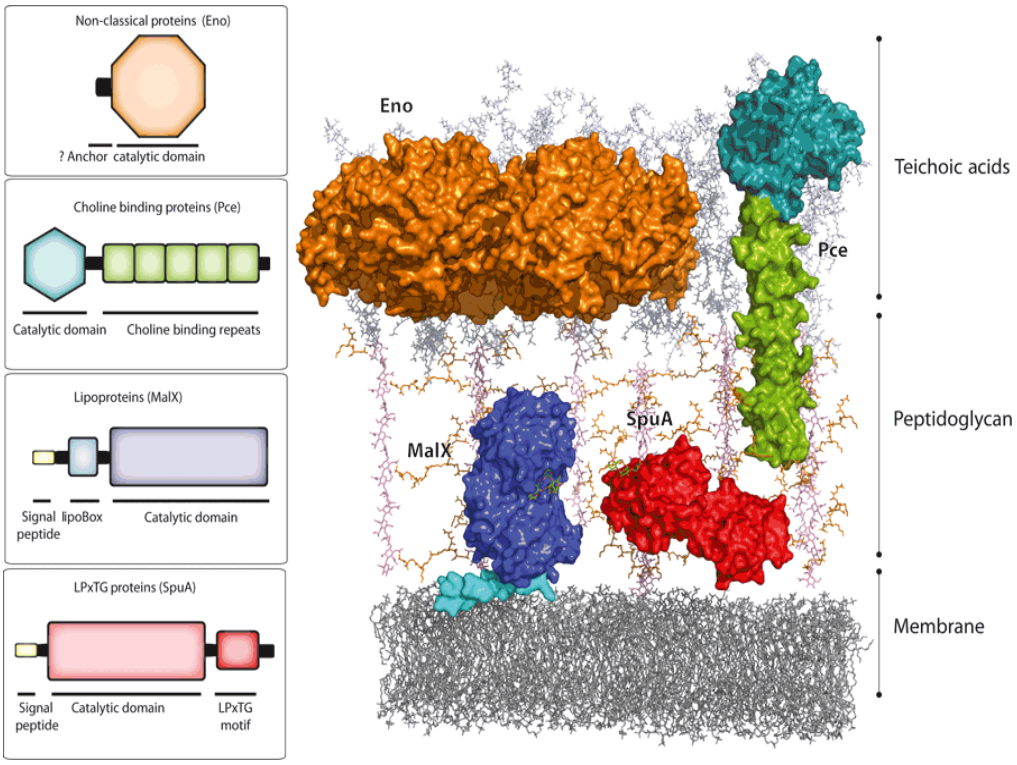

Figure 2: **Schematic representation of the cell surface of pneumococci, including various cell surface structures such as the PGN layer, TAs, and different surface proteins**. The surface proteins comprise non-classical proteins, lipoproteins (LP), LPxTG proteins and choline-binding proteins (CBPs). Figure is taken from ref (12).

1.2.2.2 Capsule polysaccharide (CPS)

Louis Pasteur discovered the pneumococcal capsule, which is considered the most crucial virulence factor of pneumococci, as almost all clinical isolates are encapsulated[13,14]. Most CPS serotypes contribute to negatively charged bacterial surface at physiological pH, which promotes colonization of the nasopharynx by repelling sialic acid-rich mucopolysaccharides. This helps to prevent entrapment of *Spn* in nasal mucus and facilitates attachment to the surface of epithelial cells. The interaction between the CPS and its host interaction process has been widely studied and described[15].

Pneumococci produce their CPS through a highly organized processes mediated by specific proteins, which are coded by genes located in the capsule synthesis (cps) locus[16,17]. Linear polymers with repeating units (RUs) containing two or more monosaccharides represent the most basic form of CPS. On the other hand, more complex structural variants are observed in branched polysaccharides. These polysaccharides have a repeating backbone made up of one to six monosaccharides, accompanied by an extra side chain. Within various *Spn* serotypes, CPS exhibits variations in their sugar composition and the linkages connecting each of their component[15,18]. Additionally, the crucial localization of the CPS on PGN has been thoroughly investigated across nearly all known serotypes[19].

Especially the CPS structure and biosynthesis of serotype 2 strain D39 has been elucidated and discussed in detail previously. However, its attachment has been a matter of debate in recent years, mainly due to conflicting results regarding whether it involves a phosphodiester bond or a glycosidic bond[19,20]. More details about this issue are described in section 1.2.2.4.

1.2.2.3 Peptidoglycan (PGN)

PGN is a large complex molecule that is vital for resisting osmotic pressure. As the name implies, PGN consists of a glycan and peptide part (**Figure 3**). The glycan part comprises *N*-acetylglucosamine (GlcNAc) and *N*-acetylmuramic acid (MurNAc), which are connected via β-1,4-glycosidic bonds. The stem peptide chains, bound to the glycan part, consist of alternating L- and D-amino acid residues and can be cross-linked both indirectly or directly. Indirectly cross-linked stem peptides with alanyl-serine or alanyl-alanine interpeptide bridges are characteristic of penicillin-resistant strains, while penicillin-sensitive strains lack these interpeptide bridges[20].

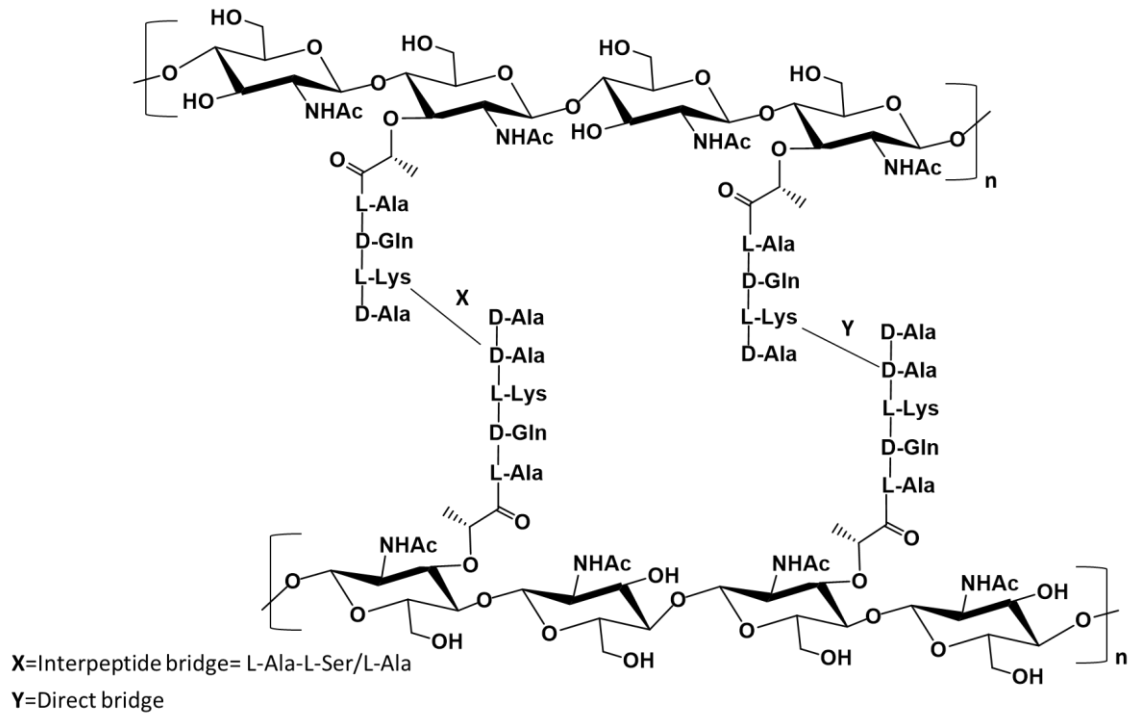

Figure 3: **Structure of peptidoglycan in *Spn*. The glycan strands are composed of alternating β-1,4-linked GlcNAc (*N*-acetylglucosamine) and MurNAc (*N*-acetylmuramic acid) residues**. The stem peptides are cross-linked either by interpeptide bridges or direct bridges. (Adapted from (2)).

1.2.2.4 Wall Teichoic acids (WTA) and lipoteichoic acids (LTA)

WTA and LTA are widely distributed polymers found in the cell-wall membrane in Gram-positive bacteria. Pneumococcal WTA (pnWTA) was firstly referred to as pneumococcal C-polysaccharide. Later, pnLTA was isolated by Goebel and Adams in 1943 and termed as pneumococcal F-antigen (Forssman antigen)[21].

Among Gram-positive species, differences in structure can be observed in the WTA and LTA indicating into distinct biosynthetic pathways involved in the synthesis of these polymers[22,23,24]. However, the structure of WTA and LTA in *Spn* share identical components of RUs and exhibit similar length distributions, indicating a common biosynthetic pathway. The RUs are joined together by phosphodiester bonds, highly complex in their composition and consist of unusual and rare amino sugars, such as 2-acetamido-4-amino-2,4,6-trideoxygalactose (AATGal), glucose (Glc), ribitol-phosphate (Rib), and two *N*-acetylgalactosamine (GalNAc) residues decorated with *P*-Cho[20,25,26]. *P*-Cho is rarely found in bacteria, and so far, *Spn* and very closely related species are known to rely on the external uptake and metabolism of choline for their growth (**Figure 4**)[27].

A computational analysis investigated the shared biosynthetic pathway of WTA and LTA in Viridans streptococci, with a particular focus on the non-pathogenic strain *S*. *pneumoniae* R6. These analyses investigated the formation of a common precursor molecule, the polymerization process leading to the formation of TAs, and the transportation of these molecules across the cytoplasmic membrane.

Different enzymes encoded by a combination of 16 known and hypothetical genes are responsible for the synthesis of the TA repeating unit (TA-RU)[27]. The composition of pneumococcal WTA and LTA has been studied over the years. Initially the RU structure was defined as AATGal-Glc-RibP-GalNAc-(*P*-Cho)-GalNAc-(*P*-Cho) with the number of RUs differing based on the strain[28,29]. Subsequent NMR analysis of RUs in pnLTA provided more stereochemical details, including both within RU components and between adjacent RUs. The study confirmed that the first repeating unit is connected to the glucose-diacylglycerol lipid anchor (→3)-α-D-Glcp-(1→3)-acyl$_2$Gro) in a β-configuration. The next RUs are then bound to the preceding unit by α-configurated AATGal moieties[30]. The current known pnLTA structure is depicted in the following figure.

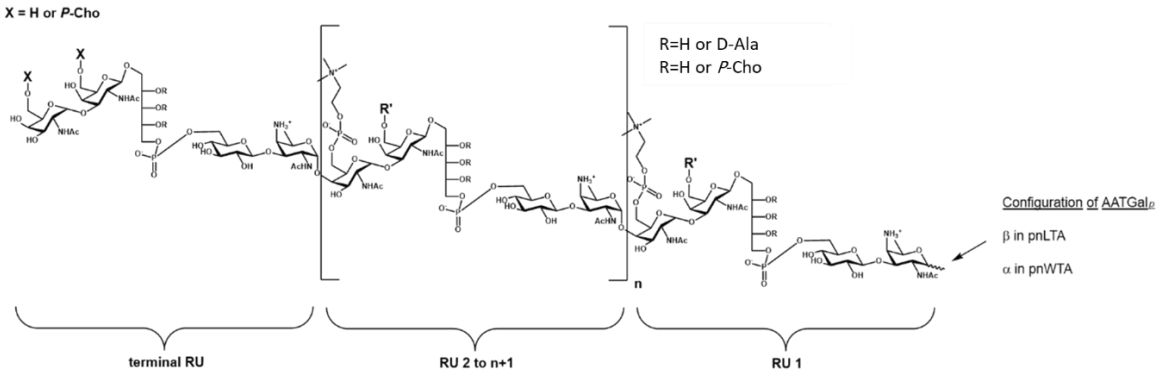

Figure 4: **The current structural model for pneumococcal LTA is composed of repeating units (RUs), each containing AATGalp, Glcp, Rib-ol-5-P, and two GalpNAc residues**. All RUs are linked by α-1 bonds, except for the first RU, which is β-1-linked. Additionally, the RU chain is bound to a Glcp-DAG molecule. Partial substitution of the hydroxyl groups on Rib-ol-5-P by D-alanine occurs to varying extents. This figure is adapted from 29.

TA polymer biosynthesis steps take place intercellularly in a similar way until their export to the extracellular membrane, where they differ in their attachment-mediated enzymes and anchors. The attachment of WTA and LTA in numerous Gram-positive bacteria has been a topic of debate for many years. Regarding the WTA attachment, certain members of the LCP family of phosphotransferase proteins (including Cps2A, LytA, and Psr) in nearly all Gram-positive bacteria have been pinpointed as key factors in facilitating the connection between complex carbohydrate polymers like WTA polymers and CPS to PGN. Mutation in this family frequently exhibit modified cell wall structures, changes in autolysin activities, decreased antibiotic resistance and diminished virulence[31,32,33]. For instance, in *Staphylococcus aureus*, studying single, double, and triple deletion mutants uncovered distinct phenotypes associated with each of the three proteins[34]. The ligase activity of these proteins has been confirmed using chemoenzymatically produced WTA and PGN as substrates[35].

In *S. pneumoniae*, all three LCP orthologs appear to be localized at the cell membrane, anchored by their N-terminal end and accumulate at septal sites. One study has utilized

anti-type 2 capsule antiserum to demonstrate that single *cps2A* or *psr* mutants had reduced capsule production. The *cps2A-lytR* double mutant displayed significant impairments in growth and cell morphology, resulting in the release of approximately half of the total capsule material into the culture supernatant. These findings suggest that the three LCP proteins in *Spn* likely have partially overlapping functions in attaching CPS to the C6-OH of the MurNAc residues of the PGN[36].

On the other side, SPD_1672 of *Spn* has been identified as putative lipoteichoic acid ligase (TacL) responsible for attachment of pnLTA. The *tacL* mutant displayed reduced virulence in mouse infection models of acute pneumonia and systemic infection. Also, in vitro analyses showed a decrease in its ability to adhere to lung epithelial cells. Despite the significant impact of *tacL* deficiency on pathophysiology in vivo, there was only a minimal effect on the growth rate observed in in vitro growth analyses using both complex and chemically defined mediums. Microscopic examination using field emission scanning electron microscopy (FESEM) and transmission electron microscopy (TEM) showed that the *tacL* mutant maintained its typical diplococci appearance, indicating no significant changes in bacterial morphology. However, the absence of *tacL* resulted in altered levels of specific choline binding proteins (CBPs), including PspC, Pce, and CbpJ, which are known to play roles in autolysis, competence, and virulence of *Spn*[37]. **Figure 5** illustrates the current understanding of the pneumococcal cell wall, emphasizing the modes of attachment for TA polymers.

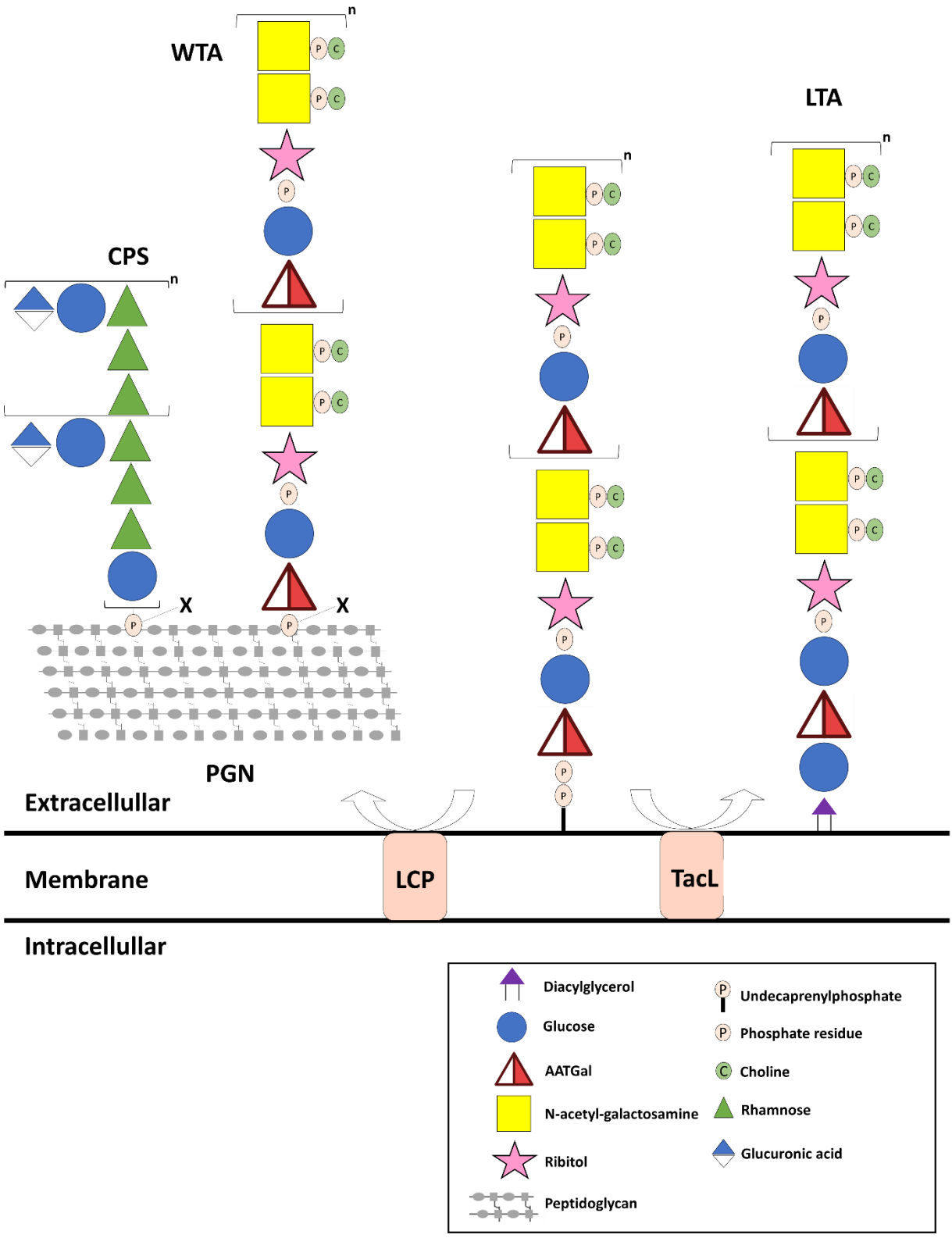

Figure 5: **The current knowledge of the pneumococcal cell wall highlights mainly the structural components of capsule polysaccharides (CPS) and teichoic acid (TA), as well as the final step in the attachment of TA in serotype 2**. The X linkage remains matter of debate. Adapted from 36.

1.2.3 Bacterial plasma membrane

The plasma membrane is a vital barrier with variation in its composition among organisms. While there has been extensive research on eukaryotic membranes, bacterial cytoplasmic membranes have received less attention and therefore are relatively understudied. However, in the last few years, the importance of bacterial lipidomics is growing intensively, especially in the search for novel bacterial lipid biomarkers as diagnostic tools and the development of antibiotics. The reason for the increasing interest in microbial lipidomics arises also from the fact that the bacteria are able to develop resistance mechanisms associated with alterations in their lipid membranes. Examples of resistance mechanisms related to cell membrane include cell wall thickening, alteration of phospholipid composition, changes in net surface charge and adjustment of membrane fluidity. Bacterial membrane lipids are mainly composed of glycerolipids (GLs) and glycerophospholipids (GPs). However, their composition can differ extensively and change over time. This variation is influenced by bacterial strains as a factor and the conditions in their environment[38,39].

1.2.3.1 Pneumococcal lipids

GLs and GPs families have been previously reported as major constituents of pneumococcal membrane lipids. In general, GLs and GPs structures contain a glycerol-based backbone connected to fatty acid (FA) chains through ester bonds. GLs usually comprise a glycerol molecule combined with one, two, or three fatty acid chains. This leads to the formation of mono-, di-, or triacylglycerol (MAG, DAG, or TAG). GLs can also consist of a hexose component, commonly glucose, galactose, or a combination of both, which is directly linked to DAG through the activity of a glycotransferase enzyme[40,41,42]. These kind of GLs are not limited to *Spn* alone; they are also present in other Gram-positive species. Glucosyldiacylglycerol (GlcDAG), galactosylglucosyldiacylglycerol (GalGlcDAG) and DAG have been reported as pneumococcal GLs (**Figure 6 A**).

GPs, on the other hand, are made of a glycerol phosphate backbone with a head group attached at the *sn*-3 position. The remaining two positions are linked to FA components via ester bond. Seven classes of GPs are commonly recognized, mainly distinguished by the chemical structure of their head group: phosphatidic acid (PA), phosphatidylserine (PS), phosphatidylglycerol (PG), cardiolipin (CL), phosphatidylcholine (PC), phosphatidylethanolamine (PE), and phosphatidylinositol (PI)[43,44]. The first studies on pneumococcal lipids have demonstrated that *Spn* can contain in its cell wall PA as well as anionic phospholipids like PG and CL. Other phospholipids, such as PS, PE and PI have not been observed[43,45]. Recent studies have shown that *Spn* can scavenge zwitterionic phospholipid PC when it is grown in a medium supplemented with yeast extract or human serum. This phenomenon is likely attributable to the bacterium's ability to incorporate the PC head group (originating from the supplemented medium) with *Spn* acyl chains,

resulting in the producing of PC[46]. The currently known GPs in *Spn* are illustrated in **Figure 6 B**.

Despite their prevalence, our understanding of GLs role in Gram-positive bacteria and more specifically in *Spn* is limited[47]. One suggested role of GLs, as seen in *Mesorhizobium loti*, is to serve as a phospholipid replacement under conditions where phosphate is limited[48]. Besides their known function as lipoteichoic acid anchors, they could also be recognized by the host's immune system; for instance, the GlcDAG of *Spn* can be recognized by natural killer T cells via a CD1d-dependent process[49,50]. However, their full roles remain largely unknown. The fact that streptococcal glycolipids stimulate the human immune system suggests their role in the streptococcal membrane could be more important than just acting as lipid anchors for lipoteichoic acids. GPs are common components of cellular membranes in both mammalian and bacterial cells. They serve key biological functions, acting either as secondary messengers or precursors for the generation of such messengers. The biosynthesis pathway for GLs and GPs are complicated due to the engagement of multiple enzymes. These pathways, along with their associated enzymes, have been previously examined and elucidated in detailed way[43,44].

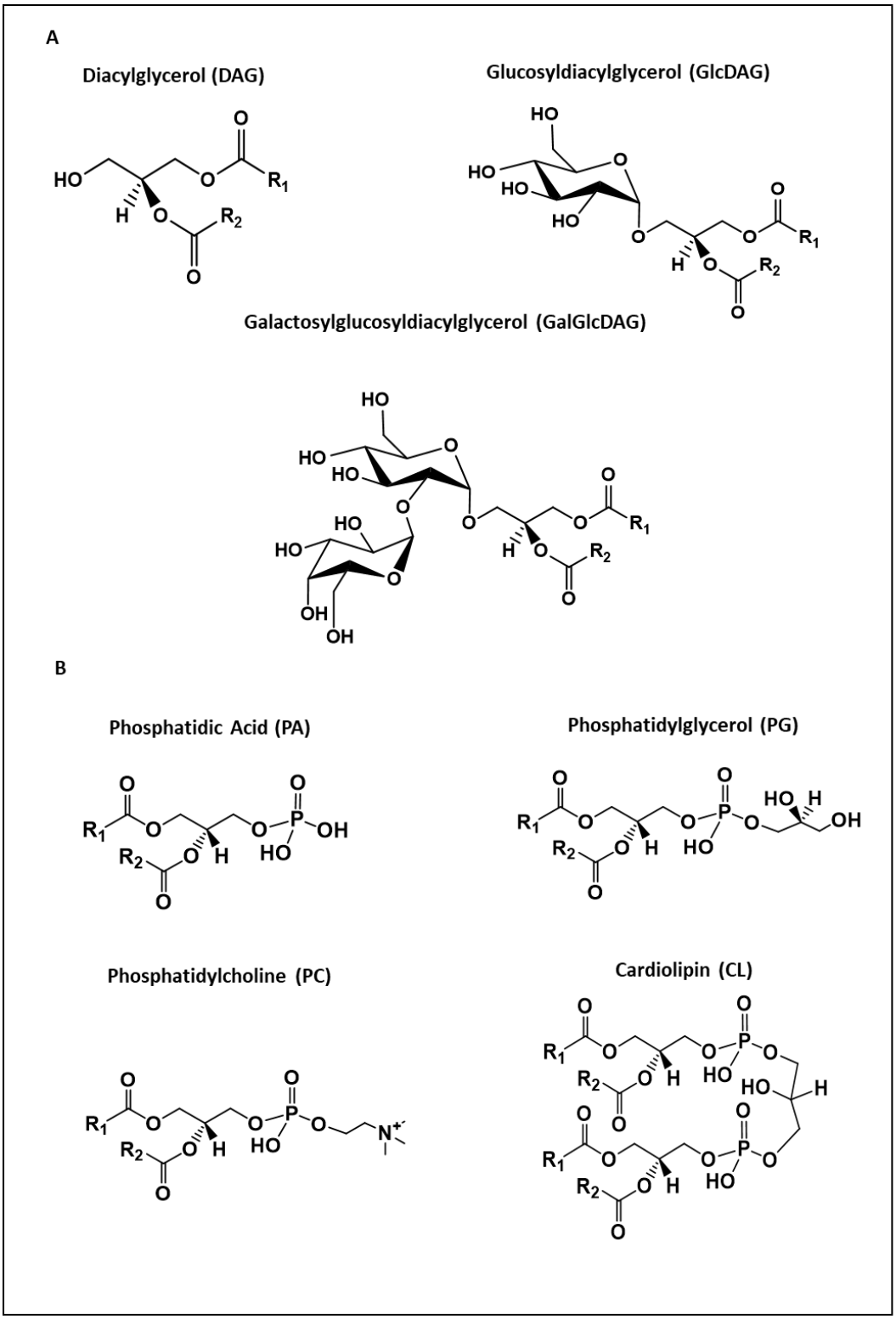

Figure 6: Identified lipid classes in *Spn* so far. In Panel A: the glycerolipids family is shown, which includes three lipid classes: DAG, GlcDAG, and GalGlcDAG. Panel B: represents the glycerophospholipids, encompassing four lipid classes in *Spn*: CL, PG, PA, and PC.

1.2.4 Lipidomics concept

Lipidomics is defined as the qualitative and quantitative description of the complete set of lipids, known as the lipidome, present in the cells, tissue, or organism. The first study which mentioned the term 'lipidome' was published in 2001[51]. Driven by the intense improvements in mass spectrometry (MS), lipidomics has experienced continuous growth in the last ten years, leading to a deeper understanding of the diverse structures and biological roles of lipids[52]. General workflows for lipidomic analysis consist of sample preparation, extraction, measurement and data processing.

1.2.4.1 Lipid nomenclature

Lipid nomenclature is essential to describe the enormous variety of lipids in an organized way. To precisely describe the chain length and degree of saturation of a single fatty acid, the numbers of carbons and double bonds are written and separated with a colon.
A standardized approach for classifying lipid species was developed, detailing the level of information obtainable through various analytical methods, ranging from broad categories to specific isomers[53]. For instance, PC 34:1 serves as the suitable shorthand notation for diacylglycerol phosphatidylcholine species, whereas PC 16:0/18:1 represents the same lipid species but provides additional molecular information regarding the fatty acid length and degree of saturation. Furthermore, the nomenclature PC 16:0/18:1 [9Z] delves deeper, containing additional details about the location of the double bond on the 9th carbon atom from the tail end of the chain, and "Z" signifies the cis configuration of the double bond.

1.2.4.2 Lipid extraction

There are several factors to consider when extracting lipids for analysis. Lipids can be extracted using monophasic or biphasic systems. Biphasic systems are often favored because they can eliminate polar interferences in the aqueous layer that might cause bias during the analysis. However, when employing LC-MS and specifically RPLC-MS approaches, polar impurities can be separated during elution, making monophasic systems a viable alternative for lipid extraction. The type of solvent used in the biphasic system leads to further subdivisions within this category[54,55].
An important example of the biphasic system is the methyl-*tert*-butyl-ether (MTBE) method, as a solution to the common difficulties associated with the chloroform-methanol-water extraction process. In this system, MTBE is used instead of chloroform and as result of its lower density, it floats when combined with methanol and water. This has the advantageous effect of positioning the separated lipid-containing organic phase on top of the aqueous phase. This method eliminates the need to cross the aqueous phase with a pipette when collecting the organic phase. This extraction process proved its effectiveness through comparative evaluations with the Bligh and Dyer method, employed for *E*. *coli* and plasma lipidome profiling. It exhibited similar or slightly better recoveries compared to those achieved with the well-established Bligh and Dyer techniques[56].

Taken together, these developments in lipid extraction procedures have earned the MTBE-based lipid extraction protocol widespread acceptance for large-scale lipidomics studies.

1.2.4.3 Mass spectrometry lipidomics

MS-driven lipidome analyses can be categorized into two approaches: LC-MS/MS based lipidomics (A) or shotgun lipidomics (B). Each one has its own advantages and pitfalls.

1.2.4.3.1 LC-MS/MS based lipidomics

The combination of high-performance liquid chromatography with tandem mass spectrometry (LC-MS/MS) is an implemented method in the field of lipidomics. It offers exceptional selectivity, efficiency, and reproducibility for lipid analysis. In the liquid chromatography system (LC), specifically reversed-phase liquid chromatography (RPLC) and hydrophilic interaction chromatography (HILIC), are the major techniques used for lipid analysis among various column chromatography separation methods. RPLC utilizes the principle of hydrophobicity to separate analytes, where the elution order is determined by factors like carbon chain length and degree of unsaturation in the acyl chains of the lipids being analyzed. In contrast, HILIC separates analytes based on their hydrophilic and amphiphilic characteristics, particularly focusing on the properties of their head groups[57,58,54]. In summary, RP chromatography is ideal for separating non-polar and moderately polar lipids, while HILIC is more suitable for the analysis of polar lipids.

1.2.4.3.2 Shotgun lipidomics

Shotgun lipidomics, a method that involves the simultaneous injection of all analytes without prior separation, was employed as the analytical approach in this study. This method, in terms of the MS-acquisition mode, can be carried out by using data independent acquisition (DIA) or data dependent acquisition (DDA) mode. In the DDA method, selected, e.g. the top 10 or 15 most abundant, ions from the preceding MS^1 full scan are chosen for subsequent isolation and fragmentation experiments. In contrast, in DIA mode, abundant and middle abundant precursors are fragmented and recorded. DIA mode in recent years is becoming more popular due to its ability to cover wide range of lipidome. In both modes, effective data interpretation normally demands the use of a spectrum library or dedicated search engines[59]. These tools help in the process of uncovering and isolating potentially interesting lipids from the complex recorded spectrums.

The shotgun lipidomics methodology, similar to the shotgun proteomics approach, enables rapid identification of the most abundant lipids. One of the main advantages of the shotgun lipidomics, particularly when based on the DIA approach, is its potential for high throughput. However it's important to mention that this method is particularly effective at detecting major lipids while it shows difficulties when it comes to quantifying low abundant lipids, even if they have potential biological significance[60].

In summary, shotgun lipidomics and LC-MS/MS have their limitations. The shotgun method is constrained by ion suppression and poor sensitivity for very low-abundance lipids. In contrast, LC-MS/MS provides high-quality analyses for lipidomics by optimizing sensitivity with sample separation, making it the preferred method for less abundant bioactive lipids (e.g. sphingolipids or oxidized lipids). However, shotgun lipidomics is rapid and robust for global lipid profiling, remaining popular for studies addressing general biological questions due to its coverage of a high number of identified lipids[61].

1.2.4.4 Lipid identification

In the past, shotgun lipidomics mainly utilized triple quadrupole mass spectrometers. During that time, lipid identification relied on a combination of one precursor scan and one neutral loss scan at a time. The used instruments had lower mass resolution to detail precise masses of fragment precursors[62]. Today, however, advanced tandem mass spectrometers like those in the Orbitrap and Q-TOF families offer high-resolution spectra with high mass accuracy. This accuracy allows the matching of detected molecular masses with their elemental compositions, hence ensuring reliable lipid identification across numerous related samples. The advantages of employing high-resolution tandem mass spectrometers for these applications have been underscored[63,64]. These state-of-the-art instruments offer high acquisition speeds and sensitivity, enabling fragmentation of nearly all potential peaks. Consequently, a thorough dataset is created that includes the masses of all precursors and their produced fragments.

LipidXplorer is a widely used open source bioinformatic tool for lipid identification in shotgun lipidomics datasets. It consists of two data processing steps: firstly, all MS^1 and MS^2 spectra are compiled into a unified flat-file database known as MasterScan. During the importing process, the software aligns related MS^1 and MS^2 spectra based on the characteristics of the mass spectrometric peaks (lock mass). This means all collected data from a complex shotgun lipidomics study are combined into a single experiment dataset. The second step is the writing of so-called Molecular Fragmentation Query Language (MFQL) files. Each MFQL file outlines structure-specific ions for different lipid classes. These structure-specific ions can include precursor and fragment ions recorded from the MS and MS/MS datasets. By combining high-resolution MS^1 with fragmentation patterns seen in MS^2, the MFQL files enable the investigation of complex lipid extracts, without requiring a reference lipid database. Also, adding or adjusting files to identify potential lipid classes or species is relatively simple with this setup. However, the complexity of shotgun datasets presents a significant challenge. In a standard workflow, once lipids are extracted and the mass spectrometry analysis is performed, the dataset from a single experiment may comprise many MS and MS/MS spectra, leading to over 100,000 unique peaks. Only a small subgroup of these peaks, usually in the hundreds, can eventually be definitively identified as lipids[65,66,67].

Another software called ALEX has been developed for analyzing high-resolution shotgun lipidomics data. It utilizes a target list generated from the ALEX lipid database to identify lipid species. However, this software has a limitation in that its database does not cover all lipid classes. Therefore, it can only detect lipid species that are already included in its database[68].

1.2.4.5 Lipid quantification

To accurately quantify endogenous lipids and reduce errors caused by lipid extraction and data acquisition processes, the use of lipid-internal standards (IS) is essential and usually are added prior to the extraction[60]. Various lipid quantification strategies have been employed, including the use of synthesized standards with non-natural fatty acid chain numbers, although these may exist in trace amounts in biological samples. Another method involves heavy isotope-labeled lipid standards (authentic standards), which are known for analysis of lipid mediators. They are effective but often expensive and limited in availability. A recent way is performed by using SPLASH® single-vial prepared lipidomic analytical standard from Avanti polar lipids. It contains deuterium-labeled lipids representing major lipid classes in human plasma. Before analysis, it is recommended to conduct a pre-screening process to identify predominant lipid classes or species, facilitating the creation of a customized internal standard. However, using a reference standard for every target lipid species may not be practical due to cost or availability constraints. Upon the development of tailored internal standard, lipid quantification can be achieved by utilizing calibration curves. This method generally employs authentic standards and is well-suited for targeted lipidomics studies[58,69]. For untargeted lipidomic studies, it is a common practice to normalize individual ion peak intensities using an internal standard for each lipid class. The subsequent ratio of the analyte to the internal standard is then multiplied by the concentration of the internal standard to derive the concentration of the lipid species[60,70,71,72]. This calculation can be performed using software such as Excel, or by using custom programming scripts, such as those written in R[73].

1.3 Scope of thesis

Our understanding of how genetic factors, biosynthesis processes, and environmental influences shape microbial lipidomes is still limited, highlighting a significant knowledge gap. This gap is particularly pronounced in the case of *Streptococcus pneumoniae* (*Spn*), where only qualitative data are available. This thesis focuses on establishing a robust and validated shotgun-workflow to enable high-accuracy quantitative analysis of lipids in wild-type and specific mutant strains used as model systems.

The LTA to WTA ratio in *S. pneumoniae* and closely related strains lacks accurate data. Two earlier studies, one from 1975 on *S. pneumoniae*[74] and another from 1993 on *S. oralis*[75], provided the only available data. These studies used radioactively labeled molecules and found LTA to WTA ratios of around 10-15% to 85-90%. Recent research suggests that LytR overexpression increases WTA relative to LTA, potentially playing a significant role[76]. This study addresses the growing need for an analytical method to precisely determine the WTA/LTA ratio by using the improved understanding of LTA/WTA structures and isolation techniques in *Spn*. The aim is to validate these ratios in Wt and Δ*LytR* strains by a GC/MS-based methodology.

Another goal of this work was to elucidate the nature of capsule attachment in *Spn*, particularly focusing on the D39 *Spn* serotype 2 strain. The mechanism of attachment to PGN in this strain is matter of debate due to conflicting findings[18]. This thesis seeks to clarify the attachment process in the D39 wild type strain, addressing the knowledge gap in this area.

2) Results and Discussion

2.1 Optimization of a GC-MS based method for pneumococcal teichoic acid quantification

2.1.1 Importance of the study

The ratio of wall teichoic acid (WTA) to lipoteichoic acid (LTA) influences the pathogenicity of *Spn* by affecting the anchoring of choline-binding proteins, which are crucial for bacterial virulence and host cell interaction. Until now, limited information existed regarding the exact proportion of LTA to WTA in *S. pneumoniae* or the genetically closely related species. Two early studies have explored this topic. The first one (1975) investigated the LTA/WTA ratio and reported a 10:90 (LTA/WTA)[77]. The used methodology involved cultivating pneumococci in a medium containing choline chloride marked with radioisotopes. This allowed to separate radioactively labelled WTA from LTA and has revealed that most of the labelled choline was incorporated into fractions containing WTA, with only a minor fraction being integrated into fractions containing LTA. Two decades later, another study employed a similar approach using radioactively labeled cultures on *S. oralis*, which demonstrated comparable TA biosynthesis to *S. pneumoniae*[27]. It has shown that the WTA content also ranged between 80-90%, while the LTA content stayed at approximately 10-20%[75].

As mentioned in the introduction, three enzymes (Cps2A, Psr, and LytR) are anticipated to participate in attaching the TA-precursor chain to the PGN for WTA as well as CPS formation. However, it remains uncertain which pathway (enzyme) is the main player in this process and how the levels of WTA and LTA are regulated. In very recent research, also by using radioactive choline, the overexpression of LytR has led to a notable increase in WTA compared to LTA[78]. This suggests that LytR may play a significant role in WTA attachment, potentially making it the primary player in this process.

Taking all mentioned information together, it becomes clear that establishing the precise WTA/LTA ratio remains a substantial challenge and a pivotal inquiry in the examination of *Spn*. Dr. Franziska Marwitz in her PhD. thesis initiated the task of developing an analytical method to determine the WTA/LTA ratio by GC/MS[79]. This part of my thesis sheds light on further enhancements to the method, with the final goal of validating the ratios in *Spn* D39 Wt compared to the isogenic Δ*lytR* mutant.

2.1.2 Principle of TA chemical quantification

Pneumococcal TA is a large heterogenous molecule with varying weight based on how many repeating units it contains[30]. Due to difficulties in quantification such large complex molecule as native molecule, the idea was to look for unique features in the studied molecule for quantification. When comparing various pneumococcal cell wall components such as PGN, TA, and the CPS, it is clear that ribitol could serve as reference point for

quantification. Ribitol is TA-specific sugar alcohol and is not found in other cell wall constituents. More information about cell wall components in *Spn* is shown in **Figure 5**.
To separate WTA from LTA and quantify their respective ribitol content, a series of isolation steps were carried out as illustrated in **Figure 7**. To determine the WTA/LTA ratio in the whole bacterial material, aliquots were collected at various time points during the purification protocol. Aliquots were first taken before and after cell disruption via the French press (samples 1 & 2, **Figure 7**). After boiling with SDS and ultracentrifugation, it was possible to separate the supernatant containing LTA from the pellet containing WTA, and both were subjected to a wash step with ethanol to reduce the SDS content. Aliquots for quantification were taken from both washed fractions (samples 3 & 4, **Figure 7**). The washed supernatant then underwent multiple steps until pure LTA was obtained, using hydrophobic interaction chromatography, from which aliquots for quantification were taken (sample 5, **Figure 7)**. Regarding WTA isolation, in the case of capsulated strains, the presence of capsule sharing the same anchoring point (MurNAc) hindered WTA isolation. The attachment of capsule on PGN sugar has been suggested by previous biochemical study[36] and is described in section 2.2.1. Therefore, the crude SDS-free WTA-PGN-CPS complex (sample 3, **Figure 7**) was used for ribitol quantification in WTA.

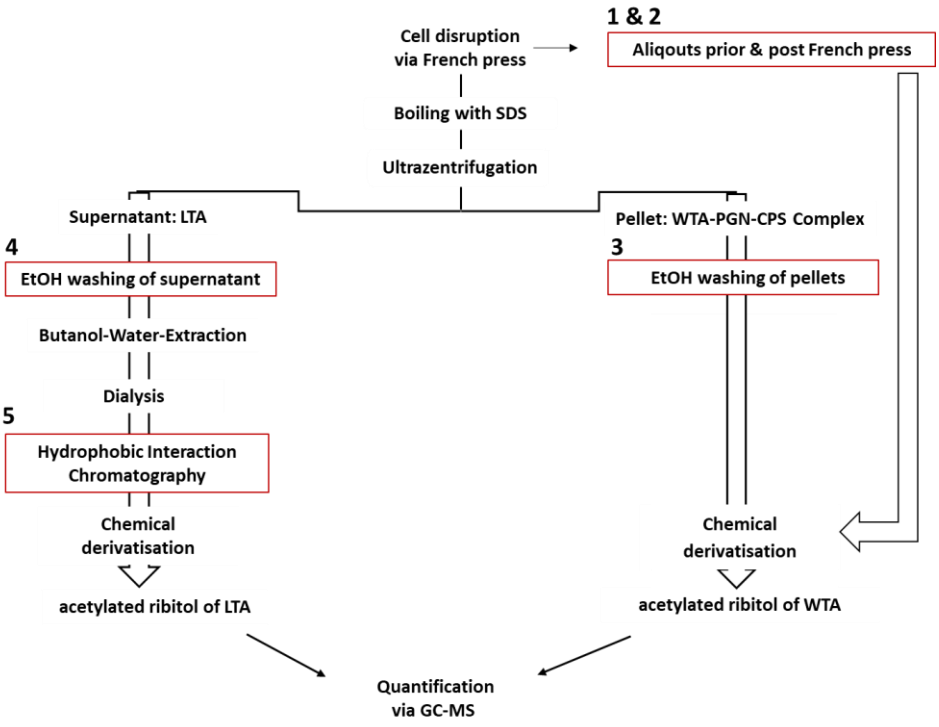

Figure 7: Workflow illustrating the processing of cell material for the isolation of LTA and WTA. Samples for quantification were taken at selected time points during the extraction, highlighted with a red box.

2.1.3 Selection of internal standard and investigation of the dynamic range

In previous experiments, specific chemical treatments were found to be crucial for breaking down the pnTA into their sugar components. The initial treatment involved the use of hydrofluoric acid (HF) for 72 h at 4°C. Its purpose was to disrupt the phosphodiester bond linking the repeating units within the TA backbone. Another important treatment is subjecting the HF-treated RUs (no longer connected) to 4 M trifluoroacetic acid (TFA) for 4 h at 100 °C. This treatment cleaves the glycosidic bonds connecting TA monosaccharide components. During these treatments, ribitol undergoes partial hydrolysis forming 1,4-anhydroribitol within both LTA and WTA structures; however, complete hydrolysis does not occur. Therefore, for accurate ribitol determination, it's essential to measure both ribitol and its hydrolysed product (1,4-anhydroribitol).

After completing the extraction steps as well as subsequent sampling as shown in **Figure 7**, an internal standard (IS) has been spiked not only to pooled samples but also to pure calibrants (ribitol and 1,4-anhydroribitol standards). The addition of an IS usually facilitates the normalization of the instrumental response and adjustment of overall analytical variations during the measurement process as well as systemic errors arising from the presence of interfering compounds within the matrix. This addition is particularly important to obtain accurate estimates of the concentration-response relationship. In this context and after several attempts for IS selection, sorbitol was selected as the surrogate standard for quantifying ribitol and 1,4-anhydroribitol **(Figure 8)**. Care was taken in the selection of sorbitol as the IS, considering factors such as its absence in bacterial cell components, non-origin from the growth medium, lack of overlap with the target molecules, and the presence of a similar fragmentation pattern to the target molecules. Another point to highlight is that due to the long purification process involved in LTA isolation, sorbitol was solely introduced into pooled samples and not at the beginning of extraction procedures. Adding polar sugars upfront in the pnTA extraction is inefficient as they are likely to be lost during the subsequent purification steps.

A

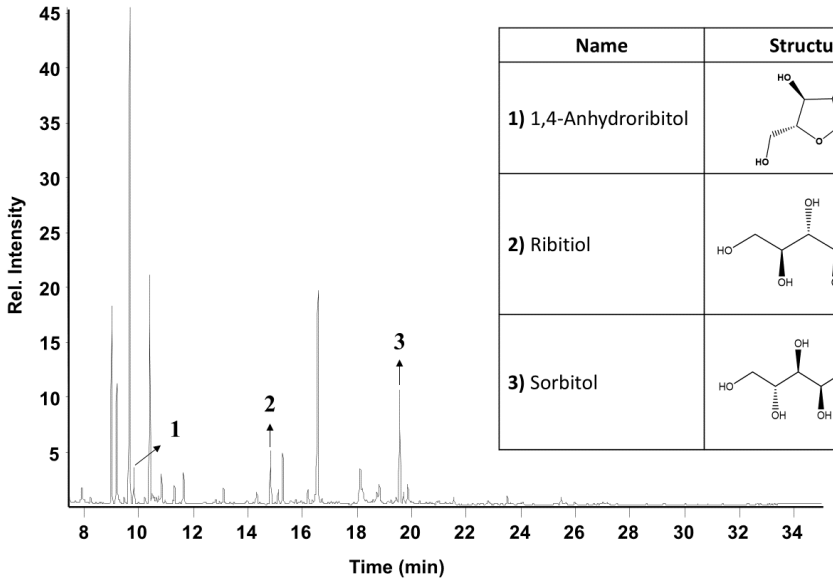

B

Name	Structure	Retention time
1) 1,4-Anhydroribitol		9.8
2) Ribitiol		14.9
3) Sorbitol		19.6

Figure 8: **Chromatographic properties of sorbitol (internal standard), endogenous ribitol, and its hydrolysis product 1,4-anhydroribitol, as determined for teichoic acid quantification**. **A**: Total ion chromatogram of the derivatized monosaccharide components from WTA-PGN-CPS intact. **B**: Table containing the chemical structures and associated retention times for the highlighted peaks seen in A. Specifically, peak number 1 corresponds to 1,4-anhydroribitol, peak 2 represents ribitol, and peak 3 indicates the selected internal standard (sorbitol) for teichoic acid quantification.

After identifying the retention time of internal standard, standard solutions of calibrants were prepared at seven different concentrations (0.5, 0.75, 1, 2.5, 5, 7.5, 10 µg/mL), each spiked with 2.5 µg/mL of the IS. Each spiked calibrant series was independently prepared in duplicate, and every concentration was measured as a technical replicate. Prior measurement, all of the calibrants went through strong methanolysis and derivatization with pyridine and acetic anhydride to make the molecules measurable in GC-MS. More information about this derivatization is described in section (4.5.2.1.5).

As shown in **Figure 9**, the results from the spiked calibrants have demonstrated a strong correlation between the normalized area of the tested calibrant on the intensity of the IS across the entire range of concentrations investigated. Below the lowest concentration used (0.5 µg/mL), there were challenges in detecting the calibrants, particularly 1,4-anhydroribitol. Consequently, for both ribitol and 1,4-anhydroribitol, a dynamic range of 0.5 µg/mL to 10 µg/mL was employed for quantifying ribitol as well as its hydrolyzed form as content of WTA and LTA.

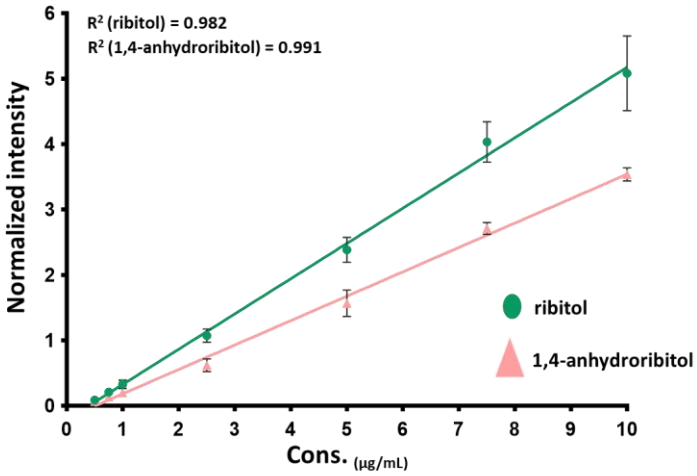

Figure 9: **Calibration curve for ribitol and 1,4-anhydroribitol, normalized to the internal standard intensity with corresponding R2 values**. The calibration curve was generated from two replicates, with error bars indicating the standard deviation.

2.1.4 Designing and preparation of a matrix-matched calibration curve

To develop an analytical method for quantification goals in a biological system, it's important to distinguish between two approaches: external calibration and internal (In-sample) calibration. External calibration involves creating a single calibration curve that can be used for multiple study samples. Different methods are available for external calibration, depending on the availability of the analyte and the matrix. The main approaches include: authentic analyte in an authentic matrix, authentic analyte in a surrogate matrix, surrogate analyte in an authentic matrix, and surrogate analyte in a surrogate matrix. On the other hand, internal calibration is performed directly on each sample, resulting in a unique calibration curve for each one. The primary consideration is the availability of the analyte, whether it's authentic or surrogate. Further details about the difference have been extensively discussed in literature[96].

In our specific study, due to the presence of the target analytes (ribitol and 1,4-anhydroribitol) naturally in the samples and the absence of an analyte-free matrix, the only possible approach was using authentic analyte in an authentic matrix. To determine the authentic matrix, a matrix sample was selected from the pooled samples, using the WTA-PGN-CPS complex (pooled sample 3, Wt **Figure 7**) as a good indicator of the biological sample's complexity. To estimate and remove the endogenous background signals, a blank matrix sample was also prepared. All matrix calibration and the blank matrix samples were prepared in three different aliquots and analysed under identical conditions using GC-MS in duplicate runs to reduce sample-to-sample variations. **Figure 10** illustrates the preparation of the matrix and blanks samples.

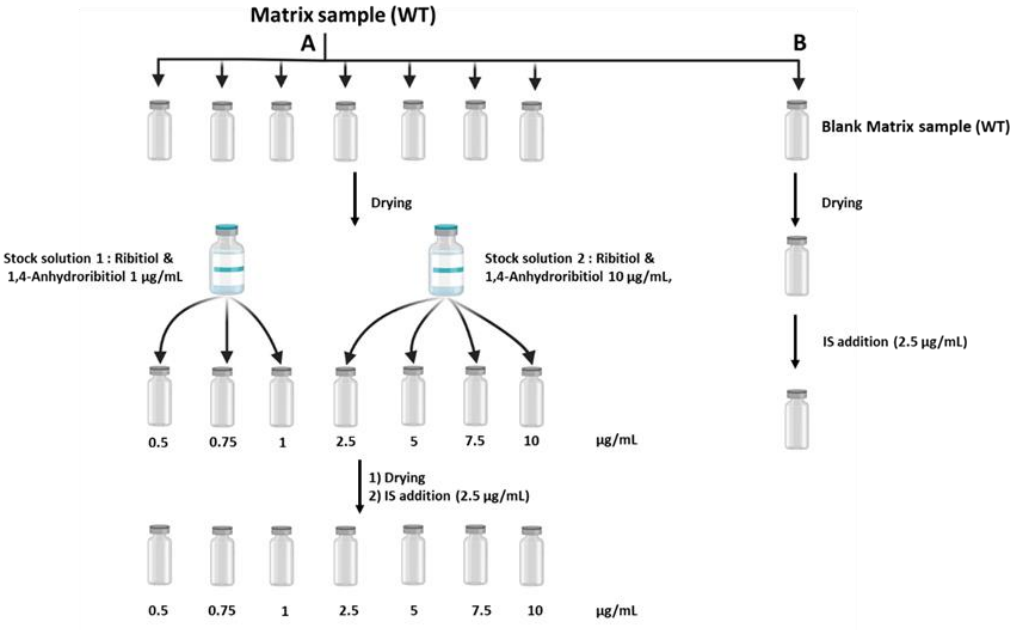

Figure 10: Preparation scheme for matrix matched calibration sample (A) and Blank matrix sample (B)

The matrix and blank samples have undergone various treatments (sections 4.5.2.1.2, 4.5.2.1.3, 4.5.2.1.4, 4.5.2.1.5), been spiked with previously determined calibrant concentrations, and analysed by GC-MS to evaluate the linearity (**Figure 11 A**). The background peak area from the blank matrix samples was subtracted from the peak area of the spiked matrix samples (**Figure 11 B)**. Following background subtraction, the averages of the three background-free calibration curves were computed for ribitol and 1,4-anhydroribitol, as depicted in **Figure 11 C**. Notably, a good correlation was observed, with R^2 values of 0.95 for ribitol and 0.93 for 1,4-anhydroribitol. Quality control (QC) aliquots were prepared to monitor instrument performance and detect any systematic errors during the analytical sequence. QC aliquots were matrix-matched, spiked with concentrations of 2.5 µg/mL and 7.5 µg/mL of authentic standards (ribitol and 1,4-anhydroribitol), and also spiked with IS (sorbitol, 2.5 µg/mL).

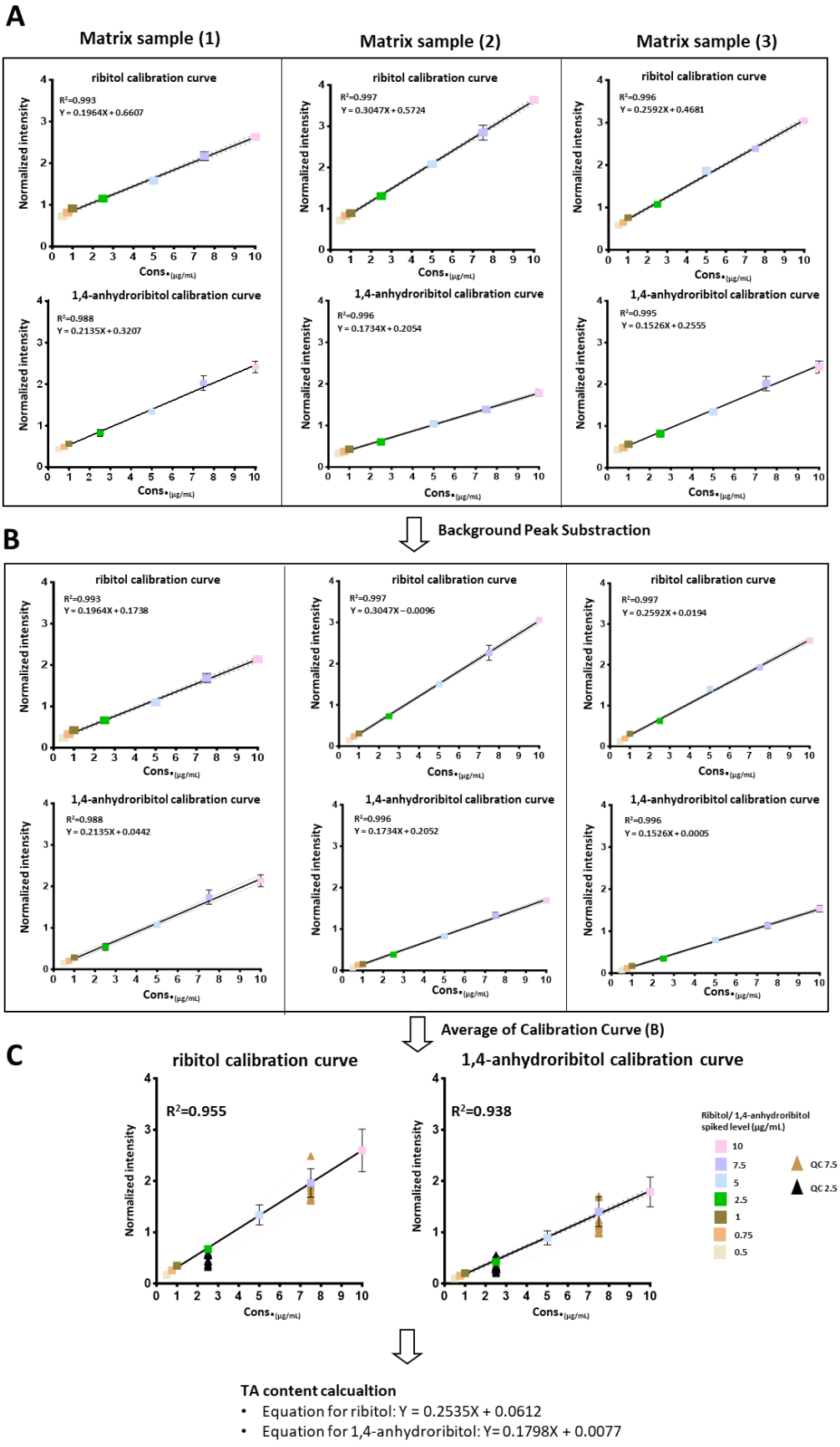

TA content calcualtion

- Equation for ribitol: Y = 0.2535X + 0.0612
- Equation for 1,4-anhydroribitol: Y= 0.1798X + 0.0077

Figure 11: **Used Calibration curves for the quantification of pneumococcal teichoic acid in three different matrix samples**. **A**: Matrix-matched calibration curve spiked with various concentrations of calibrants. **B**: Background-free matrix-matched calibration curve. **C**: Averaged background-free matrix calibration curve used for calculating ribitol and 1,4-anhydroribitol content in pooled samples.

2.1.5 Application of the quantification method to the *lytR* deletion strains

Pooled samples from both the Wt and Δ*lytR* mutant strain were measured under the same conditions as the matrix-matched calibration samples. In addition, all QC samples were analysed under identical conditions, in duplicate, both before and after the experimental runs. Most of the QC samples met the acceptance criteria, exhibiting a standard deviation under 50% (**Figure 11 C**). Based on this, the resulted equations, derived from the averaged calibration curves, were used to determine the ribitol and 1,4-anhydroribitol content in pooled samples from the Wt and Δ*lytR* strains. In the context of matrix matched calibration curves, particularly in this study for determining the ratio of WTA/LTA, certain back calculations were necessary. Correction factors were considered and calculated to determine the percentage of LTA and WTA in the initial bacterial material (**Figure 12**). Following the correction calculations, it was concluded that, on average, the *Spn* Wt strain contained approximately 16% LTA and 84% WTA. In contrast, the Δ*lytR* strain had approximately 37% LTA and 62% WTA. These calculations interpreted the respective percentages of WTA and LTA within the initial total teichoic acid content.

These preliminary results for the studied strains were in good agreement with the literature, confirming two key findings. Firstly, the ratio of WTA/LTA in the wild-type corresponds to previously reported values[74,75,79]. Secondly, the *lytR* gene appears to play a central role in WTA anchoring to the pneumococcal cell wall and *lytR* gene deletion influenced the ratio of WTA/LTA. This finding is also in line with what has been recently published about the role of LytR in ratio of WTA/LTA[78]. It is important to mention that all pure calibrants, matrix-matched calibration curves, QC and pooled samples were measured within a defined time range to prevent possible degradation during sample storage and to ensure device performance. However, a limitation of this study is that these results are based on a single biological replicate from each studied strain due to the intensive effort required for sample preparation, optimization of the quantification method and certain issues related to sample storage and device performance.

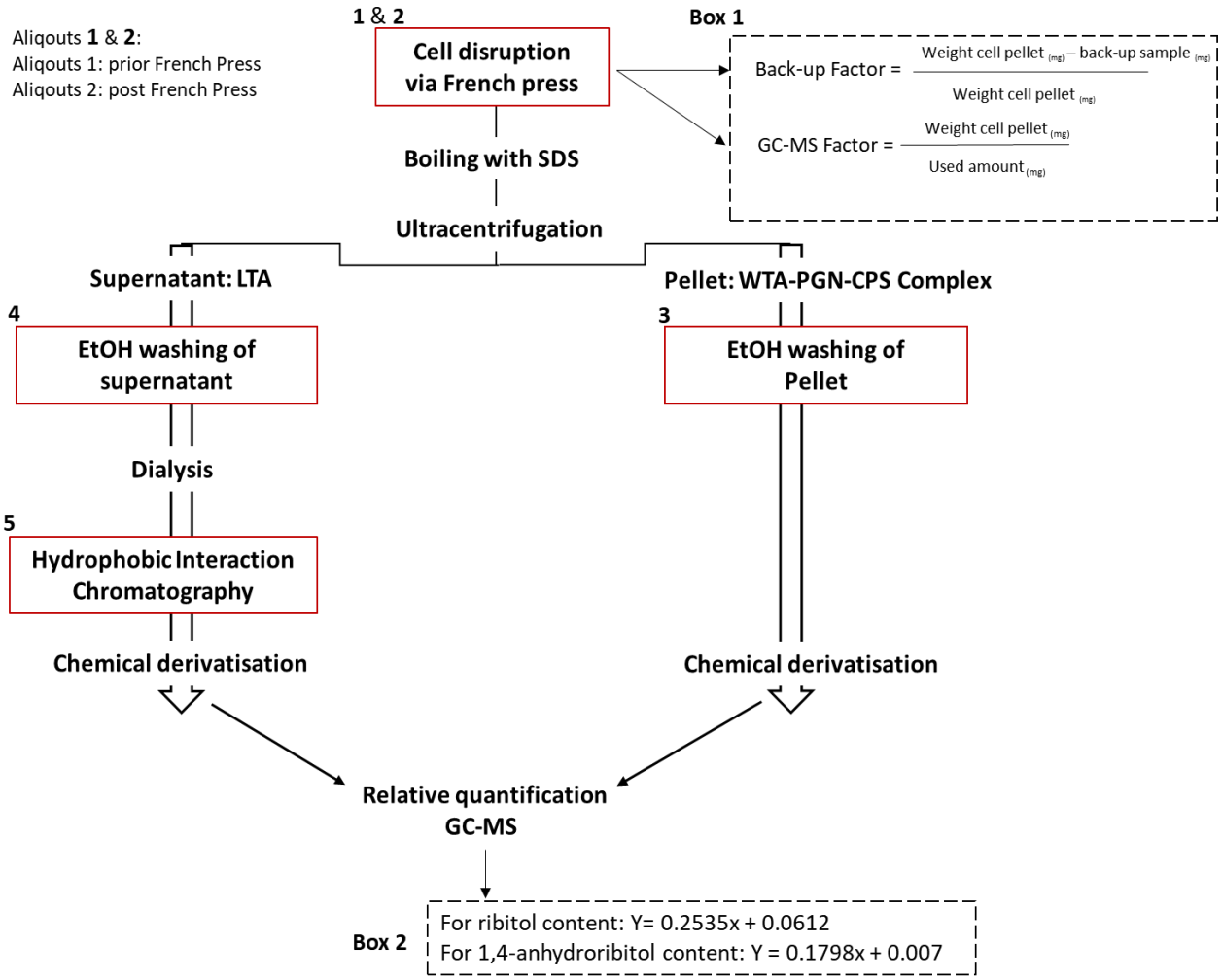

Calculation steps

1. Back-up and GC-MS factors are calculated for pooled samples (see Box 1 as an example).
2. For each measured GC-MS sample:
   a. Ribitol and 1,4-anhydroribitol content is calculated using the equations provided in Box 2.
   b. The calculated ribitol and 1,4-anhydroribitol content is summed.
   c. The sum is then multiplied by the corresponding GC-MS factor to determine ribitol content in the full material weight.
4. These calculations are performed for each technical measurement.
5. The average of the results from 2 technical replicates is calculated.
6. The ratio of found Ribitol content in samples (3, 4, 5) to the ribitol content found after cell disruption (sample 2) is calculated.
7. The calculated ratios for samples (3, 5) are summed.
8. The percentage of each part in relation to the sum part is then determined.

Figure 12: **Isolation scheme and used calculation steps for GC/MS-based quantification of TAs in *S. pneumoniae*.** The red boxes indicate the time points at which samples were taken for quantification. A backup sample indicates the taken amounts of each pooled sample, while the GC-MS sample represents only the amounts which is measured in GC-MS. Calculations steps and used equations are presented.

2.1.6 Conclusion and outlook

Determining the precise quantity of pneumococcal wall components, such as WTA and LTA, has long posed a significant challenge for researchers in this field. Historically, radioactive labeling of choline has been employed in previous studies to ascertain the WTA/LTA ratio. However, this thesis has successfully introduced an optimized methodology that eliminates the necessity for radioactive labeling, rendering it a more accessible and safer approach.

Initial results from this optimized method show a clear impact of LytR on the teichoic acid ratio. In the *lytR* deletion strain, the ratio was 37% LTA and 63% WTA, compared to 16% LTA and 84% WTA in the wildtype strain. This quantification technique now lays a robust basis for further investigations into other LCP genes that may not only influence teichoic acid quantity but also impact the quantity of capsule polysaccharides. This proof of principle method should be applied on other LCP members to explore their influence on teichoic acid ratio, including more biological replicates for each strain.

2.2 Investigation of the pneumococcal capsule attachment

2.2.1 Importance of the study

The capsule in *S*. *pneumoniae* is a known key factor for causing disease and colonizing the nasopharyngeal cavity. While there is considerable knowledge about the synthesis of these glycopolymers, less is known about the attachment processes on the bacterial surface. Early study showed that the CPS in *Spn* D39 serotype 2 formed a phosphodiester linkage with the C6 position of the MurNAc residue within the PGN[35]. However, a recent study has questioned this assumption, showing that the CPS instead utilizes a direct 1,6-glycosidic bond to attach to GlcNAc residue of PGN specifically at it reducing Glc[17]. Based on that, the nature of the capsule attachment enzymes in D39 *Spn* serotype 2 remains controversial due to conflicting findings regarding the location of CPS attachment as well as the nature of the bonding involved[19]. Therefore, for this part of the thesis, the D39 wild-type strain (serotype 2) was cultivated in full medium and further used for investigation of the capsule attachment.

2.2.2 Capsule attachment investigation requires multiple hydrolysis steps

2.2.2.1 Enzymatic degradation of the peptide cross-linking in wall teichoic-peptidoglycan-capsule complex

The WTA-PGN-CPS complex (156 mg) was isolated following the procedures outlined in the materials and methods (4.5.2.1). The complex mixture underwent initial disruption through the action of the LytA enzyme, whose mechanism of action has been previously described[37,81]. In brief, it removes the stem peptides from the glycosidic part by acting as a *N*-acetylmuramoyl-L-alanine amidase (NAMLAA). Following the LytA treatment, centrifugation was carried out. Aliquots from resulting pellets (81.2 mg) and supernatant (279.4 mg) went through multiple treatments (4.5.2.1.2, 4.5.2.1.3) and preparation steps (4.5.2.1.4, 4.5.2.1.5) until they were analyzed using GC-MS.

Since intact CPS, TA and PGN polymers have a large molecular weight and cannot be directly detected by GC/MS, specific sugars within their structures were chosen as indicators for each polymer. In this study, ribitol (Rib) and rhamnose (Rha) were chosen as representative molecules for TA and CPS, respectively. Meanwhile, *N*-acetyl glucosamine (GlcNAc) and *N*-acetyl muramic acid (MurNAc) were identified as characteristic components for the glycan strands of PGN.

Rib, MurNAc, GlcNAc, and Rha were detected in the MS spectrum through comparison with standards that underwent similar derivatization as the samples. Post centrifugation of the LytA-treated complex, the Rha was found in both fractions (pellets and supernatant). The pellets were selected for additional analysis since they also contained GlcNAc and MurNAc (**Figure 13 A**).

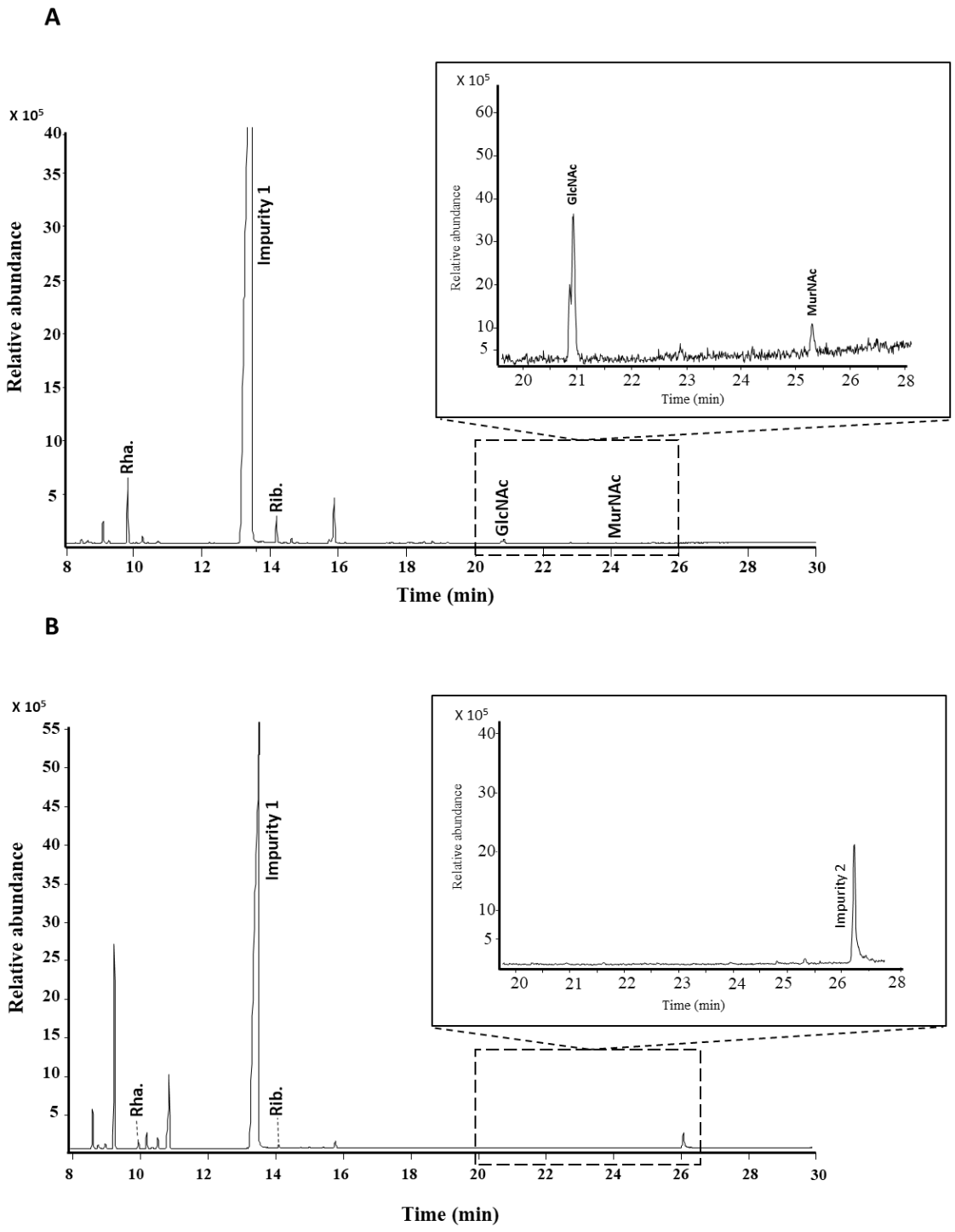

Figure 13: Total ion chromatogram representing the derivatized monosaccharide components from the WTA-PGN-CPS complex following LytA treatment. Panel A illustrates the digested and derivatized components isolated from the pellet after centrifugation. Panel B depicts the supernatant remaining after this centrifugation step. Rha: rhamnose, Rib: ribitol, MurNAc: *N*-acetyl muramic acid, GlcNAc: *N*-acetyl glucuronic acid.

The peptide-free complex (pellet post LytA treatment), which contains the glycan chain from hydrolyzed PGN with WTA and CPS, was treated with mutanolysin and lysozyme to cleave the glycosidic bond between glycan building blocks (GlcNAc and MurNAc). The used enzyme amounts were determined based on previous work[36]. After centrifugation, the soluble material was collected, and both the supernatant and pellet were analyzed using GC-MS. The supernatant was chosen for further analysis because it showed high levels of Rib, GlcNAc, and MurNAc (**Figure 14**).

The use of size exclusion chromatography (SEC) to purify the LytA-treated PGN-WTA complex from a non-capsulated sample has been previously described[37]. The same method was applied on a capsulated sample for three main purposes: first, to decrease the mixture's heterogeneity (peptide, salts); second, to distinguish CPS/WTA glycan moieties based on their weight differences; and lastly, to check if this method would provide enough material for NMR investigation (**Figure 15**).

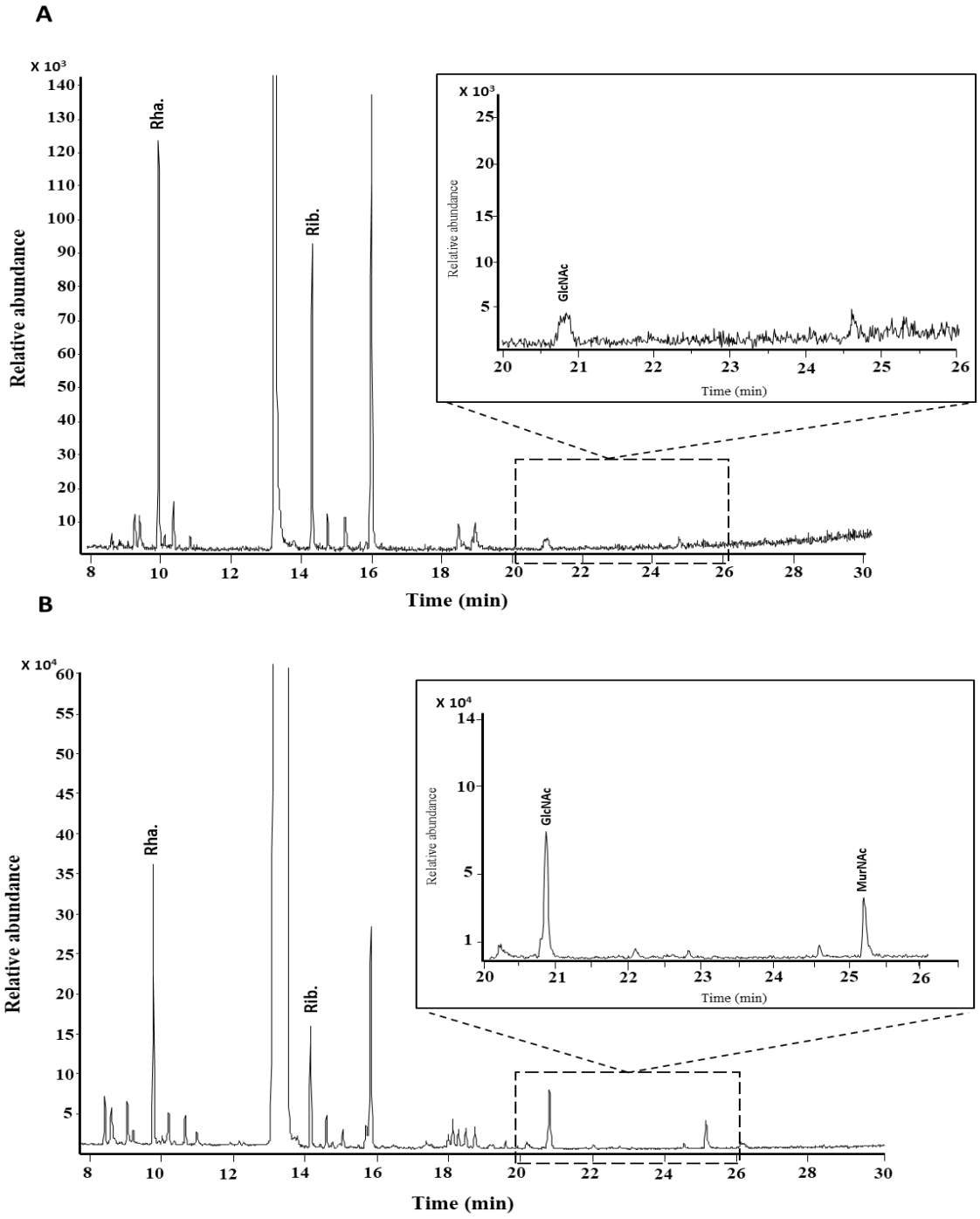

Figure 14: Total ion chromatogram spectra illustrating the derivatized monosaccharide components from the LytA-treated WTA-PGN-CPS complex following mutanolysin/lysozyme treatment and centrifugation. Panel A displays the spectrum obtained from the resulting pellet, while panel B exhibits the spectrum of the resulting supernatant. Abbreviation like figure 13.

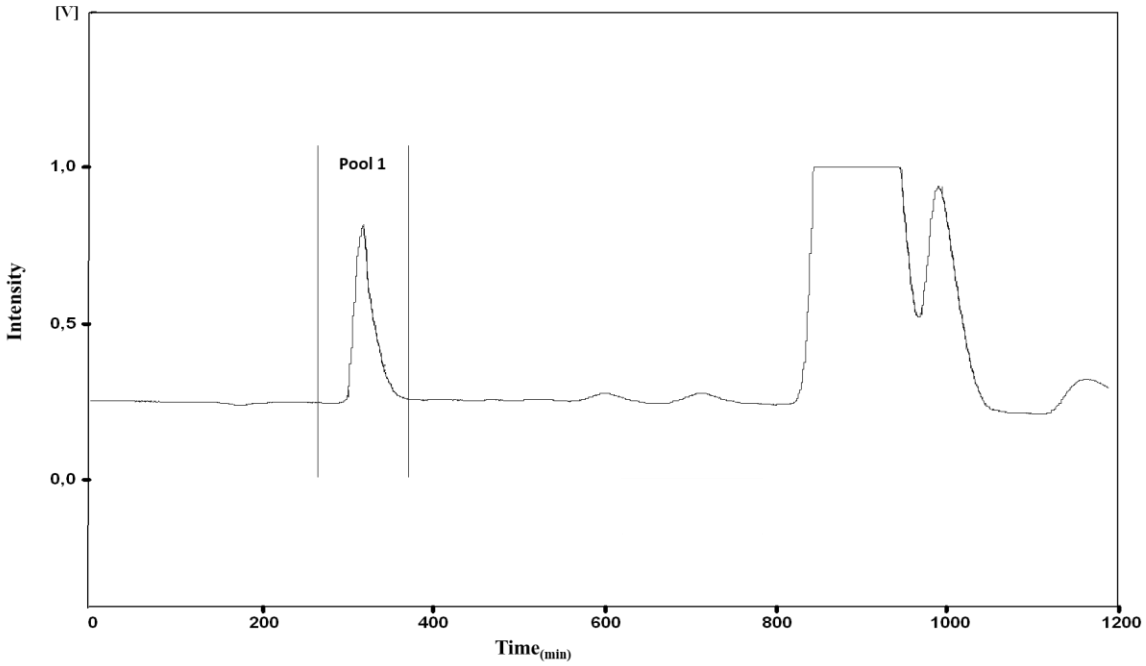

Figure 15: **Size exclusion chromatography (P30) for the isolation of CPS and pnWTA moieties bound to small PGN derived saccharides from *Spn* D39 Wt**. Pool 1 was used for further NMR analysis.

Pool 1 was collected, weighted (1.56 mg), and subjected to NMR analysis. Upon comparing the ^{1}H NMR spectrum of pool 1 (**Figure 16**, violet) with the previously published ^{1}H NMR spectrum for WTA-PGN (**Figure 16**, green), clear similarities or near features were observed. This suggests that, on one hand, separation was not achieved, while on the other hand, emerging peaks in the chemical shift range of 4.5, 5.0 and 5.3 ppm were noticed. These distinct peaks correspond to the anomeric proton signals characteristic of the capsule-rhamnose. The same trend was observed when the supernatant (post mutanolysin and lysozyme treatment) was dialyzed three times against water (**Figure 16**, red) or used as it is without any separation for NMR analysis (**Figure 16**, blue).

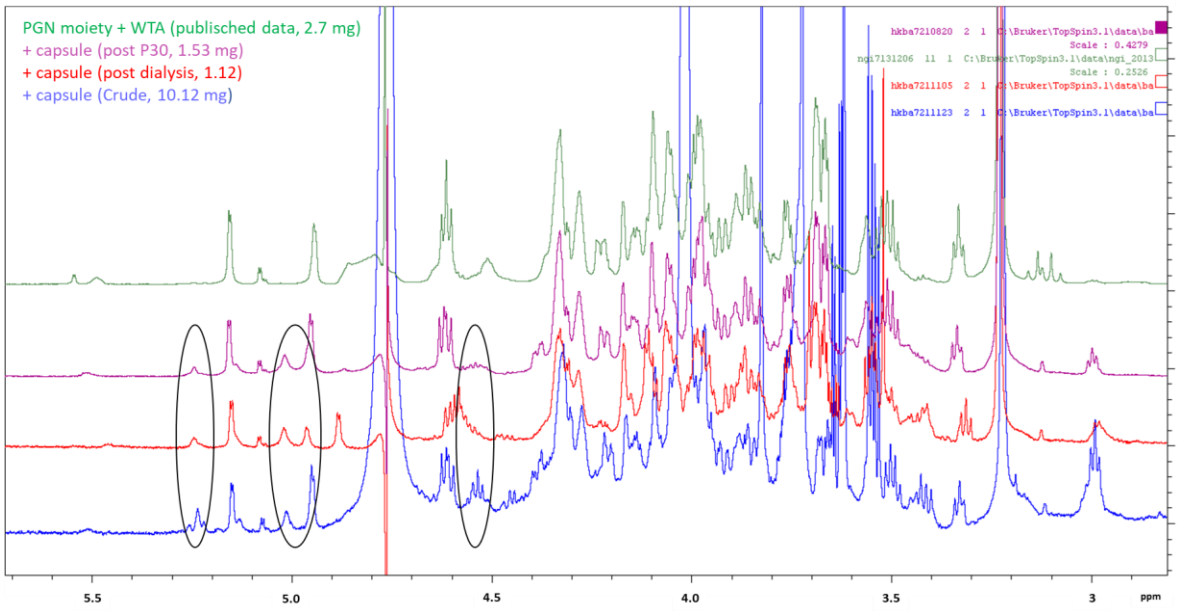

Figure 16: **^{1}H NMR spectra show WTA-PGN-CPS or WTA-PGN moieties following treatment with mutanolysin and lysozyme**. The color-coded spectra reveal key distinctions: violet spectra represent purified WTA-PGN-CPS moieties obtained via SEC, red spectra depict dialyzed WTA-PGN-CPS moieties, and blue spectra illustrate crude WTA-PGN-CPS moieties without purification steps. Green spectra, from published data of the group (36), serves as a comparison, representing WTA-PGN moieties post SEC. A black circle indicates the presence of an anomeric proton, which originates from the capsule and is not present in the WTA-PGN spectra.

To answer the question related to the nature of the linkage (a phosphodiester or a glycosidic bond) between the CPS and PGN, analysis by ^{31}P NMR has revealed peaks identical to those obtained in the WTA-PGN spectrum (-1 to -2 ppm, **Figure 17**, green). However, the presence of small peaks in this region in all conducted experiments on WTA-PGN-CPS (whether purified by SEC, dialysis, or used in its crude form) has complicated the conclusive determination of the attachment nature (**Figure 17**, violet, red, blue).

A) ^{31}P NMR spectra

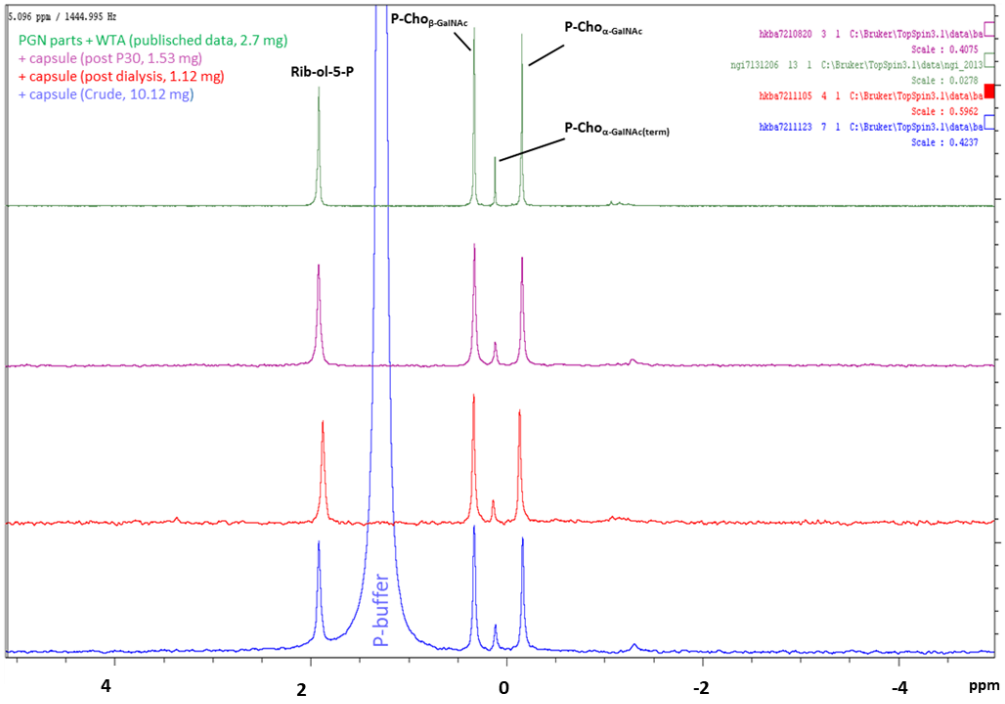

B) ^{31}P NMR spectra-zoom

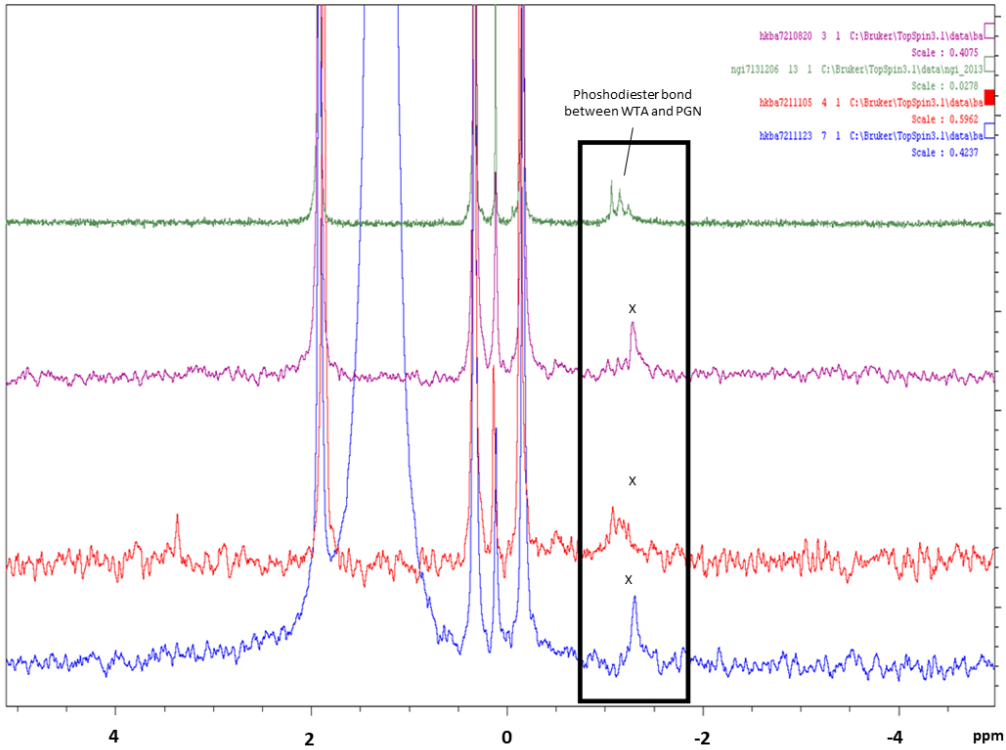

Figure 17: **^{31}P NMR spectra reveal the presence of WTA-PGN-CPS or WTA-PGN moieties after treatment with mutanolysin and lysozyme**. In A, the ^{31}P NMR spectrum is presented, including assignments of the main signals originating from pnWTA. B shows the same spectrum as panel A but with an adjusted Y intensity scale. The black box (-1 to -2 ppm) highlights attachment-specific peaks. The attachment between WTA and PGN (green) is identified as a phosphodiester bond based on prior research (30). However, the attachment between CPS and PGN (marked as "x") was challenging to interpret due to its low intensity and co-elution of both polymers at SEC. For more details about color-coded samples, please refer to the description in figure 16.

The presence of pnWTA and CPS peaks in same spectrum is also challenging for data interpretation in 2D-NMR. So, to facilitate the separation between WTA-PGN and CPS-PGN using SEC, the collected pool 1 (**Figure 15**) was subjected to alkaline hydrolysis. This treatment has previously shown that it cleaves the glycosidic bond between glucose and ribitol in the WTA backbone, resulting in the formation of two fragmented molecules. One of these molecules contained AATGal with Glc, while the second one consisted of Rib with two GalNAc units. Following the alkaline treatment, the resulting substance was loaded onto a SEC column (P10) to separate resulted-TA saccharides from CPS-PGN complex (**Figure 18**). However, the resulting amounts of all pools were very low, which made the measurement and interpretation using NMR to reveal the nature of CPS attachment not possible. Moreover, HR-MS was not suitable for adequately addressing the type of question at hand. It should be mentioned that the starting material weighed 156 mg, but the final product amounted to a mere 600 µg (pool 1, **Figure 18**), highlighting a substantial loss throughout this procedure.

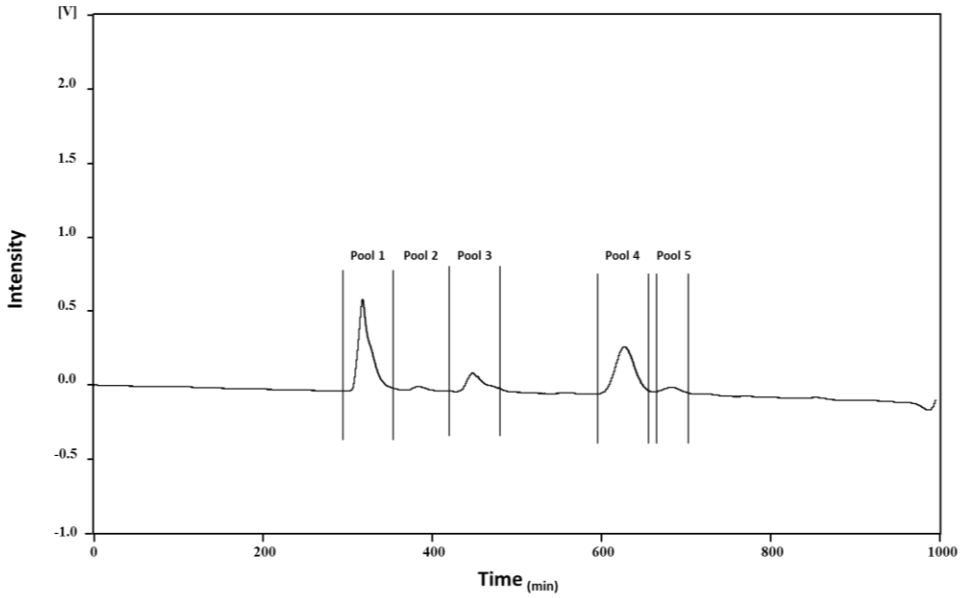

Figure 18: Size exclusion chromatography (P10 column) was employed to isolate PNG-CPS from PNG-WTA moieties post alkaline treatment. Pools were collected, weighed, and subsequently analyzed by NMR for pool 1 and MS for pools 2 and 3.

Despite extensive efforts, a conclusive determination of the attachment nature remained unsolved in this thesis. Additional investigations and refined analytical approaches are needed to tackle the complexities presented by the coexistence of CPS and PGN-WTA sugars in the NMR spectra. One potential solution involves using anion exchange chromatography to enrich the purified pool with negatively charged CPS in order to make elucidation process possible, as previously proposed[82]. However, adjustments to the protocol are needed to effectively explore the attachment between CPS and PGN.

Another possible path related to this question is the construction of a *cps2C or cps2D* mutant. The *cps* locus in *Spn* serotype 2 is represented by Cps2A, Cps2B, Cps2C and Cps2D. Cps2C or Cps2D are known to be part of a phosphoregulatory system involved in regulating the capsule production. Previous study found that deleting *cps2C* or *cps2D* resulted in the production of only short chain polymers, as determined by immunoanalysis[83]. Based on these data, construction of such a single mutant could potentially facilitate the interpretation of the NMR spectrum. The premise being that the large size of the CPS might be suppressing the linkage bond peak in the case of a full-length CPS chain.

Unfortunately, despite the efforts of colleagues at Greifswald University to construct this mutant, technical challenges associated with gene construction hindered its successful acquisition during the timeframe of this thesis.

2.2.3 Conclusion and outlook

While this study presented an experimental approach to determine the CPS-PGN attachment in *Spn*, final answers remain elusive. Further investigations are needed in this area. Potential methods might include incorporating anion exchange chromatography and exploring the *cps2D* mutant approach to delve deeper into these intricate structures. Both approaches, whether utilizing anion exchange or specific mutations, aim to yield highly purified CPS-PGN pneumococcal material. This purified material will be helpful in identifying the nature of the bond and the key factors behind the linkage.

2.3 Analysis of *Streptococcus pneumoniae* lipidome

2.3.1 Importance of the study

Many studies on the virulence of streptococci have mostly focused on pathogenic factors such as secreted proteins, surface polymers, adhesins, and mechanisms for sensing the extracellular environment[84]. However, there is still a lack of knowledge related to the lipid composition in the cellular membrane, even for the one of most extensively studied pathogens with critical risks for human health.

Earlier studies mainly used techniques like thin-layer chromatography to analyze extracted membrane lipids[45,43]. However, this method lacked the molecular specificity and sensitivity required for identification at molecular lipid level. GPs like PA, PC, PG and CL, along with GLs like GlcDAG, GalGlcDAG and DAG have been identified in the investigated streptococcal species[85]. A recent study combined normal phase chromatography with MS to describe the lipidome profile in *S. pneumoniae*. It also showed detection of the zwitterionic phospholipid PC occurred when cultured in media supplemented with human serum or yeast extract[45].

The here presented work explores the connection between some important genes and how they impact the lipidome. The lipid composition of the pneumococcal membrane in targeted strains as well as in the wild-type strain have been investigated and compared. The examined strains are: 1) Δ*tacL*: TacL is responsible for the attachment of the polymeric teichoic acid chain on the glycolipid anchor; 2) Δ*lgt*: Lgt catalyzes the diacylation of preprolipoproteins via a thioester bond by transferring a diacylglycerol moiety from a PG precursor; 3) Δ*cps*: the enzymes of the *cps* cluster are responsible for capsule polysaccharide formation.

2.3.2 Shotgun lipidomics

2.3.2.1 Optimizing sample preparation for lipidomics of pneumococci

The success of a lipidomics study relies on proper sample collection and processing. Inappropriate sampling and pre-analytical conditions can alter lipid concentrations due to enzymatic degradation or oxidation[59]. Since existing *Spn*-lipidome studies are qualitative[85], this thesis aimed to optimize sampling and pre-analytics to minimize sample variability and batch effects, enabling high-confidence quantitative data.

To guarantee reproducible results, all samples underwent the preparation process outlined in **Figure 19**. Briefly, bacteria were grown in full media to avoid stress or starvation that could impact the lipidome. Culture aliquots were carefully dispensed into identical tubes to minimize variability and butylated hydroxytoluene (BHT) was added to prevent oxidation during lipid extraction. Samples were immediately processed, and extracted lipids were stored at –80 °C until analysis. Detailed descriptions of the sampling

strategy, lipid extraction, and MS acquisition methods are provided in section 4.6.1, 4.6.2 and 4.6.3, respectively.

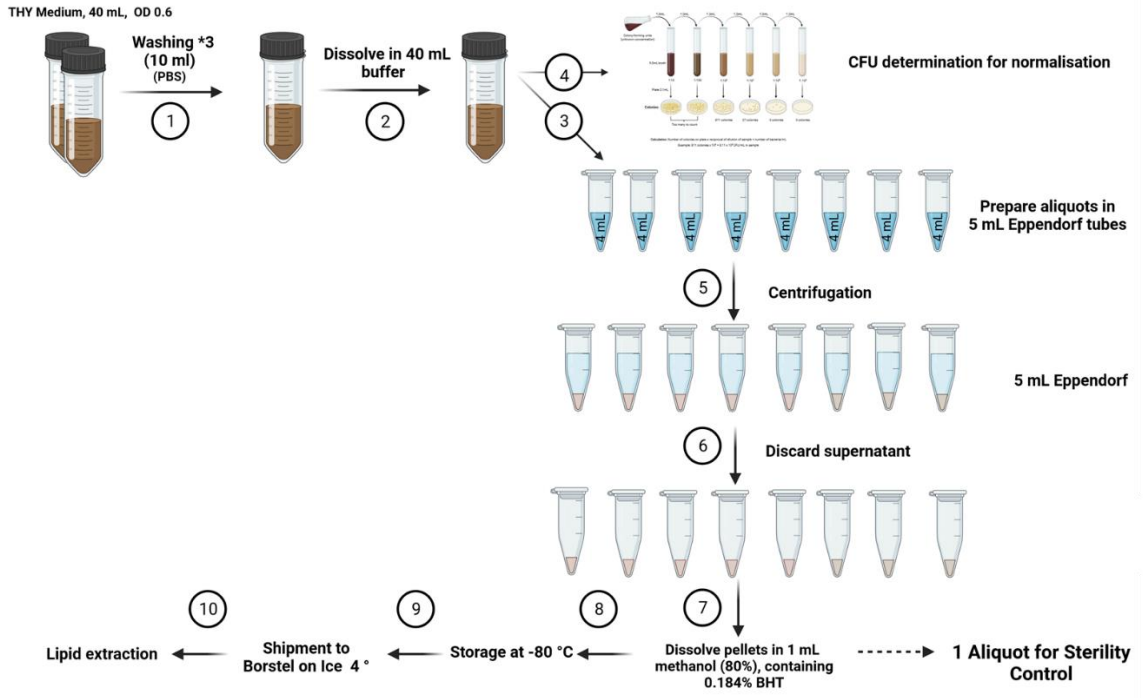

Figure 19: **Scheme of sampling strategy for *Spn* lipidomics investigation**. The figure was made using BioRender.com

2.3.2.2 Development of a customized pneumococcal internal standard

Conducting a pre-screening investigation in lipidomics studies is crucial for accurately describing the lipidome of any biological system. This investigation is particularly important in quantitative studies because it helps to select an appropriate internal standard that closely matches the endogenous lipidome's quantity. In this study, a pre-screening test was performed on both the Wt and targeted mutant strains using an in-house modified internal Splash standard, commonly used for plasma lipidome analysis. The internal Splash standard comprises 14 deuterated lipid species from Avanti, along with 5 in-house spiked deuterated lipid species with varying ratios (**Table 9**).

20 µL of the in-house modified internal Splash standard were added to each sample, followed by lipid extraction. Lipid extracts were injected and ionized using chip-based electrospray ionization in both positive and negative modes, and the resulting mass spectra were used for identification with LipidXplorer software. For quantification, each lipid's quantity is determined based on the corresponding lipid species of deuterated internal standard within the same lipid class.

It's worth noting that the modified internal standard does not include lipid species from the GlcDAG or GalGlcDAG classes, previously reported in *Spn*. Therefore, in this pre-

screening study, these two lipid classes were quantified based on the concentration of the deuterated PG (15:0-18:1(d7)), which is initially used for PG content estimation.
According to the findings from the initial screening study (**Figure 20**) and as expected, the *Spn* lipidome consists of GLs and GPs. DAG and CL were identified as the most abundant lipid classes, accounting for approximately 43% to 34% of the entire lipidome, respectively. Additionally, PG, PA, PC, GlcDAG, and GalGlcDAG were found to be present in a similar range (between 3% to 8%) in the total lipidome. Moreover, only a very small quantity of TAG (<2%) was detected, not only in the wild type but also in other studied strains.

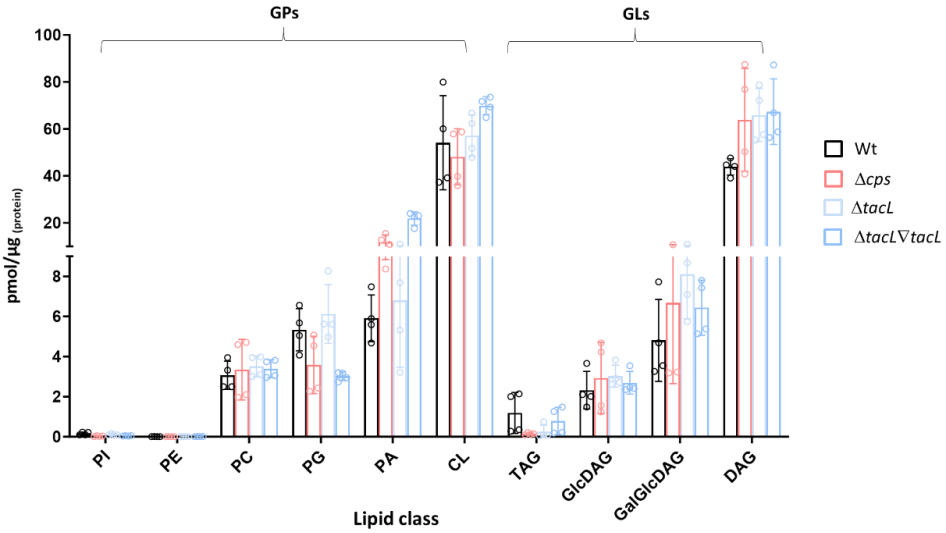

Figure 20*:* **Pneumococcal lipid profiling derived from pre-screening test.** GPs: Glycerophospholipid, GLs: Glycerolipid. Error bars represent standard deviation. The pre-screening investigation was carried out on two biological replicates.

Based on the pre-screening investigations, a customized internal standard (*Spn* IS) was developed to mirror the real pneumococcal lipidome. This *Spn* IS includes carefully selected lipid species, strategically chosen to quantify the detected endogenous lipid classes. Incorporating at least one lipid species tailored for quantifying each lipid class is common for high-quality lipidome quantitative datasets. The concentrations of utilized lipid species were determined to mimic their quantity in **Figure 20**. So based on that, CL and DAG have been used with the highest number of equivalents, followed by PC, PG, PA, PI, PE, MAG, and GalDAG, while TAG held the lowest number of equivalents among the lipid species in the final *Spn* IS. All used lipid species are deuterated except for GalDAG 18:3. This particular lipid was chosen based on recent study which found that having one fatty acid chain with 3 double bonds in *Spn* is uncommon[85]. In the *Spn* IS spectrum, certain peaks (**Figure S1**, marked as "x") were observed, which are artifacts originating from detergents and plasticizers, as often reported in lipidomics studies[86]. **Table 1** summarizes the lipid species used in the customized *Spn* IS, providing information about their use in direct MS infusion, detection mode, adducts, theoretical mass and observed mass.

Table 1: Customized pneumococcal internal standard mix (*Spn* IS) employed for lipidome quantification.

Lipid species	Chemical formula	Adduct	Monoisotopic mass	Number of equivalents	pmol in 20 µl
15:0-18:1-d7-TAG	$C_{51}H_{49}D_7O_6$	$[M+NH_4]^+$	829.799	0.1	12.31
15:0-18:1-d7-PC	$C_{41}H_{73}D_7NO_8P$	$[M+H]^+$	753.613	0.2	25.29
15:0-18:1-d7-PG	$C_{39}H_{67}D_7NaO_{10}P$	$[M-H]^-$	740.546	0.2	26.17
15:1-18:1-d7-PA	$C_{36}H_{61}D_7NaO_8P$	$[M-H]^-$	666.509	0.2	26.35
15:0-18:1-d7-PI	$C_{42}H_{75}D_7NO_{13}P$	$[M-H]^-$	828.562	0.2	24.85
15:0-18:1-d7-PE	$C_{38}H_{67}D_7NO_8P$	$[M-H]^-$	709.552	0.2	26.78
18:1-d7 MAG	$C_{21}H_{33}D_7O_4$	$[M+NH_4]^+$	381.371	0.2	26.19
18:3 GalDAG	$C_{45}H_{74}O_{10}$	$[M+CH_3COO]^-$	833.542	0.4	49.15
15:0-18:1-d7 DAG	$C_{36}H_{61}D_7O_5$	$[M+NH_4]^+$	605.583	1	120.05
18:2/18:2-18:2/18:2-d5-CL	$C_{81}H_{143}D_5N_2O_{17}P_2$	$[M-2H]^{2-}$	725.508	1	122.10

2.3.2.3 Pneumococcal lipidome annotation

Once the components and required quantities of the *Spn* IS were decided, pneumococcal cell samples spiked with customized *Spn* IS have been subjected to MTBE extraction (section 4.6.2) and analyzed by MS (section 4.6.3) to determine the accurate lipid composition.

Lipid identification was carried out using the LipidXplorer software, effectively aiding the structural characterization and identification of numerous lipid species within the studied strains. The identified lipid classes in *Spn* are PC, CL, PG, DAG, GlcDAG and GalGlcDAG. The generated MFQL queries for lipid identification primarily relied on the MS^1 (precursor level) as well as on MS^2 level (molecular level) for most lipid classes, except for CL and lysolipids. Additional details regarding the lipid annotation mechanisms and the used MFQL scripts are outlined in section 1.2.4.4 and 4.6.9, respectively.

Figure 21 provides further insights into the potential fragmentation pattern (MS^2) of the most abundant lipids in the wild type. GLs like DAG species generate $[M+NH_4]^+$ ions that fragment to lose a hydroxy group and ammonia (*m*/*z* 579, **Figure 21 A**). Abundant fragments indicating fatty acid loss and ammonia (*m*/*z* 341 and 313) are observed. Acetate adducts of GlcDAG and GalGlcDAG exhibit simpler patterns in negative mode, each with two prominent fatty acid loss fragments (**Figure 21 C** and **E**). A very low-abundance ion corresponding to [GalGlc-H_2O] was also observed. Therefore, the sugar moieties for GlcDAG and GalGlcDAG were additionally used as a third identifying fragment in the MFQL script, improving confidence in GLs identification.

GPs like PG readily ionize as $[M-H]^-$ ions, generating informative fragmentation patterns dominated by prominent fatty acid carboxylate ions (**Figure 21 B**). CL species, on the other hand, form doubly charged ions in negative mode, fragmenting primarily into fatty acid ions (**Figure 21 D**). The pneumococcal PC produces abundant $[M+H]^+$ ions upon positive mode analysis, fragmenting to yield a prominent phosphocholine ion at *m*/*z* 184 (**Figure 21 F**). The structurally informative fragment ions corresponding to the FA chain are in low abundance. Although high-resolution mass spectrometry played a paramount role in precise determination, the exact molecular assignment of a significant number of peaks (e.g., DAG) remains ambiguous.

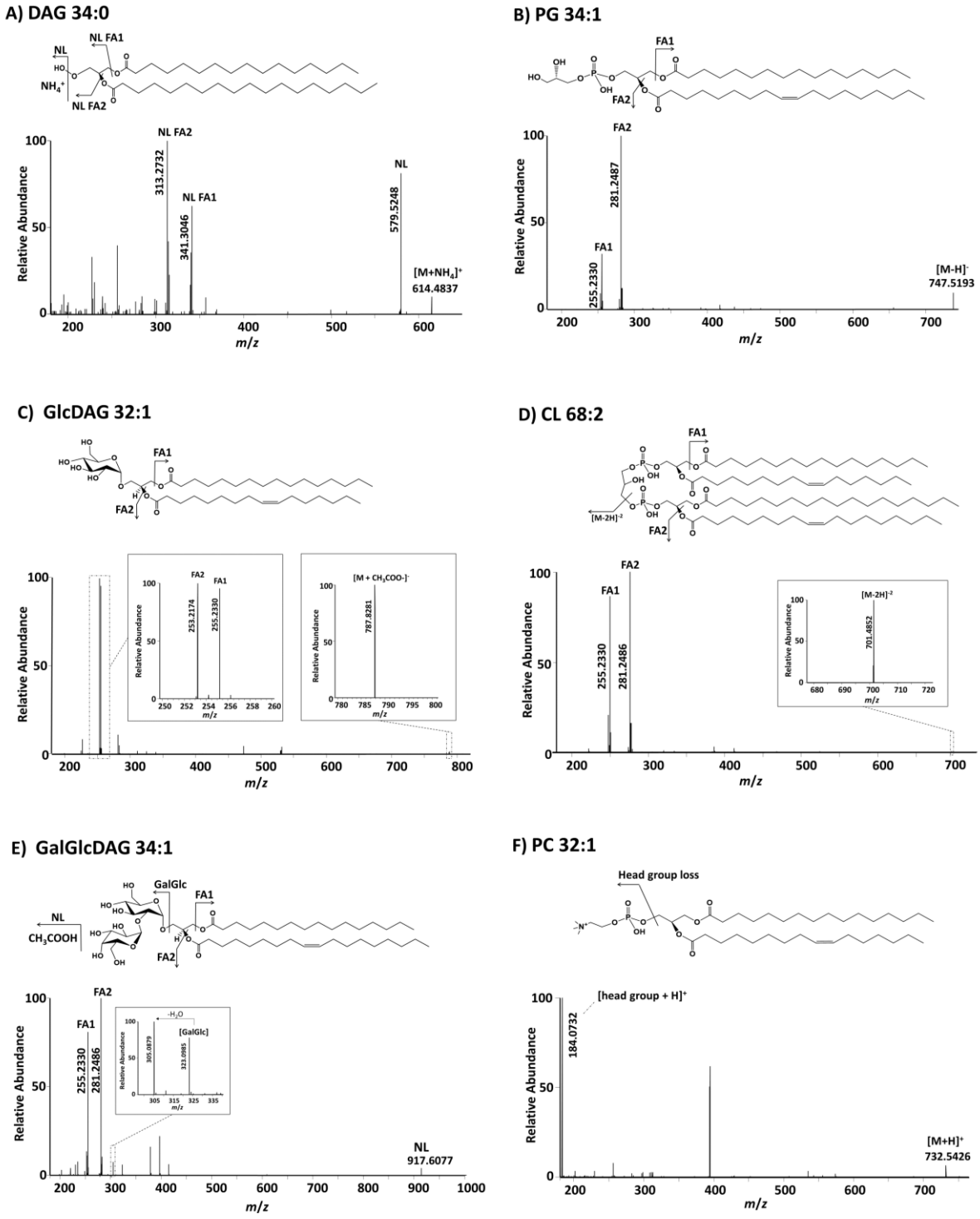

Figure 21: **Molecular structural analysis of pneumococcal lipids at the precursor and fragment leve**l.
The different panels show exemplary MS^2 spectra that are used for structural identification of the different lipid species by customized MFQL search files, using the fully automated search engine LipidXplorer. Potential fragmentation mechanisms are shown above each panel. Annotated fragments are indicated in the chemical structure of distinct species, with an asterisk (*) representing the fragment without an adduct. Exact fatty acid positions are not known and might be interchanged.

2.3.2.4 Quantification of pneumococcal lipidome

Accurate quantifying of the pneumococcal lipidome needs not only suitable internal standards, but also a consistent maintenance of the sample preparation condition and bacterial count (**Table 8**). The overlapping issue of fatty acids originating from different lipid classes poses a significant challenge for precise quantification. To reduce this potential error, quantification was performed based on precursor ion values at the MS^1 level.

The lipidome identified through LipidXplorer was subjected to processing using LxPostman, a R shiny application developed in the group[73]. This automatic tool streamlines data cleaning, calculations and provides the ability to subtract background signals from the target analyte to exclude biases introduced during the extraction process. The used settings are described in section 4.6.4. Following LxPostman processing, a methodically unified strategy was operated for data clean-up and management. In the beginning, the lipidome data for every investigated strain were organized, and the averages of technical replicates were calculated, considering 2 aliquots per batch. Subsequently, a filtering criterion was manually applied to retain only those lipid species that were consistently present in a significant majority (50%) of the dataset, thereby enhancing the data's reliability. As a result of this filtering process, the number of remaining lipid species in the wild type and non-encapsulated strain was 141 species.

The number of remaining lipid species was comparatively lower in the Δ*tacL*, Δ*tacL*∇*tacL* and Δ*lgt* mutant strains. Notably, it should be mentioned that lysolipids constitute a minor component among the lipid species. Thus, the count of these particular lipid species displayed considerable variation among the strains under investigation (**Figure 22**).

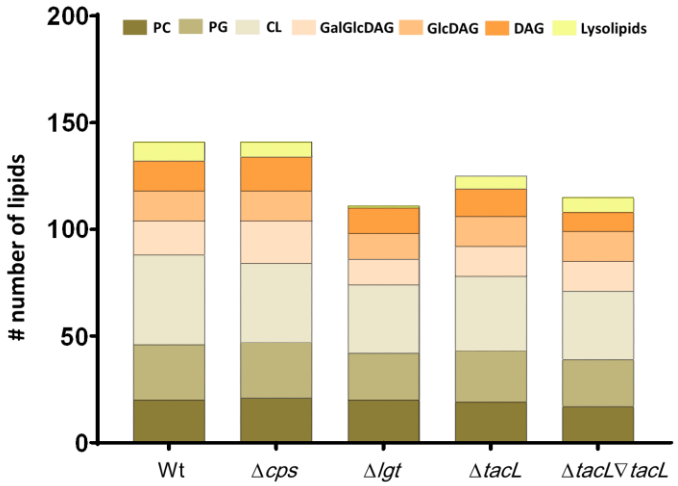

Figure 22: Comparison of the number of detected lipid species after filtering among studied pneumococcal strains. In the Wt and Δ*cps* strains, 141 lipid species were reported, while in Δ*tacL*, Δ*tacL*∇*tacL* and Δ*lgt* strains, 125, 115, and 111 lipid species were observed, respectively.

To ensure precise quantification in *Spn* as well as in any biological system, the concentrations of the filtered lipids under investigation were normalized based on the

protein content. By summing up the concentrations of the filtered normalized lipid species within each lipid family, it was demonstrated that the composition of the pneumococcal membrane in the wild-type strain is comprised of GLs (71%) and GPs (29%). In terms of dominant lipid classes, the order is as follows: GlcDAG (29%), GalGlcDAG (26%), PG (21%), DAG (17%), CL (6%), and PC (2%) (**Figure 23 A**). This distinctive distribution pattern of predominant lipid classes, quantified for the first time in *Spn*, was previously only described qualitatively[44]. As shown in **Figure 23 B**, 15 lipid species have demonstrated their collective contribution of over 60% to the entire lipidome, with nearly all of them belonging to the GLs family. This observation has been thoroughly validated across six distinct biological replicates employed in the study, all consistently highlighting the presence of the same reported lipids within the wild-type strain.

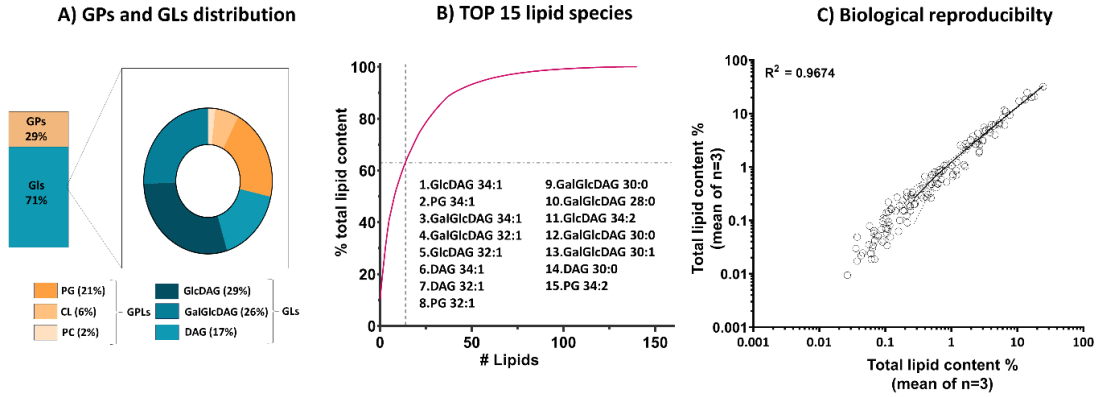

Figure 23*:* **Exploring the lipidome in pneumococcal wild-type strain D39. A**: A pie chart illustrating the distribution of detected lipid classes with their respective percentages in the entire lipidome. **B:** Cumulative lipid abundance, where fifteen lipid species constitute over 60% of the total lipid content. panel **C:** linear regression demonstrating biological reproducibility with data obtained from six biological replicates.

Another essential aspect to consider in lipidomics studies is the reproducibility of reported lipid species concentrations across diverse biological replicates. A strong linear correlation (R^2 = 0.967) between biological replicates in the wild-type strain (**Figure 23 C**) demonstrates this reproducibility, validating the reported concentration values. A similar pattern has also been observed among all other studied strains (**Figure 24**).

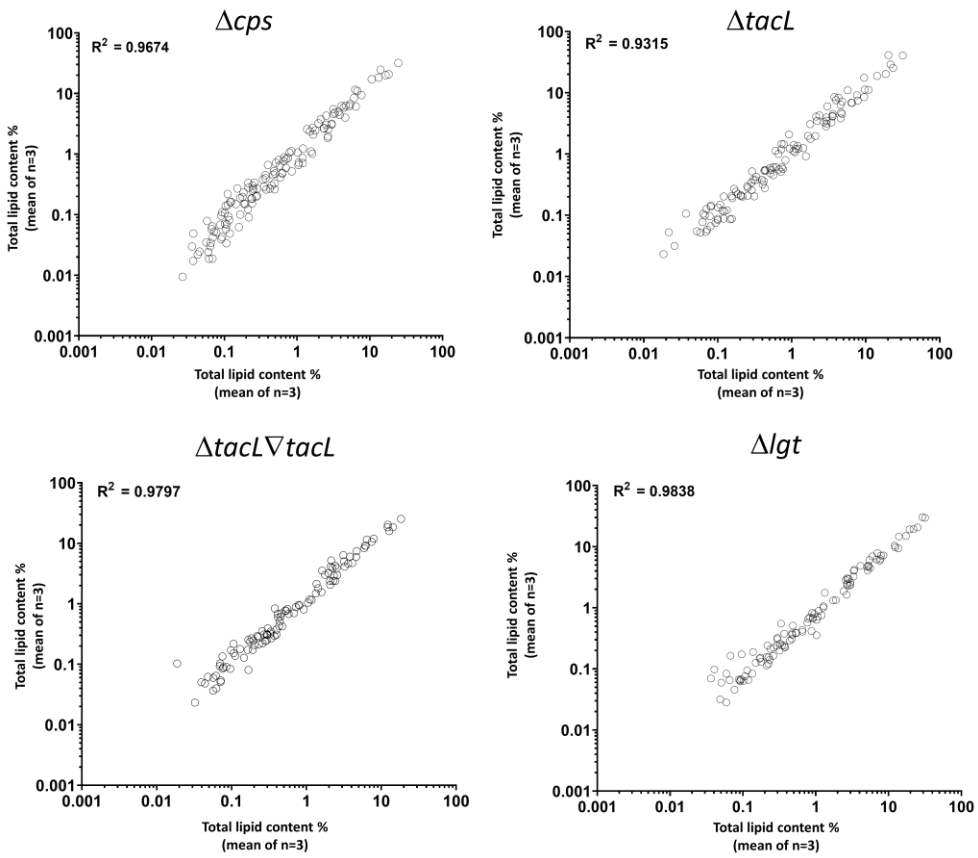

Figure 24: **Biological reproducibility of the lipidomics screen for *Spn* D39 Δ*cps*, Δ*tacL*, Δ*tacL*∇*tacL*, and Δ*lgt***. The graphs display a linear correlation of lipidome data derived from the mean of six independent biological replicates taken from the studied bacterial sample. The R2 values are indicated in the panels.

Regarding the gene knockout effect on lipids compositions, a notable deviation has been identified at the lipid class level. This difference primarily manifests within the GLs category and is particularly evident when comparing the Δ*cps* samples to the Wt. By contrast, the deletion of the *tacL* and *lgt* genes displayed no obvious impact on the lipid composition of the pneumococcal membrane, despite their contribution on membrane structure or components. These outcomes remained consistent whether the data was normalized by protein content or molar percentage (**Figure 25 A**).

This study has also confirmed the detection of PC lipid when *Spn* is cultivated in a complete medium supplemented with yeast extract. This interesting finding has previously been extensively examined[84]. Previous study concluded that *Spn* possess the capability to scavenge both fatty acids and head groups, in contrast to staphylococci and enterococci, which exclusively scavenge host fatty acids[85]. Further investigation is needed in this area to understand the effects of incorporating host-derived fatty acids and lipid classes into the pneumococcal membrane. Additionally, the majority of lipid classes exhibited a considerable dynamic range spanning more than two orders of magnitude (**Figure 25 B**).

As demonstrated in **Figure 22**, over 100 lipid species were identified across all studied strains. The detailed quantities of these lipid species in each strain, compared to the wild type, are provided in the supplementary data (**Figure S1 to S9**). Examining the top 15 lipid species among the studied mutants revealed a dissimilarity in their ranking compared to the Wt. As in the Wt, most of these species originated from the GLs family (**Figure 25 C**).

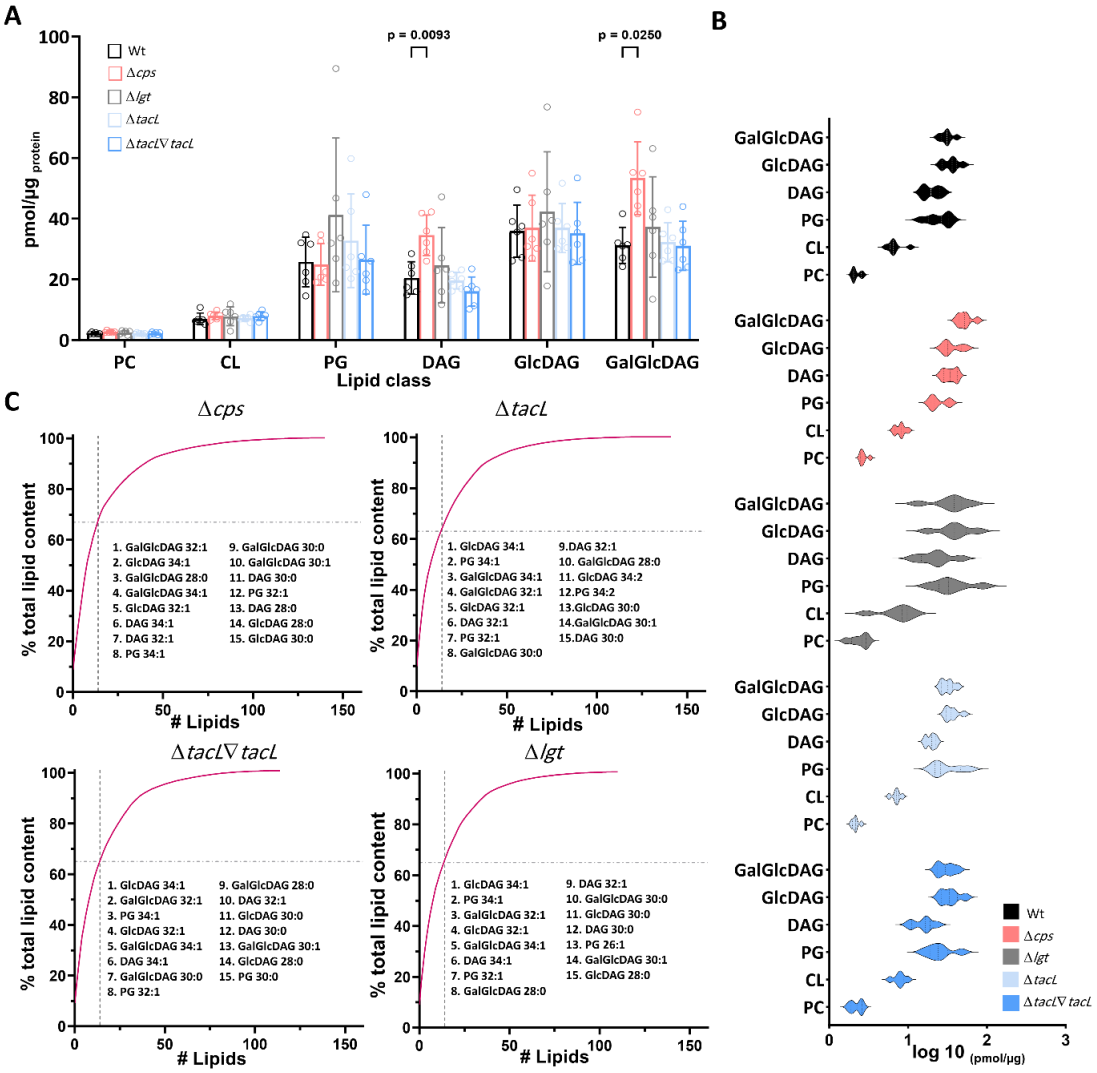

Figure 25: Quantitative lipidomics analysis of *S. pneumonaie*. A: Illustrates the relative distribution of major lipid classes in the wild type and the examined mutants, stated in pmol/µg protein. Statistical analysis was performed using a two-way ANOVA test, followed by a false discovery rate correction at 5%. All data points represent the means of six biological replicates, error bars represent standard deviation. **B:** Presents a box plot depicting the dynamic range of the pneumococcal lipidome under the investigated conditions. This analysis encompasses two lipid families (GLs, GPs) across six lipid classes and includes 141 lipid species for the Wt and Δ*cps* samples, 125 for Δ*tacL* and 115 for its complemented strain. For Δ*lgt*, 111 lipid species were involved within these categories. **C:** Demonstrates the cumulative lipid abundance, revealing that the top fifteen specific lipid species account for over 60% of the total lipid content in the studied strains.

The change in GLs levels between Wt and Δ*cps* was the reason for conducting a more in-depth investigation of these two strains. Clustering analysis emerges as a widely used statistical technique to identify patterns among lipid species. In this study and prior to data clustering, more targeted filtering steps were applied to the Wt and Δ*cps* datasets, where a threshold of 90% occupation was applied. Any data that did not meet the mentioned criteria were excluded. As a result, the total number of lipid species was reduced from 141 to 101, representing the common lipid species shared between the two groups. Importantly, the evaluation of the proportion of these 40 excluded species in comparison to the entire lipidome revealed that they constituted just 1% of the whole. These careful data cleaning measures were crucial in enhancing the reliability and confidence in the reported lipidome.

The application of a clustering approach to the six biological replicates has revealed distinct alterations in lipid species expression upon capsule knockout. As shown in **Figure 26 A**, saturated and monounsaturated lipid species appear to be up-regulated or more prominently featured, whereas polyunsaturated lipid species are noticeably less dominant. This pattern suggests that the elimination of the capsule may expose the membrane to a high extent to environmental conditions, potentially affecting its saturation state. Such changes have been linked to alterations in the biophysical properties in *Listeria monocytogenes*. Specifically, the accumulation of straight-chain saturated fatty acids leads to tightly packed bilayers, resulting in a higher phase transition temperature and lower permeability[3]. This might suggest that the *Spn* also potentially regulates its membrane fluidity and permeability as a response to environmental change. Furthermore, a clear observation is the clustering of lipid species within each group, which could further enhance the confidence of this finding. Thus, the clustering analysis underscores the similarity between distinct biological replicates cultivated at different time points, adding another layer of certainty to the study.

To value the extent of the observed difference, a series of multiple unpaired t-tests followed by a false discovery rate (FDR) of 5% was conducted. This approach enabled the identification of lipidome alterations that are particularly significant in non-encapsulated samples and pass the established threshold (p-value of 0.05). Meanwhile, for the horizontal axis, threshold values of ±0.5 for fold changes were adopted, an accepted criterion for characterizing metabolic shifts within biological systems[87] (**Figure 26 B**). Most of the lipids with higher levels in the non-capsulated samples belong to the GLs group, such as GalGlcDAG, GlcDAG, and DAG. **Figure 26 C** shows alterations in GLs and GPs in comparison to the wild-type.

In conclusion, the knockout of the capsule has certainly resulted in a shift in the membrane lipid composition when compared to the wild type. This alteration primarily shows changes in the saturation state, with the non-capsulated strain exhibiting elevated levels of saturated or mono-unsaturated species, particularly evident in glycerolipid species.

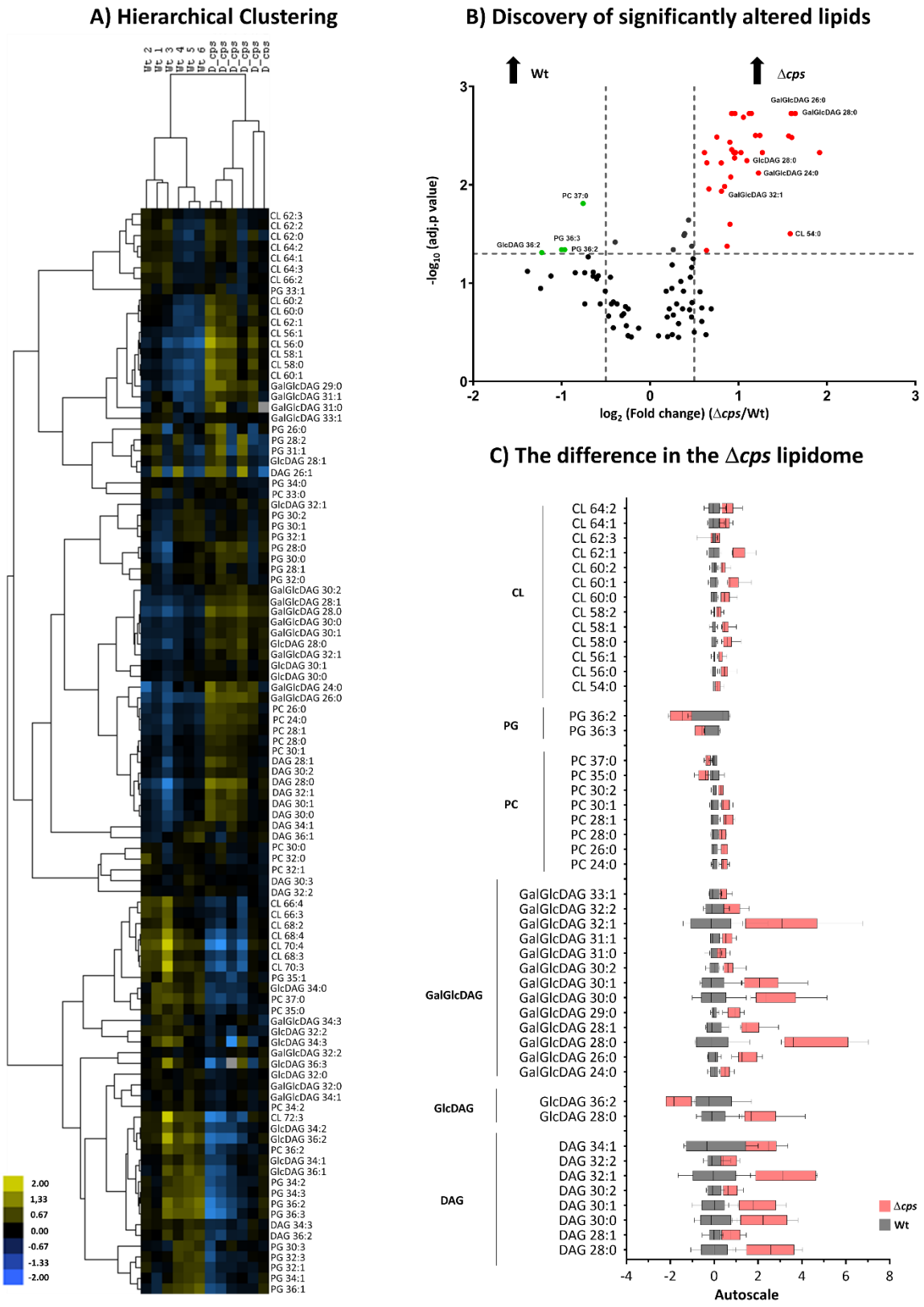
A) Hierarchical Clustering
wt 2
wt 1
wt 3
wt 4
wt 5
wt 6
Δ_cps
Δ_cps
Δ_cps
Δ_cps
Δ_cps
Δ_cps
CL 62:3
CL 62:2
CL 62:0
CL 64:2
CL 64:1
CL 64:3
CL 66:2
PG 33:1
CL 60:2
CL 60:0
CL 62:1
CL 56:1
CL 56:0
CL 58:1
CL 58:0
CL 60:1
GalGlcDAG 29:0
GalGlcDAG 31:1
GalGlcDAG 31:0
GalGlcDAG 33:1
PG 26:0
PG 28:2
PG 31:1
GlcDAG 28:1
DAG 26:1
PG 34:0
PC 33:0
GlcDAG 32:1
PG 30:2
PG 30:1
PG 32:1
PG 28:0
PG 30:0
PG 28:1
PG 32:0
GalGlcDAG 30:2
GalGlcDAG 28:1
GalGlcDAG 28.0
GalGlcDAG 30:0
GalGlcDAG 30:1
GlcDAG 28:0
GalGlcDAG 32:1
GlcDAG 30:1
GlcDAG 30:0
GalGlcDAG 24:0
GalGlcDAG 26:0
PC 26:0
PC 24:0
PC 28:1
PC 28:0
PC 30:1
DAG 28:1
DAG 30:2
DAG 28:0
DAG 32:1
DAG 30:1
DAG 30:0
DAG 34:1
DAG 36:1
PC 30:0
PC 32:0
PC 32:1
DAG 30:3
DAG 32:2
CL 66:4
CL 66:3
CL 68:2
CL 68:4
CL 70:4
CL 68:3
CL 70:3
PG 35:1
GlcDAG 34:0
PC 37:0
PC 35:0
GalGlcDAG 34:3
GlcDAG 32:2
GlcDAG 34:3
GalGlcDAG 32:2
GlcDAG 36:3
GlcDAG 32:0
GalGlcDAG 32:0
GalGlcDAG 34:1
PC 34:2
CL 72:3
GlcDAG 34:2
GlcDAG 36:2
PC 36:2
GlcDAG 34:1
GlcDAG 36:1
PG 34:2
PG 34:3
PG 36:2
PG 36:3
DAG 34:3
DAG 36:2
PG 30:3
PG 32:3
PG 32:1
PG 34:1
PG 36:1
2.00
1,33
0.67
0.00
-0.67
-1.33
-2.00
B) Discovery of significantly altered lipids
Wt
Δcps
GalGlcDAG 26:0
GalGlcDAG 28:0
GlcDAG 28:0
GalGlcDAG 24:0
GalGlcDAG 32:1
CL 54:0
PC 37:0
PG 36:3
PG 36:2
GlcDAG 38:2
-log10 (adj.p value)
log2 (Fold change) (Δcps/Wt)
C) The difference in the Δcps lipidome
CL
CL 64:2
CL 64:1
CL 62:3
CL 62:1
CL 60:2
CL 60:1
CL 60:0
CL 58:2
CL 58:1
CL 58:0
CL 56:1
CL 56:0
CL 54:0
PG
PG 36:2
PG 36:3
PC
PC 37:0
PC 35:0
PC 30:2
PC 30:1
PC 28:1
PC 28:0
PC 26:0
PC 24:0
GalGlcDAG
GalGlcDAG 33:1
GalGlcDAG 32:2
GalGlcDAG 32:1
GalGlcDAG 31:1
GalGlcDAG 31:0
GalGlcDAG 30:2
GalGlcDAG 30:1
GalGlcDAG 30:0
GalGlcDAG 29:0
GalGlcDAG 28:1
GalGlcDAG 28:0
GalGlcDAG 26:0
GalGlcDAG 24:0
GlcDAG
GlcDAG 36:2
GlcDAG 28:0
DAG
DAG 34:1
DAG 32:2
DAG 32:1
DAG 30:2
DAG 30:1
DAG 30:0
DAG 28:1
DAG 28:0
Δcps
Wt
Autoscale

Figure 26: Altered lipid composition in the non-encapsulated pneumococcal strain. **A**: A complete linkage of hierarchical clustering of 101 lipid species (after applying a 90% occupation threshold) identified in six biological replicates of both *Spn* D39 Wt and Δ*cps*. Each row represents one lipid species, and each column represents one biological replicate. **B**: A volcano plot combines fold change and multiple unpaired t-test results. The x-axis displays log2 (fold change, FC), while the y-axis represents -log10 (adjusted for false discovery rate). Colorful dots indicate features with fold changes larger than (+0.05 and-0.05) with p-values greater than 0.05. Red dots represent up-regulated lipid species in Δ*cps*, while green dots represent high dominant lipid species in Wt compared to Δ*cps*. **C**: Differences in the pneumococcal lipidome of Wt and Δ*cps* are visualized using autoscaling. Samples are color-coded: grey for Wt and pink for Δ*cps*. Boxplots display the median with the interquartile range, with whiskers showing the maximum and minimum points. Data are normalized based on protein content. Selected lipid species exhibited differences as determined by multiple unpaired t-tests.

2.3.2.5 Assessment of the method robustness

Analysing lipidomics data faces a significant challenge: the impact of uncertainty originating from diverse sources of variability (biological and technical variations), potentially affecting the interpretation of studied groups. Therefore, ensuring the reliability of results becomes a critical consideration. In this study, the coefficient of variation (CV%) for all lipid species within both Wt and Δ*cps* datasets has been computed and assessed. This assessment aimed to shed light on which lipid species exhibited the most significant variability across distinct biological replicates measured at different time points. **Figure 27** illustrates that in both Wt and Δ*cps* datasets, the CV% values can exceed 50%. However, it's clear that this large variation primarily is related to the less prevalent lipid species within both groups. Conversely, the main lipid species, constituting 98% in Wt and 96% in Δ*cps* of the entire lipidome, display low CV% values, typically below 50%. This observation supports confidence in the accuracy of the measurements. This finding aligns completely with the general analytical principle that there tends to be an inverse relationship between the amount of lipids present in a sample and the coefficient of variation[88].

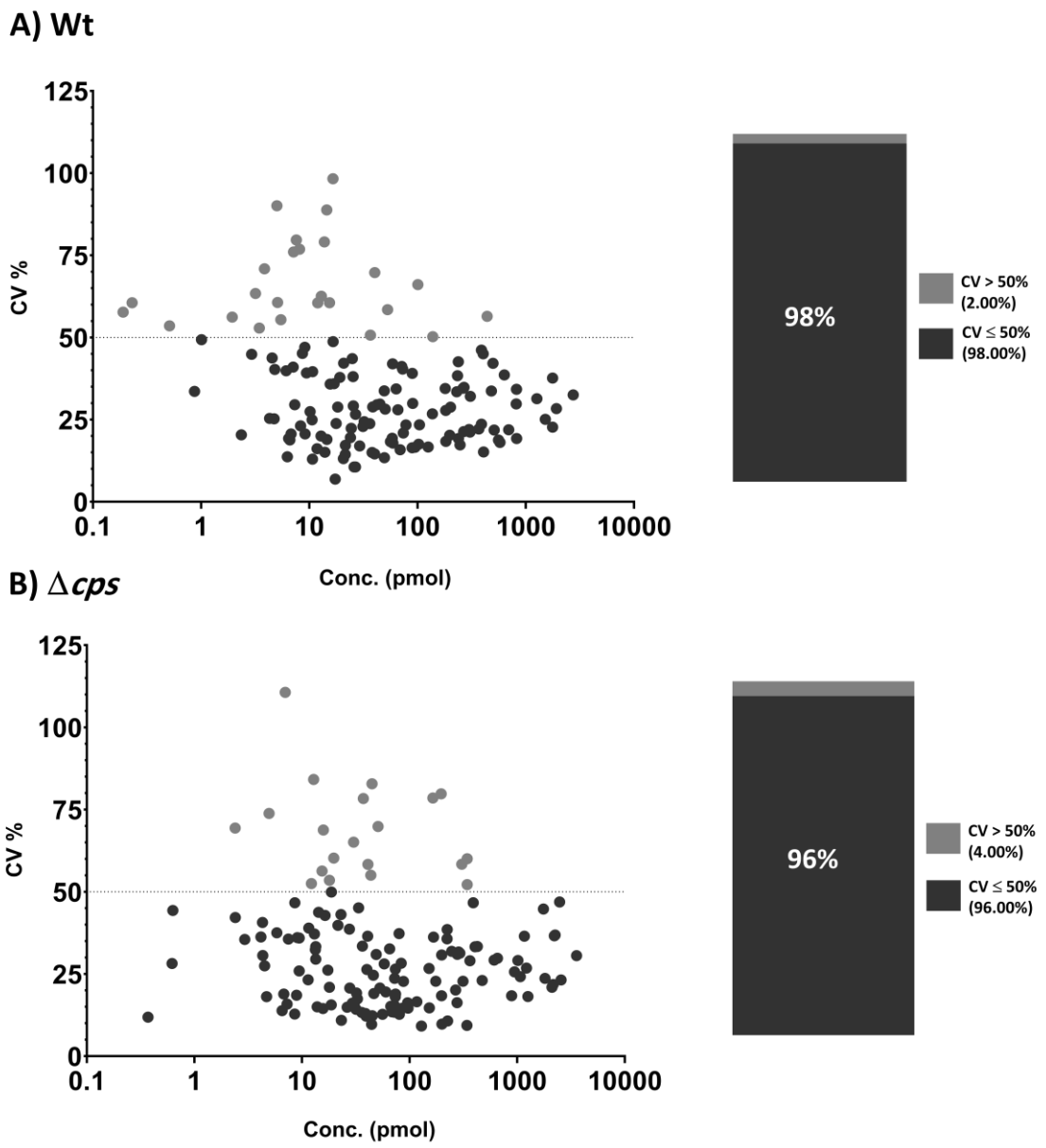

Figure 27: **The correlation between coefficients of variation and the average lipid concentrations was examined for 141 lipid species in both Wt (A) and Δ*cps* (B) datasets.** Dark points on the graph represent lipid species with low CV values, constituting more than 95% of the entire lipidome. In contrast, light points represent minor lipid species with high CV values, making up less than 5% of the entire lipidome.

2.3.3 Fatty acid analysis by GC-MS

One of the observations arising from performing shotgun lipidomics in *Spn* is that the majority of lipid species consisting of fatty acids possess even carbon numbers. To confirm that, fatty acids liberated from Wt, Δ*cps*, Δ*tacL*, Δ*tacL*∇*tacL,* and Δ*lgt* were subjected to analysis through conversion into fatty acid methyl esters (FAMEs) via saponification, methylation, and subsequent extraction. The resulted esterified fatty acids were then

subjected to analysis using GC-MS. The complete experimental details are described in section 4.6.7.

As illustrated in **Figure 28**, the semi-quantitative GC-MS analysis also reveals the prominent presence of even-numbered fatty acids within the studied *Spn* strains. Notably, myristic acid (C14:0), palmitic acid (C16:0), and oleic acid (C18:1) are the main detected fatty acids, with palmitic acid exhibiting the highest dominance, followed by oleic acid and myristic acid. Additionally, a trace amount of lauric acid (C12:0) has been observed within the examined strains. Regarding the degree of saturation, the fatty acids in *Spn* span a spectrum encompassing both saturated and monounsaturated fatty acids. It is important to note that this assay provides a relative measure of the *Spn* fatty acids and does not yield absolute quantities. For accurate quantification, individual calibration curves would have to be established for each fatty acid. This involves quantifying endogenous fatty acids based on the intensity and concentration of spiked deuterated fatty acids. The implementation of a semi-quantitative approach for fatty acid analysis was sufficient to verify the range of chain length and degree of saturation in *Spn*, which has been previously identified using the shotgun lipidomics method (section 2.3.2). Both methods have revealed the prevalence of even-numbered fatty acids across a range of saturation levels, including unsaturated, monounsaturated, and polyunsaturated species.

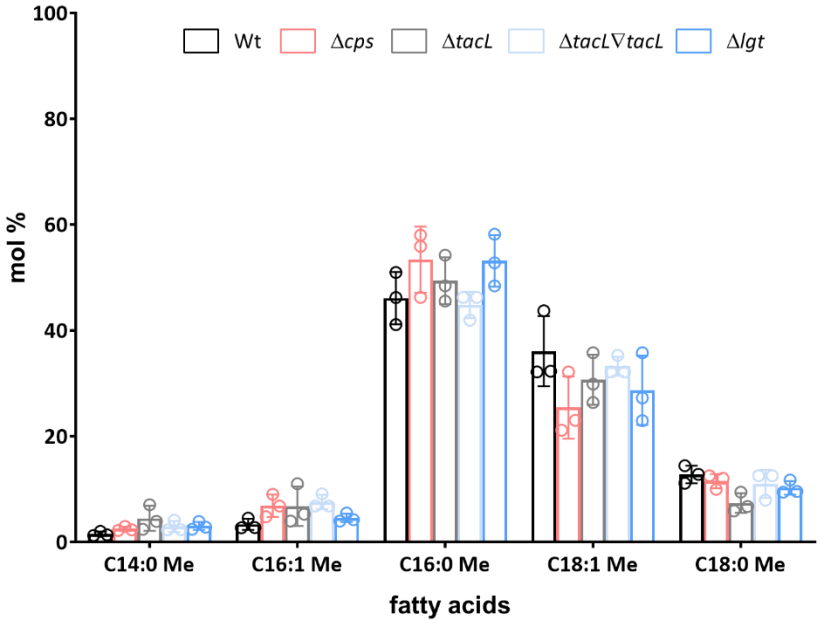

Figure 28: **Main pneumococcal fatty acids identified in the *Spn* D39 wild type and the isogenic mutant strains**. All data show the mean of six biological replicates, error bars represent standard deviation.

2.3.4 Thin layer chromatography coupled with mass spectrometry (Off-line TLC-MS)

A very common obstacle in shotgun lipidomics is the possible occurrence of overlaps among lipid species originating from distinct lipid classes. **Figure 29** illustrates the problem of overlap among the identified lipid species in the pneumococcal samples through the shotgun approach. Therefore, further check is necessary for methods that can avoid having this major challenge. One of the employed techniques is LC-MS, which has been demonstrated in various studies to improve lipid coverage and address the challenge of overlapping lipid species issue. However, this approach requires specialized equipment and expertise, which, particularly in the context of untargeted lipidomics screening, can introduce complexity to the overall setup.

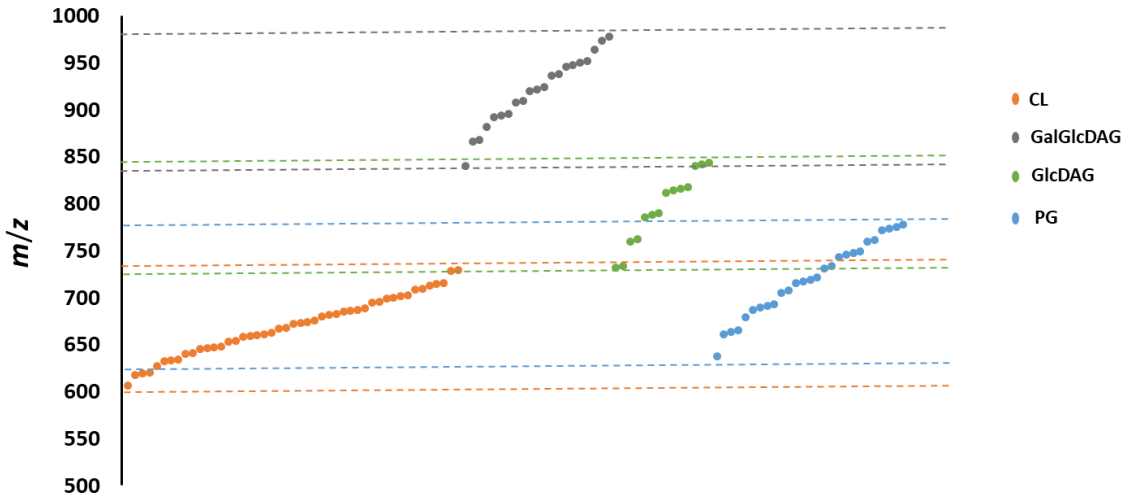

Figure 29: Overlapping phenomena among detected lipid species in the pneumococcal samples through the shotgun lipidomics.

In this study, the utilization of off-line TLC-MS was implemented to avoid the difficulties associated with the chromatography-MS setup and method development. In multiple studies, TLC-MS has been applied in lipidomics for the confident identification of various lipid classes[89,94,95]. A fundamental concern that arises when discussing lipid detection via TLC is the selection of a suitable dye that preserves the lipid structure without altering it. Moreover, ensuring the dye's compatibility with MS holds significant importance. Upon literature review, it has been determined that Coomassie staining, commonly used for protein identification, can also be employed for visualizing lipids. This staining method has demonstrated reliability and simplicity, particularly for phospholipids, without disrupting lipid chemical structure[90].

Pneumococcal lipids were extracted from dried cultures using the MTBE protocol, excluding *Spn* IS spiking. Then, different quantities were loaded onto silica TLC plates to

determine the needed amount from the extract, ensuring satisfactory intensity. The total amount of pneumococcal lipid extracts from a dried cultures (0.5 L) ranged around 100 µg, with 30 µg being identified as a well suitable quantity for TLC (**Figure 30 A**). During TLC separation, lipids are separated according to the polarity of head group and/or number of fatty acids.

As demonstrated by the results from shotgun experiments, the *Spn* membrane comprises 70% GLs. However, these GLs were hardly visible through Coomassie staining on the TLC. Consequently, a further step was made by implementing a two-step staining process on the same TLC plate. The plate was initially stained with Coomassie, followed by subsequent staining with Hannesian' stain (Mostain). This approach aimed to enhance the intensity of the GLs and GPs spots as illustrated in **Figure 30 B**.

At the lipid class level and based on Mostain TLC-stained plate, the TLC spot identification process involved running different lipid standards, including GLs and GPs, and then comparing their retention factor (R_f) values to determine the composition and characteristics of the analyzed lipid extracts.

Figure S10 illustrates a TLC plate containing lipid standards along with their corresponding R_f values. The TLC analysis of *Spn* lipid extracts has revealed lipidome classes consistent with those previously observed through shotgun experiments (section 2.3.2).

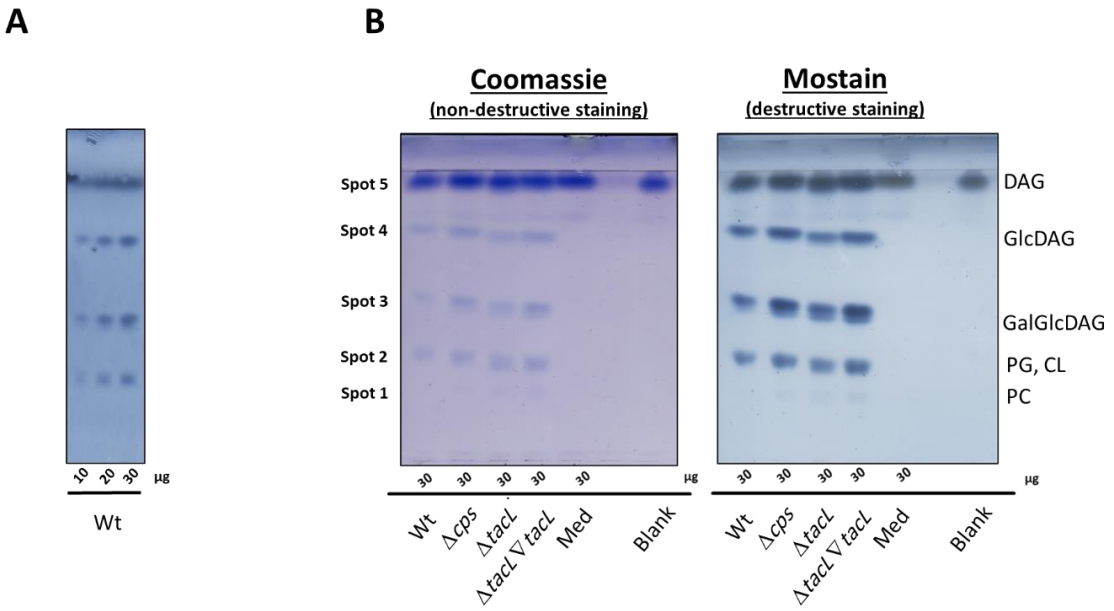

Figure 30: Separation of extracted pneumococcal lipids on TLC. **A**: 10, 20, and 30 µg of total lipid extracts from the wild type were applied to the silica TLC plate. A mobile phase of chloroform: methanol: water (60:25:4, v/v/v, respectively) was used. After separation, the plate was stained with Mostain. **B:** For the investigated strains, 30 µg of extracted lipids were applied to the TLC plate under the same conditions as in A. Following separation, the plate was first stained with Coomassie and then with Mostain.

To check the lipid species identity within separated lipid class, a new batch of *Spn* lipid extract was separated using the same conditions and exclusively stained by Coomassie. The resulting spots were carefully removed from the Coomassie-stained TLC plate and underwent a chloroform-water extraction process to isolate the lipids from the protein, salts, and silica material (detailed experimental procedure is depicted in section 4.6.8).

By employing the same acquisition mode used in shotgun investigation, the lipids extracted from Coomassie stained TLC plate were directly subjected to MS analysis and then processed qualitatively using LipidXplorer. It's important to mention that for the TLC-extracted lipids, all of used MFQL files for lipid identification were adjusted to utilize MS^1 and MS^2 for lipid identification. This adjustment reduced the overlapping issue (**Figure 29**) and thereby enhanced confidence in the reported lipid species at the molecular level.

A series of filtering steps was also applied here on annotated lipid species to remove background peaks. To eliminate possible background peaks from both the TLC plate and the post-TLC extraction tube, the ratio between the average intensity of each reported lipid species in *Spn* samples and the average in blank samples was calculated. Lipid species with a ratio below 60% were subsequently excluded from consideration to enhance the confidence level in the identified pneumococcal lipid species.

The subsequent filtering step involved the establishment of thresholds for *Spn* lipid species based on both precursor level (MS^1) and molecular level (MS^2). Specifically, at the precursor level, a threshold of 50% was set, indicating that a lipid species would be reported if the precursor was found in at least 50% of the different biological replicates. Similarly, a 60% threshold was implemented for the reporting of lipid species at the MS^2 level. It is important to mention that these filtering steps were applied to all separated lipid classes on the TLC plate, including DAG, GlcDAG, and GalGlcDAG. These steps helped to eliminate unusual fatty acid combinations and in generating high quality lipidome dataset. For instance, **Table 2** illustrates the GalGlcDAG species that were reported after implementing all mentioned filtering criteria. **Table S1** & **S2** show more information about GlcDAG and DAG species post filtering steps.

Table 2: Validated lipid species of the GalGlcDAG TLC-spot following the implementation of filtering steps. The precursor (Prec.) is the parent lipid that undergoes fragmentation to produce daughter ions (Frag.). Here, Frag A and B refer to the generated fatty acids.

GalGlcDAG		Occupation threshold				
Lipid species level	**Molecular species level**	**Prec. > 50%**	**Frag A > 60%**	**Frag B >60%**	**Observed/ calculated monoisotopic mass (Da)**	**ppm**
26:0	14:0_12:0	83	83	75	867.531/ 867.533	-2.3

28:1	16:1_12:0 14:0_14:1	100 83	100 83	91 66	893.549/ 893.547	2.2
28:0	16:0_12:0 14:0_14:0	100 100	100 100	100 100	895.562/ 895.563	-1.1
29:0	16:0_13:0	100	100	75	909.580/ 909.578	2.2
30:2	16:1_14:1	91	91	83	919.565/ 919.563	2.2
30:1	18:1_12:0 16:0_14:1 16:1_14:0	91 100 100	91 100 100	83 100 100	921.580/ 921.578	2.2
30:0	18:0_12:0 16:0_14:0	100 100	100 100	100 100	923.596/ 923.594	2.2
31:0	17:0_14:0 16:0_15:0	83 100	83 100	83 83	937.612/ 937.609	3.2
32:2	16:1_16:1	100	100	100	947.596/ 947.594	2.1
32:1	18:1_14:0 16:0_16:1	100 100	100 100	100 100	949.612/ 949.609	3.1
33:1	17:0_16:1	91	75	91	963.627/ 963.625	2.1
34:3	18:2_16:1	91	83	91	973.612/ 973.609	3.1
34:2	18:1_16:1 18:2_16:0	100 100	100 100	100 100	975.626/ 975.625	1.0
34:1	18:0_16:1 18:1_16:0	100 100	100 100	100 100	977.643/ 977.641	2.0

In the context of the GPs, successful separation between PG and CL was not accomplished on the TLC plate under the used condition. Nevertheless, it is noteworthy that the number of PG lipid species remained consistent between the shotgun and off-line TLC-MS methods. Regarding CL, while the shotgun method detected more CL species, the difference primarily involved minor CL species. In the case of PC, despite the low intensity of PC on the TLC plate, the MS measurement of the TLC pre-separated PC spot yielded a higher number of PC lipid species compared to shotgun method. Considering the challenges of overlap and low intensity, the necessity for filtering steps was considered

less significant for these specific lipid classes. However, it is important to mention that the overall number of lipid species between these methods was quite similar, with minor differences primarily attributable to minor species. Most of the major species were present in both approaches (**Figure 31 B)**.

Furthermore, it's important to report that few lipid species were solely found in TLC-MS, such as CL 70:2, PC 26:1, PG 33:0 and some DAG species. But despite these variations, approximately 80% of the lipid species detected using shotgun of the whole lipid extract (without prior TLC separation) were also detectable by the offline TLC-MS method, confirming the high-quality data obtained from both procedures, as depicted in the Venn diagram (**Figure 31 B**). These lipid species represent over 80% of the entire lipidome, while the remaining species constitute minor components.

Table S3 provides detailed information about the reported lipid species in both the shotgun and TLC-MS method. Moreover, the pre-separation of lipids on TLC before the MS experiment, especially for *Spn* glycerolipids, played a crucial role in simplifying the spectra's complexity (**Figure 31 C**) and enhancing the process of lipid annotation at the molecular level.

In summary, the offline TLC-MS experiment has demonstrated its value as a significant enhancement to the shotgun method, specifically for studying pneumococcal lipids. By separating lipids before MS analysis, it overcomes the issue of overlapping signals from different lipid classes inherent in shotgun lipidomics. This enhances confidence in lipid annotation and makes the workflow adaptable to bacterial lipidomics studies of diverse biological membranes.

A) Workflow for MS-based identification of TLC pre-separated lipids

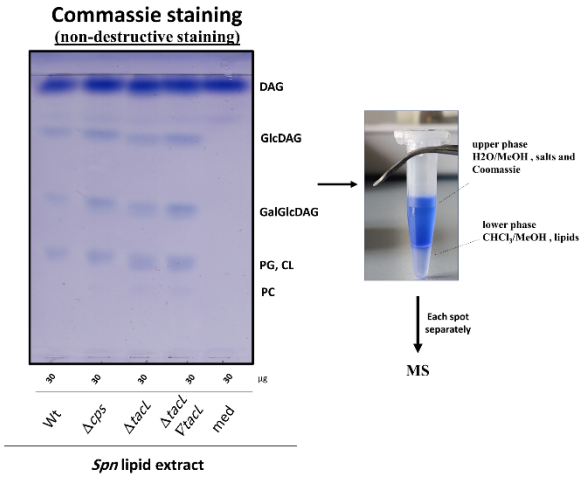

B) Comparison of identity and number of detected lipids between direct infusion and off-line TLC-MS

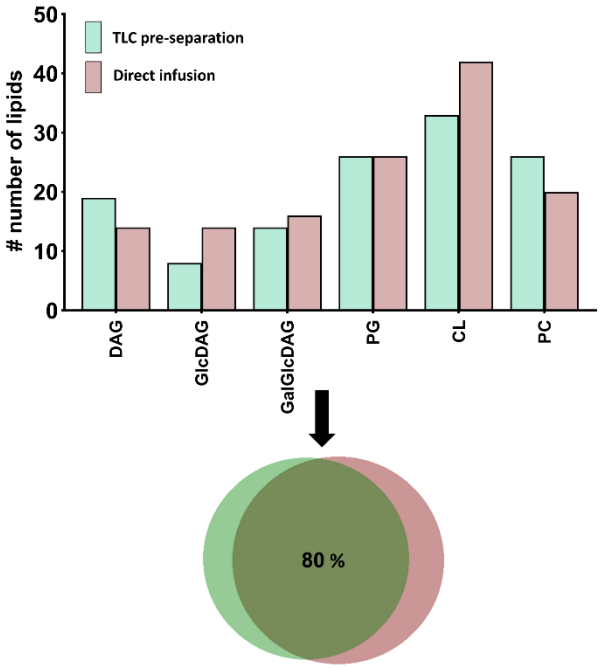

C) MS spectrum of TLC pre-separated lipids

PG and CL

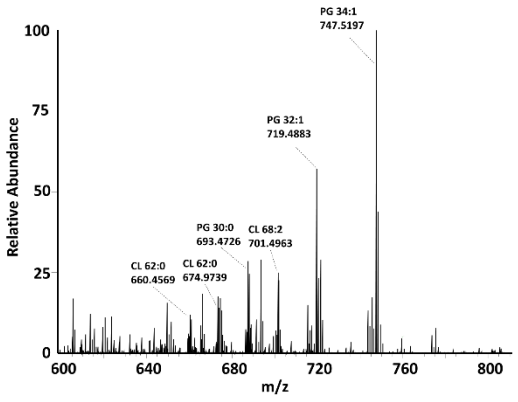

GlcDAG

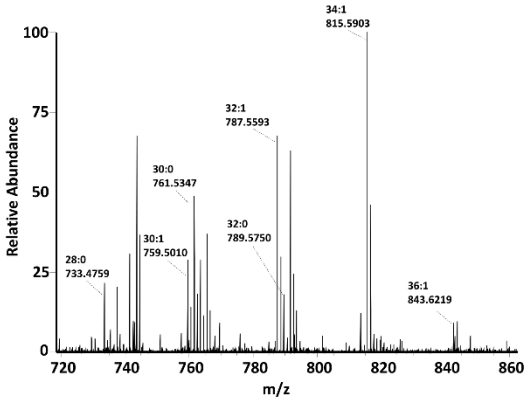

DAG

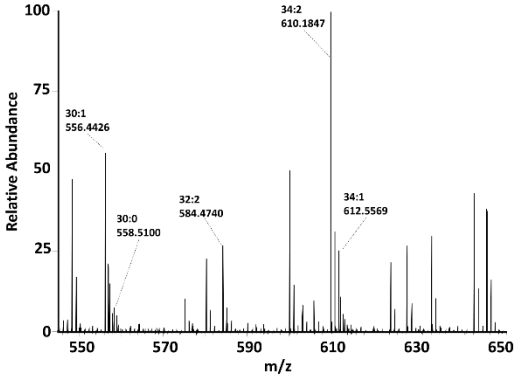

GalGlcDAG

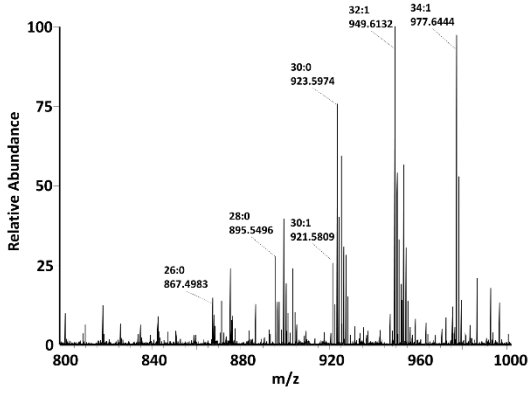

Figure 31: **A Comparison of shotgun and off-line TLC-MS approaches**. **A**: 30 µg of *Spn* lipid extract were applied on TLC, separated by using chloroform/methanol/water (65:25:4, v/v/v) as mobile phase, stained with Coomassie and then spots were removed using a scalpel and subjected to chloroform-water extraction. The lipids were obtained from the lower organic phase and subsequently subjected to MS. **B:** Comparison of number (bar) and identity (circles) of detected lipids in *Spn* D39 Wt between TLC pre-separation and shotgun methods. **C**: MS spectrum of TLC pre-separated lipids, including PG, CL, GlcDAG, and GalGlcDAG, were analyzed in negative mode, while PC and DAG were analyzed in positive mode. All lipids were identified using modified MFQL files (section 4.6.9) designed for lipid identification based on MS^2.

2.3.5 Conclusion and outlook

The membrane composition is pivotal for shaping the structure and safeguarding bacterial cells. However, the current grasp of the intricate relationship between genetic inventory, biosynthesis, and environmental factors on one side, and the composition of microbial lipidomes on the other, is still in the early stages of understanding. Specifically, for *Streptococcus pneumoniae* (*Spn*) only qualitative data was available. In this study, shotgun lipidomics was employed to investigate the impact of selected genetic mutations (Δ*tacL*, Δ*lgt*, and Δ*cps*) on the membrane lipid composition of *Spn* strain D39.

A customized mix of internal standards enabled reliable quantitative analysis. Our analysis led to the quantification of more than 100 lipids of six classes (DAG, GlcDAG, GalGlcDAG, PG, CL and PC) with GlcDAG and GalGlcDAG being the major abundant ones. Fatty acid profiling by Gas Chromatography-Mass Spectrometry and Thin Layer Chromatography combined with high resolution MS^2 were further used for identification of lipid species. Fatty acid profiling showed that palmitic acid (16:0), stearic (18:0), and oleic acid (18:1) are the predominant fatty acids. The lipidome of Δ*tacL* and Δ*lgt* strains remained largely unchanged compared to the wild type, whereas the non-encapsulated strain showed notable alteration in lipid composition. In conclusion, a reliable technique for quantitatively analyzing the lipidome in *Spn* has been developed, enabling further exploration of other mutants or growth conditions.

The developed workflow is particularly significance for less studied non-typeable pneumococci strains, which naturally lack capsules, allowing for an examination of their membrane lipid composition. Additionally, the differential lipidome composition in non-capsulated strains could be driver for in-depth biophysical membrane analysis. These efforts can deepen our knowledge of membrane biosynthesis and remodeling processes.

3) Supplementary Data

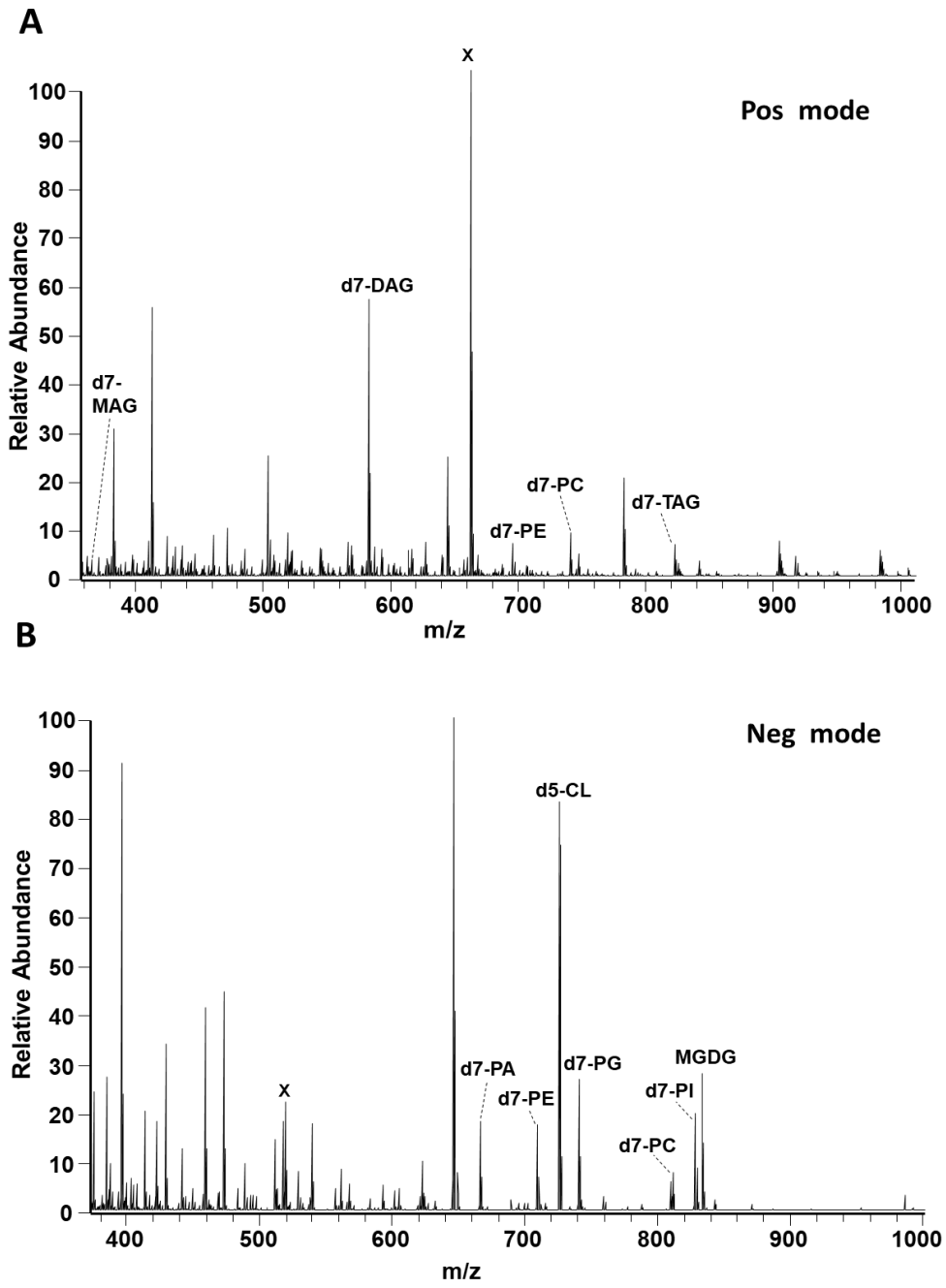

Figure S1: Spectrum illustrates the customized internal standard utilized in this study, showing the detected deuterated lipid species in both positive (A) and negative (B) modes. In the positive mode, peaks marked with "x" indicate the presence of Tris(di-*tert*-butylphenyl) phosphate as $[M+NH_4]^+$, whereas in the negative mode, the "x" peaks represent Octadecyl (di-*tert*-butyl-hydroxyphenyl)propionate as $[M-H]^-$.

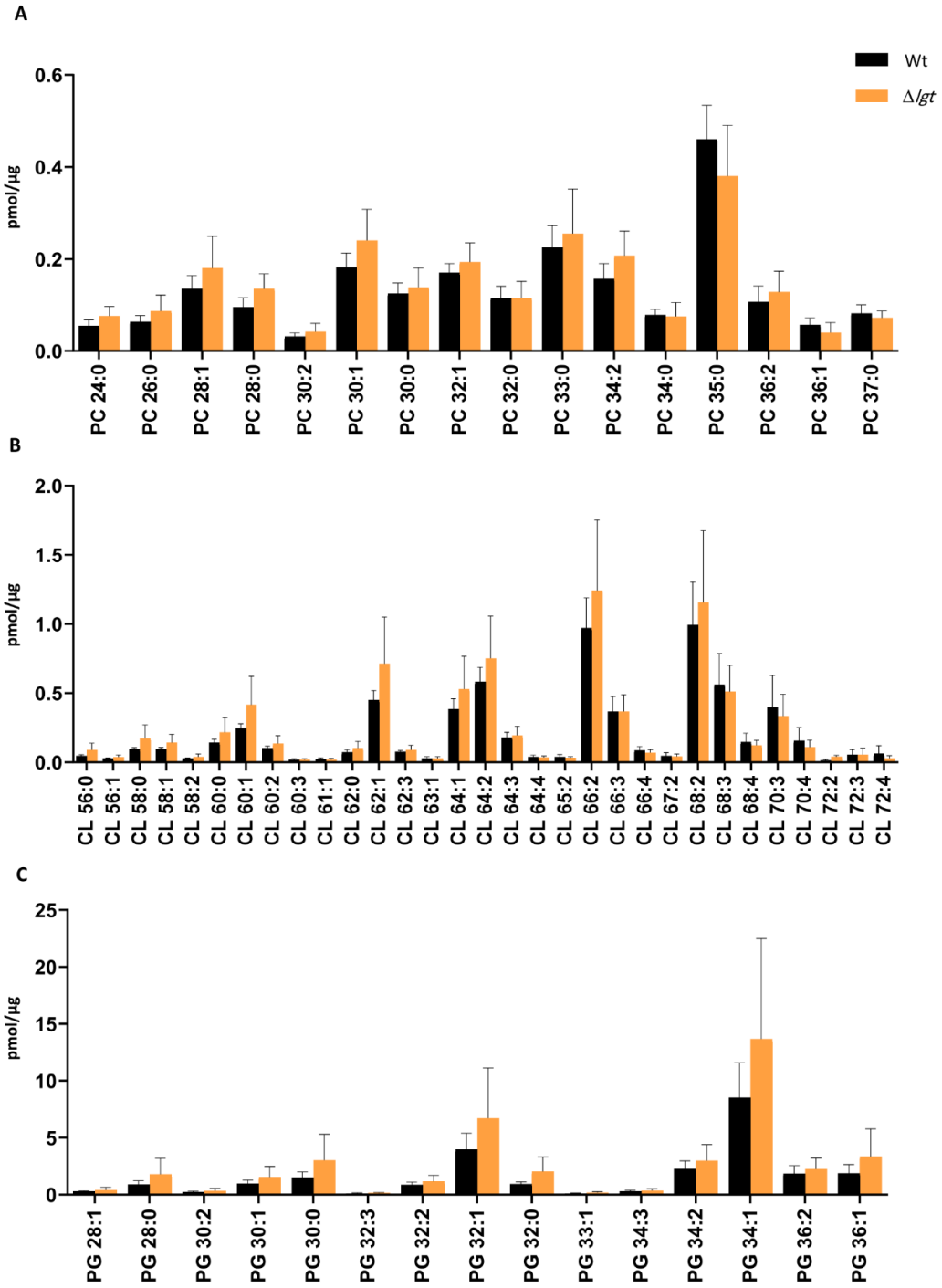

Figure S2: **Quantity of glycerophospholipids in *Spn* D39 Wt and Δ*lgt***. All data show the mean of six biological replicates. Data is normalized on the protein content. Error bars represent standard deviation. A multiple t-test was used for statistical analysis. Benjamini, Krieger and Yukutieli correction was applied to p-values using an FDR cut-off < 0.05 (*P ≤ 0.05, **P ≤ 0.01, ***P ≤ 0.001*).*

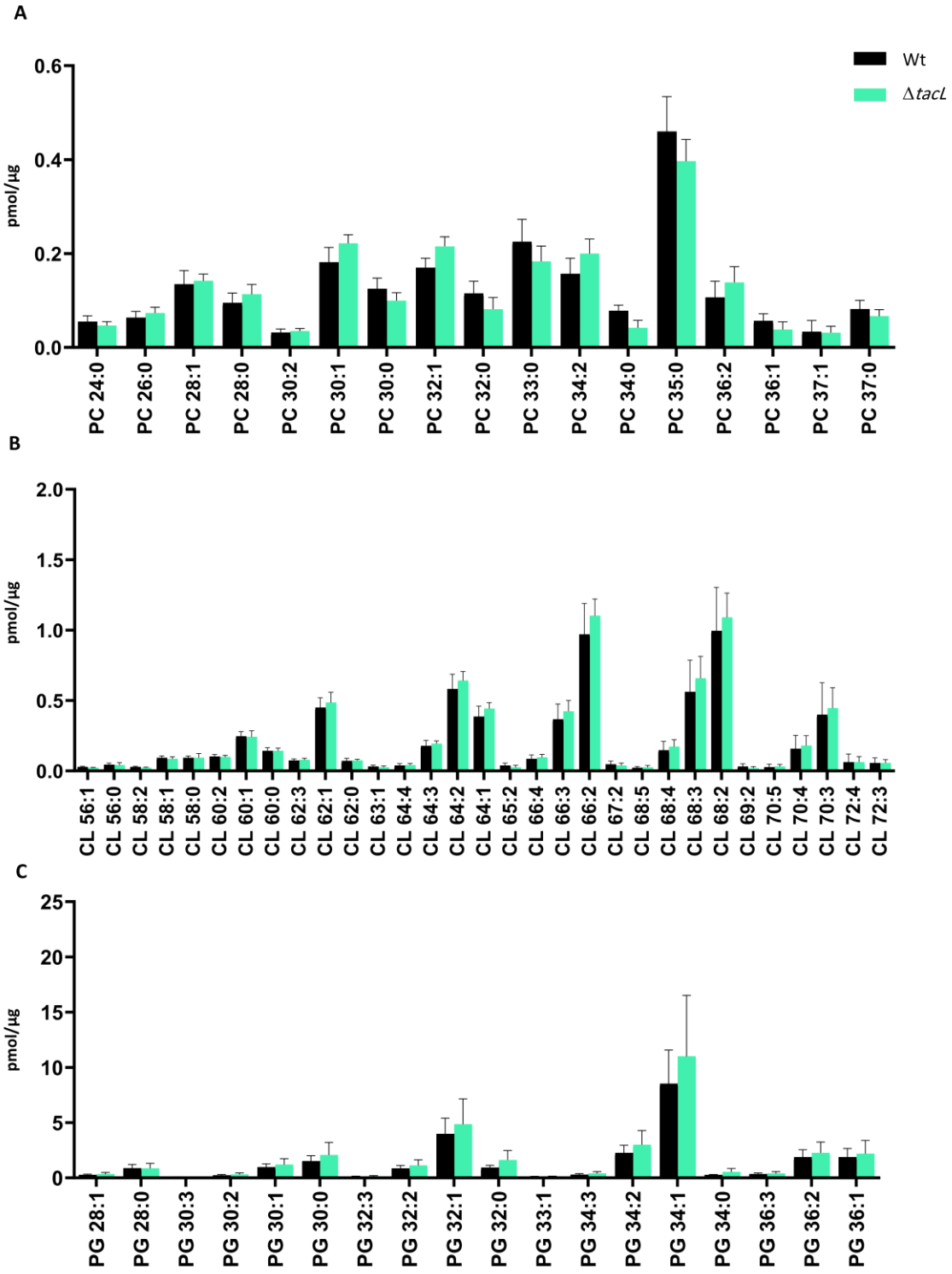

Figure S3*:* Quantity of glycerophospholipids in *Spn* D39 Wt and Δ*tacL*. All data show the mean of six biological replicates. Data is normalized on the protein content. Error bars represent standard deviation. A multiple t-test was used for statistical analysis. Benjamini, Krieger and Yukutieli correction was applied to p-values using an FDR cut-off < 0.05 (*P ≤ 0.05, **P ≤ 0.01, ***P ≤ 0.001*)*

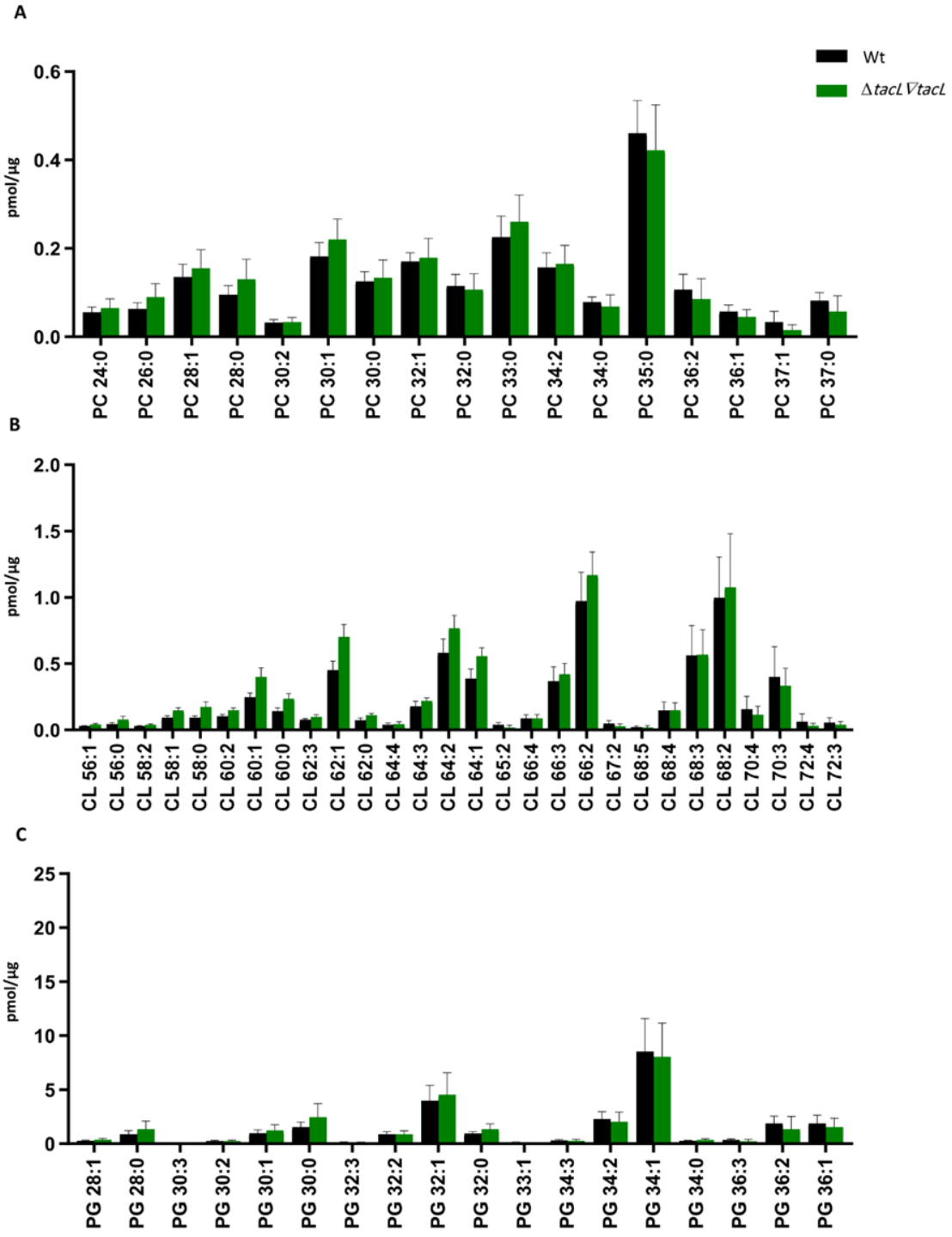

Figure S4: **Quantity of glycerophospholipids in *Spn* D39 Wt and Δ*tacL*∇*tacL*.** All data show the mean of six biological replicates. Data is normalized on the protein content. Error bars represent standard deviation. A multiple t-test was used for statistical analysis. Benjamini, Krieger and Yukutieli correction was applied to p-values using an FDR cut-off < 0.05 (*P ≤ 0.05, **P ≤ 0.01, ***P ≤ 0.001).

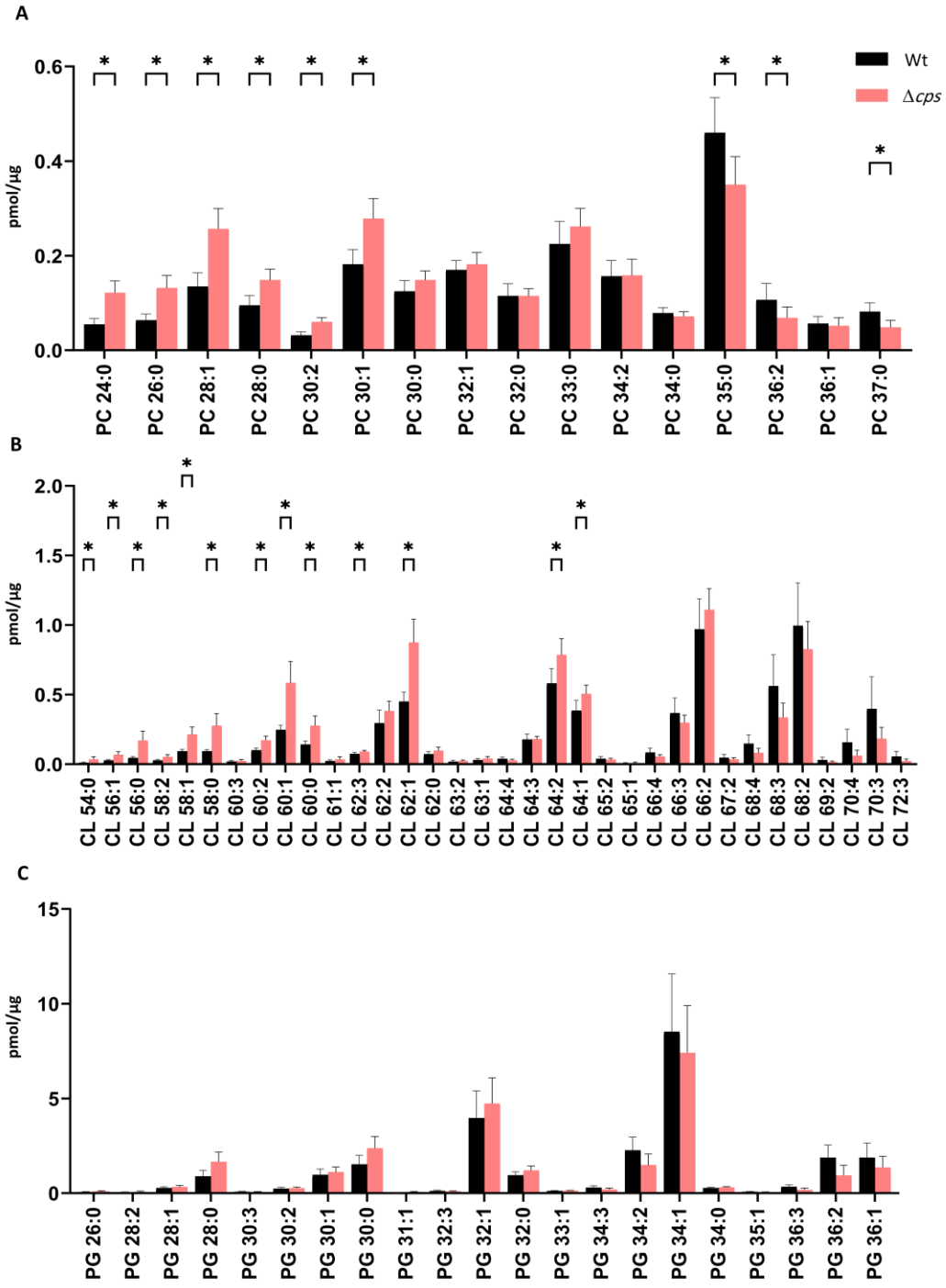

Figure S5*:* Quantity of glycerophospholipids in *Spn* D39 Wt and Δ*cps*. All data show the mean of six biological replicates. Data is normalized on the protein content. Error bars represent standard deviation. A multiple t-test was used for statistical analysis. Benjamini, Krieger and Yukutieli correction was applied to p-values using an FDR cut-off < 0.05 (*P ≤ 0.05, **P ≤ 0.01, ***P ≤ 0.001).

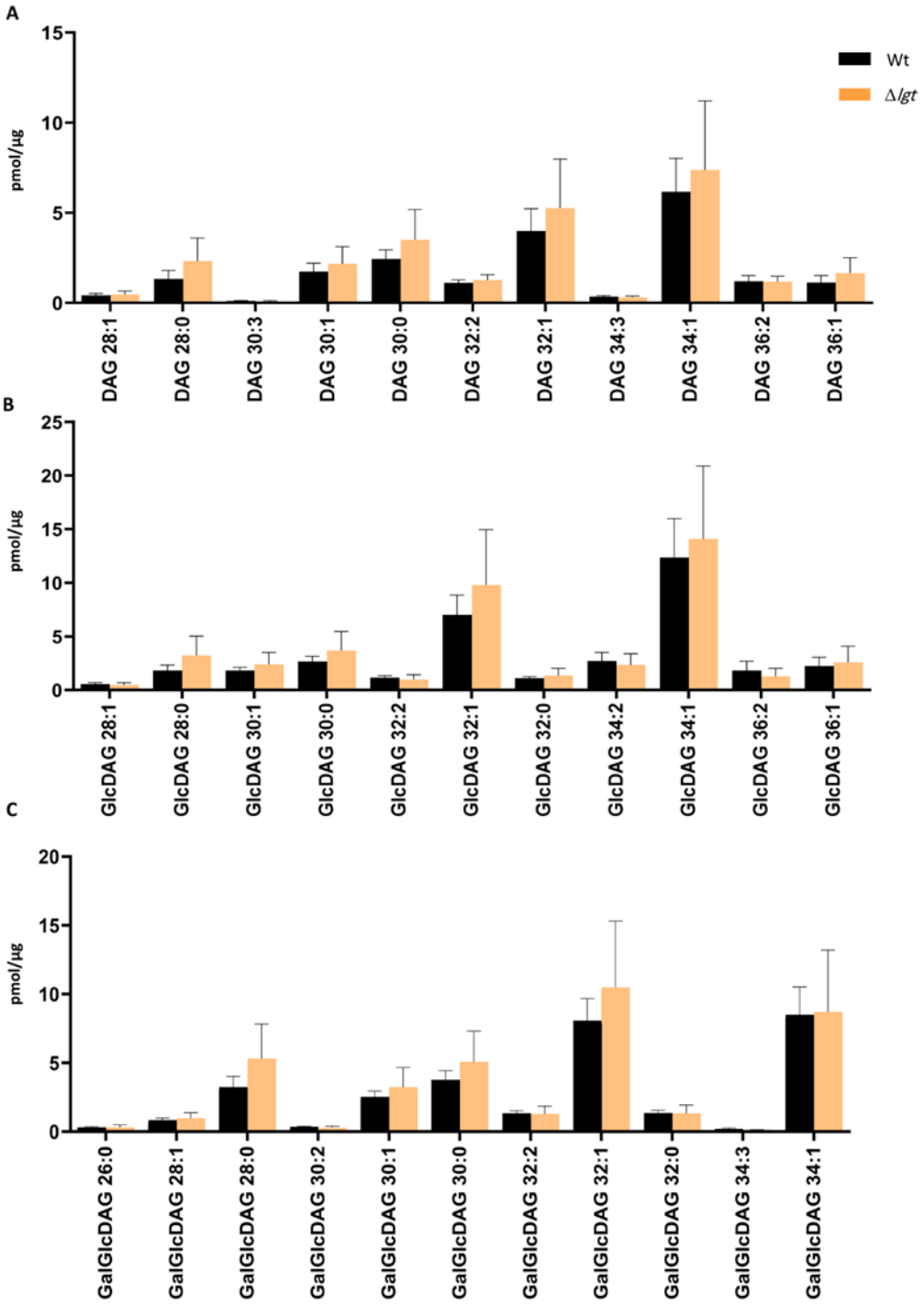

Figure S6: Quantity of glycerolipids in *Spn* D39 Wt and Δ*lgt*. All data show the mean of six biological replicates. Data is normalized on the protein content. Error bars represent standard deviation. A multiple t-test was used for statistical analysis. Benjamini, Krieger and Yukutieli correction was applied to p-values using an FDR cut-off < 0.05 (*P ≤ 0.05, **P ≤ 0.01, ***P ≤ 0.001).

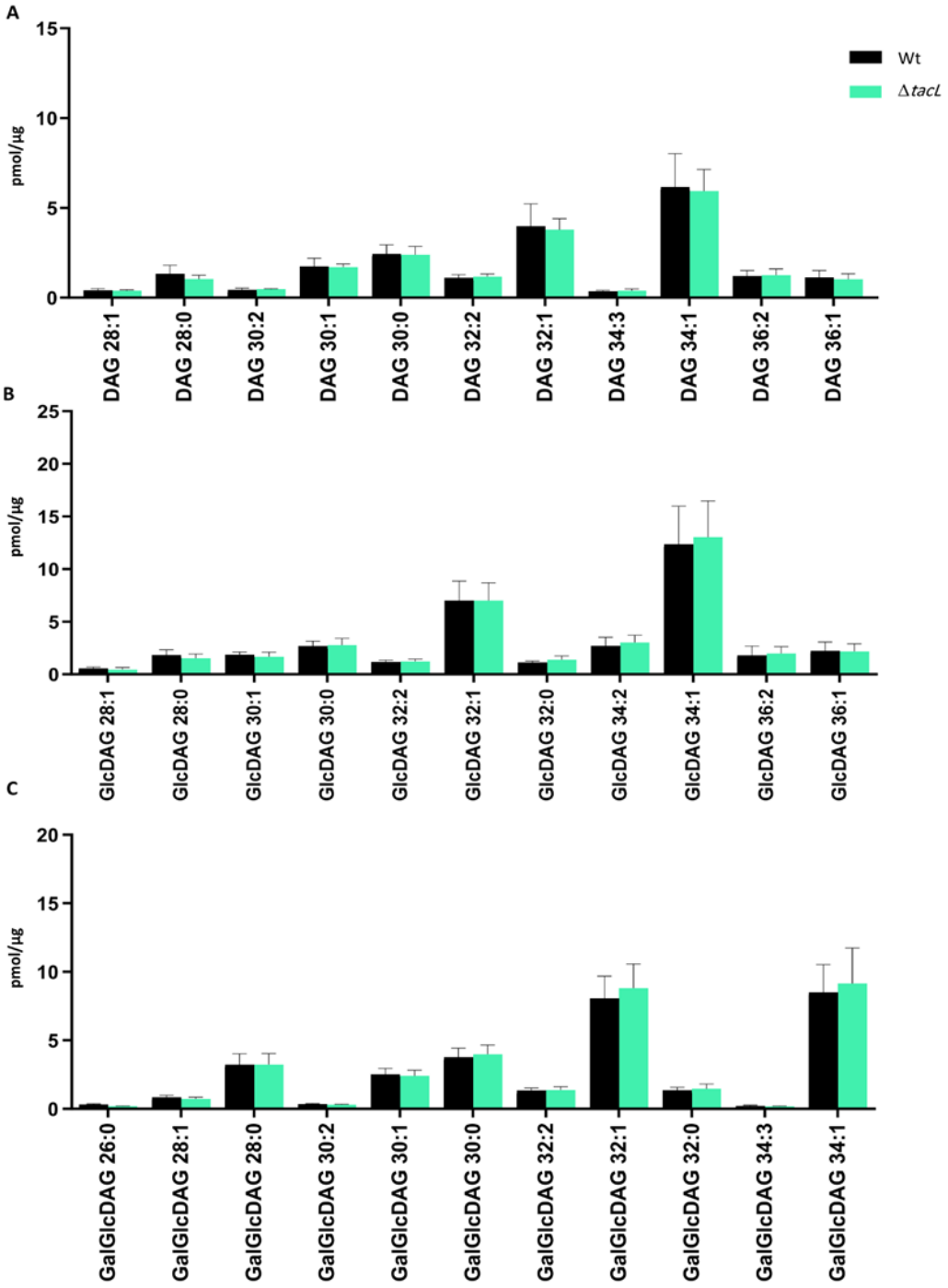

Figure S7*:* Quantity of glycerolipids in *Spn* D39 Wt and Δ*tacL*. All data show the mean of six biological replicates. Data is normalized on the protein content. Error bars represent standard deviation. A multiple t-test was used for statistical analysis. Benjamini, Krieger and Yukutieli correction was applied to p-values using an FDR cut-off < 0.05 (*P ≤ 0.05, **P ≤ 0.01, ***P ≤ 0.001).

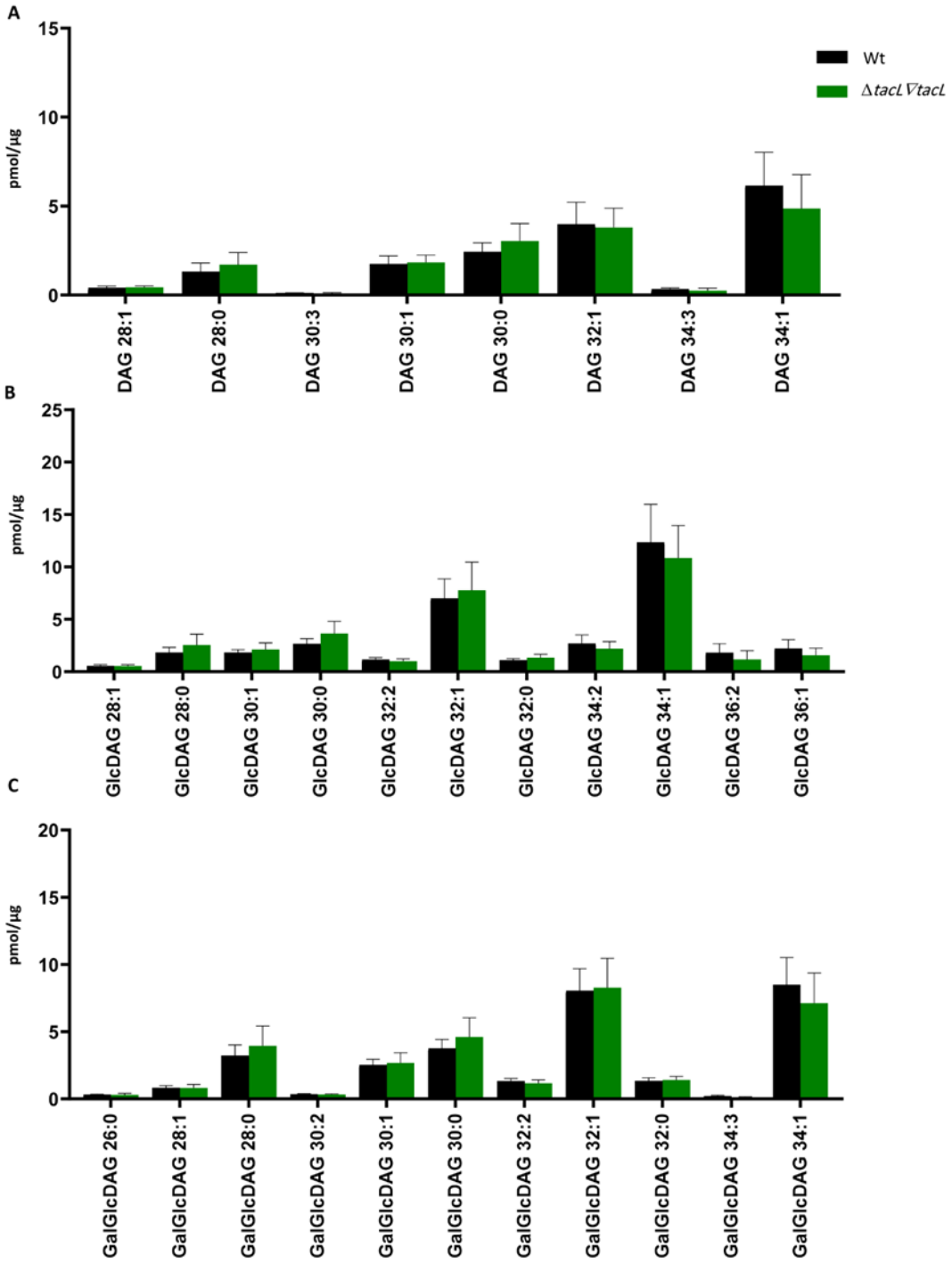

Figure S8: **Quantity of glycerolipids in *Spn* D39 Wt and Δ*tacL*∇*tacL*.** All data show the mean of six biological replicates. Data is normalized on the protein content. Error bars represent standard deviation. A multiple t-test was used for statistical analysis. Benjamini, Krieger and Yukutieli correction was applied to p-values using an FDR cut-off < 0.05 (*P ≤ 0.05, **P ≤ 0.01, ***P ≤ 0.001).

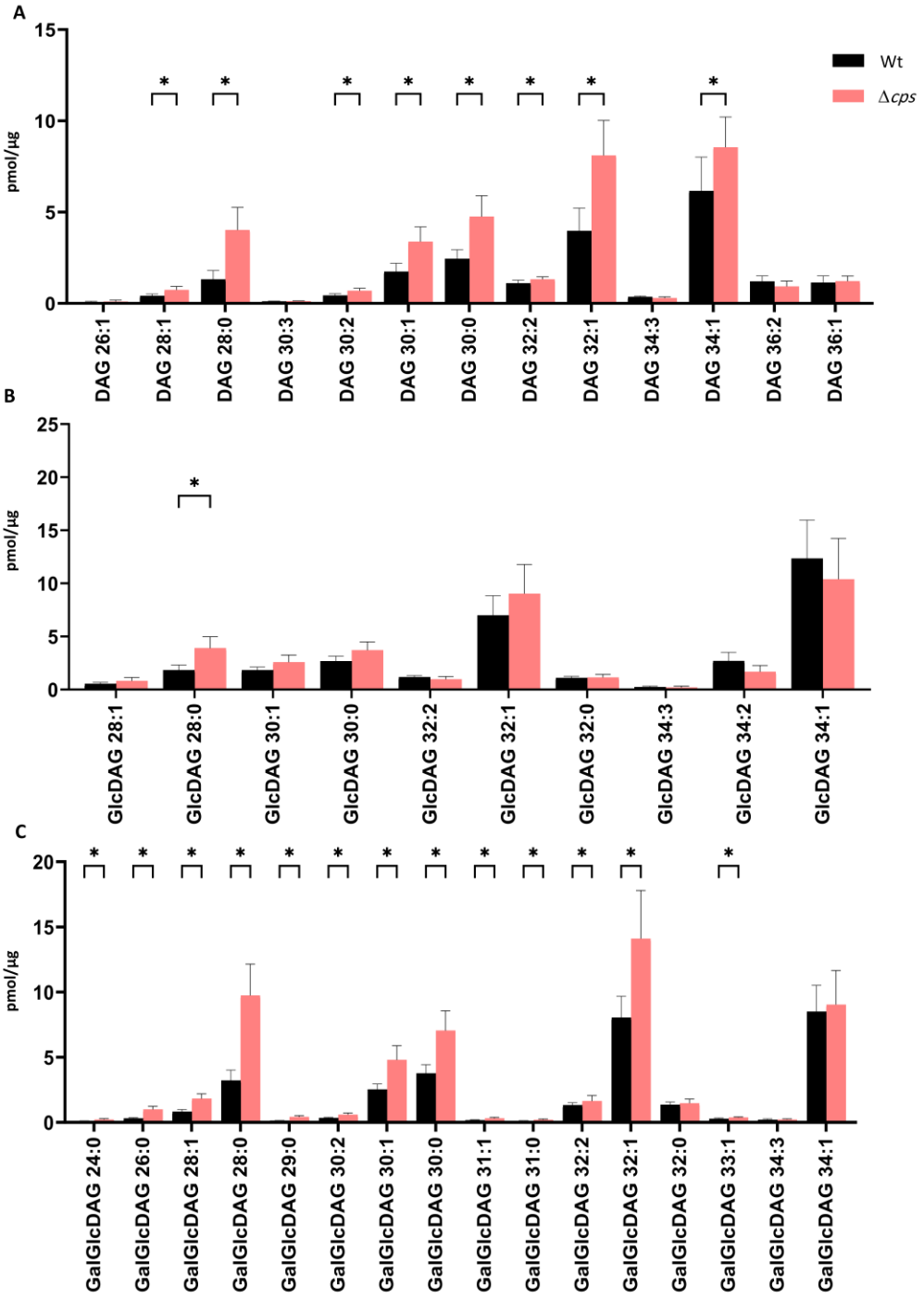

Figure S9*:* Quantity of glycerolipids in *Spn* D39 Wt and Δ*cps*. All data show the mean of six biological replicates. Data is normalized on the protein content. Error bars represent standard deviation. A multiple t-test was used for statistical analysis. Benjamini, Krieger and Yukutieli correction was applied to p-values using an FDR cut-off < 0.05 (*P ≤ 0.05, **P ≤ 0.01, ***P ≤ 0.001) (*P ≤ 0.05, **P ≤ 0.01, ***P ≤ 0.001).

A

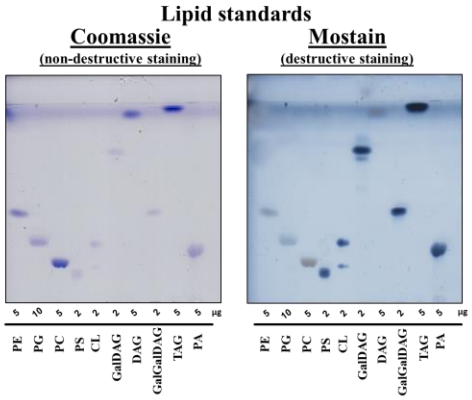

B

Lipid standard	Solvent system (R_f)
PA	0.22
TAG	0.80
GalGalDAG	0.38
DAG	0.78
GalDAG	0.64
CL	0.25
PS	0.12
PC	0.17
PG	0.26
PE	0.39

Figure S10: Separation of lipid standards on TLC. **A**: Various amounts of different lipid stands were loaded on the TLC plate, using a mobile phase composed of chloroform: methanol: water (60:25:4, v/v/v, respectively). Following separation, the plate was stained with Coomassie (left) followed by Mostain (right). **B**: Table shows the retention factor (R_f) for separated lipids in A. The retention factor is calculated by dividing the distance traveled by the lipid by the distance traveled by the solvent front. Abbreviations:
PA: phosphatidic acid; TAG: triacylglycerol, GalGalDAG: digalactosyldiacylglycerol, DAG: diacylglycerol, GalDAG: monogalactosyldiacylglycerol, CL: cardiolipin, PS: phosphatidylserine, PC: phosphatidylcholine, PG: phosphatidylglycerol, PE: phosphatidylethanolamine.

Table S1: Validated lipid species of the GlcDAG TLC-spot following the implementation of filtering steps. Abbreviation based on Table 2.

GlcDAG		Occupation threshold				
Lipid species level	**Molecular species level**	**Prec. > 50 %**	**Frag A > 60 %**	**Frag B >60 %**	**Observed/ calculated monoisotopic mass (Da)**	**ppm**
28:0	16:0_12:0 14:0_14:0	100 83	100 83	100 83	733.511/ 733.511	0
30:1	16:0_14:1 16:1_14:0	100 91	100 83	91 91	759.527/ 759.525	2.6
30:0	18:0_12:0 16:0_14:0	100 100	100 100	83 100	761.543/ 761.541	2.6
32:1	18:1_14:0 16:0_16:1	91 100	91 100	83 100	787.559/ 787.557	2.5
34:2	18:1_16:1 18:2_16:0	100 91	100 83	100 91	813.574/ 813.572	2.4
34:1	18:0_16:1 18:1_16:0	100 100	100 100	100 100	815.590/ 815.588	2.4
36:2	18:1_18:1	100	100	100	841.606/ 841.604	2.4

36:1	18:0_18:1	100	100	100	843.621/ 843.619	2.4

Table S2: Validated lipid species of the DAG TLC-spot following the implementation of filtering steps.
Abbreviation based on Table 2.

DAG		Occupation threshold				
Lipid species level	**Molecular species level**	**Prec. > 50 %**	**Frag A > 60 %**	**Frag B > 60 %**	**Observed/ calculated monoisotopic mass (Da)**	**ppm**
28:1	14:0_14:1	100	83	91	528.462/ 528.462	0
28:0	14:0_14:0	100	100	100	530.478/ 530.478	0
29:0	14:0_15:0	91	75	91	544.493/ 544.494	-1.8
30:2	14:0_16:2 16:1_14:1 14:2_16:0	91 100 100	66 100 100	91 100 100	544.478/ 544.472	11.1
30:1	14:1_16:0 14:0_16:1	100 100	100 100	100 100	556.493/ 556.494	-1.8
30:0	16:0_14:0	100	100	100	558.509/ 558.509	0
31:1	15:0_16:1 15:1_16:0	100 91	100 91	100 33	570.509/ 570.509	0
31:0	14:0_17:0	100	83	100	572.525/ 572.525	0
32:3	16:1_16:2	100	75	100	580.493/ 580.494	-1.7
32:2	16:0_16:2 16:1_16:1 14:0_18:2 14:1_18:1	100 100 100 100	100 100 83 100	100 100 100 100	582.509/ 582.509	0
32:1	16:0_16:1 14:0_18:1 14:1_18:0	100 100 100	100 100 100	100 100 100	584.524/ 584.525	-1.7

32:0	16:0_16:0 14:0_18:0	100 100	100 100	100 100	586.540 586.541	-1.7
33:1	16:0_17:1 16:1_17:0	100 100	100 91	100 100	598.540 598.541	-1.7
34:2	16:0_18:1 16:1_18:0	100 100	100 100	100 100	610.540/ 610.541	-1.6
34:1	16:0_18:2 16:1_18:1	100 100	100 100	100 100	612.556/ 612.556	0
34:0	16:0_18:0	100	91	100	614.571/ 614.572	-1.6
35:2	17:1_18:1	100	100	91	624.556/ 624.556	0
35:1	17:0_18:1	100	100	100	626.572/ 626.572	0
36:3	18:1_18:2	100	100	100	636.556/ 636.556	0
36:2	18:0_18:2 18:1_18:1	100 100	91 100	100 100	638.572/ 638.572	0
36:1	18:0_18:1	100	100	100	640.587/ 640.588	-1.6

Table S3: Common identified lipid species in pneumococcal cell extracts (Wt and Δ*cps*).The table includes information such as the observed *m/z*, ion species, corresponding lipid class and species, and the ion mode used for identification. The lipid species were identified either through direct infusion or after TLC pre-separation, as indicated. Addtionally, the table displays lipid species that were exclusively identified in one of the methods.

m/z	**Ion**	**Lipid Class**	**Ion mode**	**Shotgun**	**TLC pre-separation**
605.902	CL 54:0	Cardiolipin	Negative	x	-
618.910	CL 56:1	Cardiolipin	Negative	x	x
619.918	CL 56:0	Cardiolipin	Negative	x	x
631.918	CL 58:2	Cardiolipin	Negative	x	x
632.926	CL 58:1	Cardiolipin	Negative	x	x
633.934	CL 58:0	Cardiolipin	Negative	x	x
644.926	CL 60:3	Cardiolipin	Negative	x	x
645.934	CL 60:2	Cardiolipin	Negative	x	x
646.942	CL 60:1	Cardiolipin	Negative	x	x
647.950	CL 60:0	Cardiolipin	Negative	x	x
653.950	CL 61:1	Cardiolipin	Negative	x	x
658.942	CL 62:3	Cardiolipin	Negative	x	x
659.949	CL 62:2	Cardiolipin	Negative	x	x
660.957	CL 62:1	Cardiolipin	Negative	x	x
661.966	CL 62:0	Cardiolipin	Negative	x	x

666.957	CL 63:2	Cardiolipin	Negative	x	x
667.965	CL 63:1	Cardiolipin	Negative	x	x
671.950	CL 64:4	Cardiolipin	Negative	x	x
672.958	CL 64:3	Cardiolipin	Negative	x	x
673.966	CL 64:2	Cardiolipin	Negative	x	x
674.974	CL 64:1	Cardiolipin	Negative	x	x
680.973	CL 65:2	Cardiolipin	Negative	x	x
681.981	CL 65:1	Cardiolipin	Negative	x	x
685.966	CL 66:4	Cardiolipin	Negative	x	x
686.973	CL 66:3	Cardiolipin	Negative	x	x
687.981	CL 66:2	Cardiolipin	Negative	x	x
694.989	CL 67:2	Cardiolipin	Negative	x	x
699.981	CL 68:4	Cardiolipin	Negative	x	-
700.989	CL 68:3	Cardiolipin	Negative	x	x
701.997	CL 68:2	Cardiolipin	Negative	x	x
709.005	CL 69:2	Cardiolipin	Negative	x	-
713.997	CL 70:4	Cardiolipin	Negative	x	-
715.005	CL 70:3	Cardiolipin	Negative	x	x
716.013	CL 70:2	Cardiolipin	Negative	-	x
729.020	CL 72:3	Cardiolipin	Negative	x	-
637.409	PG 26:0	Phosphatidylglycerol	Negative	x	-
661.409	PG 28:2	Phosphatidylglycerol	Negative	x	-
663.425	PG 28:1	Phosphatidylglycerol	Negative	x	x
665.440	PG 28:0	Phosphatidylglycerol	Negative	x	x
679.456	PG 29:0	Phosphatidylglycerol	Negative	x	x
687.425	PG 30:3	Phosphatidylglycerol	Negative	x	x
689.441	PG 30:2	Phosphatidylglycerol	Negative	x	x
691.456	PG 30:1	Phosphatidylglycerol	Negative	x	x
693.472	PG 30:0	Phosphatidylglycerol	Negative	x	x
705.472	PG 31:1	Phosphatidylglycerol	Negative	x	x
707.487	PG 31:0	Phosphatidylglycerol	Negative	x	x
715.456	PG 32:3	Phosphatidylglycerol	Negative	x	x
717.472	PG 32:2	Phosphatidylglycerol	Negative	x	x
719.487	PG 32:1	Phosphatidylglycerol	Negative	x	x
721.503	PG 32:0	Phosphatidylglycerol	Negative	x	x
731.488	PG 33:2	Phosphatidylglycerol	Negative	x	-
733.503	PG 33:1	Phosphatidylglycerol	Negative	x	x
735.519	PG 33:0	Phosphatidylglycerol	Negative	-	x
743.488	PG 34:3	Phosphatidylglycerol	Negative	x	x
745.503	PG 34:2	Phosphatidylglycerol	Negative	x	x
747.519	PG 34:1	Phosphatidylglycerol	Negative	x	x
749.535	PG 34:0	Phosphatidylglycerol	Negative	x	x
759.519	PG 35:2	Phosphatidylglycerol	Negative	x	x
761.534	PG 35:1	Phosphatidylglycerol	Negative	x	x
771.519	PG 36:3	Phosphatidylglycerol	Negative	x	x
773.535	PG 36:2	Phosphatidylglycerol	Negative	x	x
775.550	PG 36:1	Phosphatidylglycerol	Negative	x	x
777.566	PG 36:0	Phosphatidylglycerol	Negative	-	x
622.444	PC 24:0	Phosphatidylcholine	Positive	x	x
648.462	PC 26:1	Phosphatidylcholine	Positive	-	x
650.475	PC 26:0	Phosphatidylcholine	Positive	x	x
670.443	PC 28:4	Phosphatidylcholine	Positive	-	x

676.491	PC 28:1	Phosphatidylcholine	Positive	x	x
678.506	PC 28:0	Phosphatidylcholine	Positive	x	x
692.521	PC 29:0	Phosphatidylcholine	Positive	-	x
702.507	PC 30:2	Phosphatidylcholine	Positive	x	x
704.522	PC 30:1	Phosphatidylcholine	Positive	x	x
706.538	PC 30:0	Phosphatidylcholine	Positive	x	x
720.553	PC 31:0	Phosphatidylcholine	Positive	-	x
726.504	PC 32:4	Phosphatidylcholine	Positive	-	x
728.520	PC 32:3	Phosphatidylcholine	Positive	-	x
732.554	PC 32:1	Phosphatidylcholine	Positive	x	x
734.569	PC 32:0	Phosphatidylcholine	Positive	x	x
748.584	PC 33:0	Phosphatidylcholine	Positive	x	x
754.535	PC 34:4	Phosphatidylcholine	Positive	-	x
756.552	PC 34:3	phosphatidylcholine	Positive	-	x
758.569	PC 34:2	Phosphatidylcholine	Positive	x	x
760.585	PC 34:1	Phosphatidylcholine	Positive	-	x
762.600	PC 34:0	Phosphatidylcholine	Positive	x	x
776.615	PC 35:0	Phosphatidylcholine	Positive	x	-
782.566	PC 36:4	Phosphatidylcholine	Positive	-	x
786.600	PC 36:2	Phosphatidylcholine	Positive	x	x
788.616	PC 36:1	Phosphatidylcholine	Positive	x	x
790.631	PC 36:0	Phosphatidylcholine	Positive	-	x
802.631	PC 37:1	Phosphatidylcholine	Positive	x	x
804.647	PC 37:0	Phosphatidylcholine	Positive	x	-
839.502	GalGlcDAG 24:0	Galactosylglucosyldiacylglycerol	Negative	x	-
867.534	GalGlcDAG 26:0	Galactosylglucosyldiacylglycerol	Negative	x	x
893.549	GalGlcDAG 28:1	Galactosylglucosyldiacylglycerol	Negative	x	x
895.565	GalGlcDAG 28:0	Galactosylglucosyldiacylglycerol	Negative	x	x
909.581	GalGlcDAG 29:0	Galactosylglucosyldiacylglycerol	Negative	x	x
919.565	GalGlcDAG 30:2	Galactosylglucosyldiacylglycerol	Negative	x	x
921.581	GalGlcDAG 30:1	Galactosylglucosyldiacylglycerol	Negative	x	x
923.596	GalGlcDAG 30:0	Galactosylglucosyldiacylglycerol	Negative	x	x
935.596	GalGlcDAG 31:1	Galactosylglucosyldiacylglycerol	Negative	x	-
937.612	GalGlcDAG 31:0	Galactosylglucosyldiacylglycerol	Negative	x	x
947.596	GalGlcDAG 32:2	Galactosylglucosyldiacylglycerol	Negative	x	x
949.612	GalGlcDAG 32:1	Galactosylglucosyldiacylglycerol	Negative	x	x
951.629	GalGlcDAG 32:0	Galactosylglucosyldiacylglycerol	Negative	x	-
963.6289	GalGlcDAG 33:1	Galactosylglucosyldiacylglycerol	Negative	x	x
973.612	GalGlcDAG 34:3	Galactosylglucosyldiacylglycerol	Negative	x	x
975.626	GalGlcDAG 34:2	Galactosylglucosyldiacylglycerol	Negative	-	x
977.648	GalGlcDAG 34:1	Galactosylglucosyldiacylglycerol	Negative	x	x

731.496	GlcDAG 28:1	Glucosyldiacylglycerol	Negative	x	-
733.511	GlcDAG 28:0	Glucosyldiacylglycerol	Negative	x	x
759.527	GlcDAG 30:1	Glucosyldiacylglycerol	Negative	x	x
761.543	GlcDAG 30:0	Glucosyldiacylglycerol	Negative	x	x
785.543	GlcDAG 32:2	Glucosyldiacylglycerol	Negative	x	-
787.559	GlcDAG 32:1	Glucosyldiacylglycerol	Negative	x	x
789.574	GlcDAG 32:0	Glucosyldiacylglycerol	Negative	x	-
811.559	GlcDAG 34:3	Glucosyldiacylglycerol	Negative	x	-
813.574	GlcDAG 34:2	Glucosyldiacylglycerol	Negative	x	x
815.590	GlcDAG 34:1	Glucosyldiacylglycerol	Negative	x	x
817.606	GlcDAG 34:0	Glucosyldiacylglycerol	Negative	x	-
839.590	GlcDAG 36:3	Glucosyldiacylglycerol	Negative	x	-
841.606	GlcDAG 36:2	Glucosyldiacylglycerol	Negative	x	x
843.622	GlcDAG 36:1	Glucosyldiacylglycerol	Negative	x	x
500.431	DAG 26:1	Diacylglycerol	Positive	x	-
528.462	DAG 28:1	Diacylglycerol	Positive	x	x
530.478	DAG 28:0	Diacylglycerol	Positive	x	x
544.493	DAG 29:0	Diacylglycerol	Positive	-	x
552.462	DAG 30:3	Diacylglycerol	Positive	x	x
554.478	DAG 30:2	Diacylglycerol	Positive	x	x
556.493	DAG 30:1	Diacylglycerol	Positive	x	x
558.509	DAG 30:0	Diacylglycerol	Positive	x	x
572.525	DAG 31:0	Diacylglycerol	Positive	-	x
570.509	DAG 31:1	Diacylglycerol	Positive	-	x
580.493	DAG 32:3	Diacylglycerol	Positive	-	x
568.494	DAG 32:2	Diacylglycerol	Positive	x	x
584.525	DAG 32:1	Diacylglycerol	Positive	x	x
598.540	DAG 33:1	Diacylglycerol	Positive	-	x
606.509	DAG 34:4	Diacylglycerol	Positive	-	x
608.525	DAG 34:3	Diacylglycerol	Positive	x	x
612.556	DAG 34:1	Diacylglycerol	Positive	x	x
624.556	DAG 35:2	Diacylglycerol	Positive	x	x
636.556	DAG 36:3	Diacylglycerol	Positive	-	x
638.572	DAG 36:2	Diacylglycerol	Positive	-	x
640.587	DAG 36:1	Diacylglycerol	Positive	x	x

4) Material and Methods

4.1 Chemicals

Table 3: List of used chemicals in this work

Chemical Name	Manufacturer
1,4-Anhydroribitol	Biosynth Carbosynth, USAs
Acetic acid, 100%	Merck, Darmstadt, Germany EMSURE® ACS, ISO, Reag. Ph Eur
Ammonium acetat (NH_4OAc)	VWR Chemicals, Hiprechrom, Leuven, Belgium
Bicinchoninic acid assay	kit Thermo Fisher Scientific, Waltham, MA, USA
Bio-Gel® P10 Media	Bio-RAD, USA Cat. #150-4144, Fine: 45-90 µm (wet)
Bio-Gel® P30 Media	Bio-RAD, USA Cat. #150-4154, Fine: 45-90 µm (wet)
Chloroform ($CHCl_3$)	Merck KGaA, Darmstadt, Germany SupraSolv for gas chromatography ECD & FID, 1.02432.2500
Citric acid	Merck KGaA, Darmstadt, Germany
Di-sodiumhydrogenphosphat	Merck, Darmstadt, Germany
DNase I	Roche Diagnostics, Indianapolis, USA DNase I from bovine pancreas grade II, Ref. 10104159001, Lot: 11733500
D-Sorbitol	Sigma-Aldrich, Steinheim, Germany
Ethanol pure 410 (EtOH)	Brüggemann Alcohol, Heilbronn GmbH, Germany
Ethylendiamintetraacetat (EDTA)	J.T, Baker, Merck, Darmstadt, Germany
Hydrofluoric acid (HF)	Sigma Aldrich, Steinheim, Germany
L(+)-Ascorbic acid	Merck, Darmstadt, Germany
Lithium chloride	Merck, Darmstadt, Germany EMSURE® ACS, Reag. Ph Eur
Lysozyme	Sigma Aldrich, Switzerland Lysozyme from chicken egg white LOT# BCBJ3179V
Methanolic hydrochloride	Upelco, Bellefonte, USA
Methanol (MeOH)	Merck KGaA, Darmstadt, Germany SupraSolv for gas chromatography ECD & FID, 1.06011.2500
Mutanolysin	Sigma Aldrich, USA Mutanolysin from *Streptomyces globisporus* ATCC 21553, 10KU
Pyridin	Merck KGaA, Darmstadt, Germany EMSURE® ACS, Reag. Ph Eur, 1.097828.1000

Ribitol	Sigma-Aldrich, Steinheim, Germany
RNase	Sigma-Aldrich Chemie GmbH, Steinheim, Germany Ribonuclease A Typ I-AS, from bovine pancreas, Lot: 28H7465, P.O. 1120
Sodiumhydroxide (NaOH)	J.T, Baker, Schwerte, Germany
Sodiumdihydrogenphosphate (NaH_2PO_4)	Merck, Darmstadt, Germany
Trifluoroacetic acid (TFA)	Merck, Darmstadt, Germany
Tris-(hydroxymethyl)-aminomethan (Tris)	Sigma Aldrich, Steinheim, Germany
Trypsin	Sigma-Aldrich Chemie GmbH, Steinheim, Germany Trypsin from bovine pancreas, Lot: #070M8709V
18:3 MGDG (synthetic) Monogalactosyldilinolenoylglycerol	Avanti polar lipids, Part of Croda International Plc, USA Avanti number: 840533P
15:0-18:1-d7-PG 1-pentadecanoyl-2-oleoly(d7)-*sn*-glycero-3-[phosphor-*rac*-(1´-glycerol)]	Avanti polar lipids, Part of Croda International Plc, USA Avanti number: 791640C
15:0-18:1-d7-PA 1-pentadecanonyl-2oleoly(d7)-*sn*-glycero-3- phosphate (sodium salt)	Avanti polar lipids, Part of Croda International Plc, USA Avanti number: 791642C
15:0-18:0-d7-15:0 TG 1,3-Dipentaceca-2-oleyol(d7)-glycerol	Avanti polar lipids, Part of Croda International Plc, USA Avanti number: 791648C
15:0-18:1-d7 DG 1-pentadecanoyl-2-oleyol(d7)-*sn*-glycerol	Avanti polar lipids, Part of Croda International Plc, USA Avanti number: 791647C
15:0-18:1-d7-PE 1-pentadecanoly-2-oleoyl(d7)-*sn*-glycero-3-phosphoethanolamine	Avanti polar lipids, Part of Croda International Plc, USA Avanti number: 791638C
15:0-18:1-d7-PI 1-pentadecanoyl-2-oleoly(d7)-sn-glycero-3-phosphoinositol (ammonium salt)	Avanti polar lipids, Part of Croda International Plc, USA Avanti number: 791641C
18:1-d7 MG 1-oleoyl(d7)-*rac*-glycerol	Avanti polar lipids, Part of Croda International Plc, USA Avanti number: 791646C
18:2 Cardiolipin-d5 1´,3`-bis[1,2-dilinoleoyl-*sn*-glycer-3-phospho]-glycerol-d5 (ammonium salt)	Avanti polar lipids, Part of Croda International Plc, USA Avanti number: 791108C
15:0-18:1-d7-PC 1-pentadecanoly-2-oleolyl(d7)-sn-glycero-3- phosphocholine	Avanti polar lipids, Part of Croda International Plc, USA. Avanti number: 791637C

4.2 Software

Table 4: List of used softwares in this work

Software	Purpose
Biorender	For creating scientific illustrations
Chemdraw	For drawing chemical structures
Clarity	For gel permeation chromatography
CorelDraw	for image editing
GraphPad Prism software version 9.4.1	For data visualization
LipidXplorer version 1.2.8.1	For lipid identification
lxPostman	For data filtering and lipid quantification.
MSD ChemStation	For GC-MS data analysis
Thermo Xcalibur Qual browser	For HRMS data analysis
Topspin 3.2	For NNR data analysis

4.3 Devices

Table 5: List of used devices in this work

Device	Manufacturer
Balance	Sartorius AG, Göttingen, Germany
Centrifuge	Eppendorf Centrifuge 5417R, Hamburg, Germany
Centrifuge 5804 R	Eppendorf, Hamburg, Germany Rotor: 5804/R: 5810/R
French Press	Constant Cell disruption system L10
Gas Chromatography/Mass Spectrometry for sugar analysis	Agilent Technologies 6890N Network GC System Autosampler: Agilent Technologies 7683B Series Injector Mass spectrometery: Agilent Technologies 5975 inert XL mass selective Detektor
Gas Chromatography/Mass Spectrometry for fatty acid analysis	Agilent Technologies 7890A Network GC System Autosampler: Agilent Technologies 7693 Series Injector Mass spectrometery: Agilent Technologies 5975C, inert XL mass selective Detektor
Lyophile (Temp.range –110 C)	Scanvac CoolSafeTM 110-4 Pro, 3450 Lynge, Denmark
pH meter	Toledo FiveEasy Plusm, Gießen, Germany
Photometer	Unicam, Germany
Q Exactive Plus mass spectrometry (HR-MS)	Thermo Scientific, Bremen, Germany
Shaker NeoMix cool	NeoLabLine, Heidelberg, Germany
Shaker MixMate	Eppendorf, Hamburg, Germany

Sorval centrifuge	Rotor: SL 250T, 14500 RPM Max Rotor: SL50T, 18500 RPM Max Thermo Scientific, Germany
SpeedVac	SPD speedVac, Thermo, Germany
TriVersa NanoMate	Advion BioSciences, Ithaca NY, USA
Ultracentrifuge	Sorvall WX Ultra Series Centrifuge, Thermo Scientific, Germany Rotor: Sorvall ® T-865, Sorvall Super T21

4.4 Consumable material

Table 6: List of used consumable materials during this work

Material	Manufacturer
Cuvette	Sarstedt AG & Co, Nuembrecht, Germany Polystyrol/Polystyrene; 10 x 4 x 45 mm; Ref. 67.742; 51588
Dialysis tubing	Roth, Mannheim, Germany Spectra/ Por® 6 Dialysis Membrane; 3,5 kDa MWCO; diameter 11,5 mm
Fractionation tube	Sarstedt AG & Co, Nuembrecht, Germany 8 mL Tubes; 100 x 13 mm; PS; 51588
1.5 mL glass vial	Macherey-Nagel GmbH & Co KG, Dueren, Germany 11,6 x 32 mm; Ref. 702 O1HP
1.5 ml screw glass vial	Macherey-Nagel GmbH & Co KG, Dueren, Germany 11,6 x 32 mm, Ref. 702004
5 mL glass vial	Macherey-Nagel GmbH & Co KG, Dueren, Germany 20,5 x 38 mm, Ref. 702 04.36
10 mL glass vial	Macherey-Nagel GmbH & Co KG, Dueren, Germany. 20,5 x 54,5 mm, Ref. 702 05.36
Pasteur pipette	BRAND GmbH & Co, Wertheim, Germany
Phosphate test Tubes	Corning, New York 14831, USA 13x100 mm; Borosilicate Glass; Pyrex® Lot No. 21214439
Stericup® Filter Unit 1,5	Merck KGaA, Darmstadt, Germany
TLC Silica gel 60F254	Merck, Darmstadt, Germany
TLC Silica gel 60F254 Glass	Merck, Darmstadt, Germany
96-well plate	Eppendorf, Hamburg, Germany

4.5 Isolation of pneumococcal cell wall components

4.5.1 Mutant construction and bacterial culture

S. pneumoniae serotype 2 strain D39 and its isogenic mutants used in this work were constructed earlier or in parallel to this thesis by Max Brendel and Dr. Thomas Kohler from the University of Greifswald using various antibiotic resistance cassettes.

Table 7: The used *Streptococcus pneumoniae* strains in this work

Serotype	Strain	Genotype	Antibiotic-resistance	Reference
2	D39	Wt		92
		Δ*cps*	Kanamycin	93
		Δ*tacL*	Erythromycin	36
		Δ*tacL*∇*tacL*	Erythromycin, Kanamycin	36
		Δ*lgt*	Erythromycin	91
		Δ*lytR*	Kanamycin	92

4.5.2 Isolation of pneumococcal glycopolymers

4.5.2.1 Extraction of lipoteichoic acid (pnLTA)

Lipoteichoic acid isolation from pneumococcal cultures followed a procedure long-term established in the group[36]. In brief, 2.5 liters of *S. pneumoniae* cultures were suspended in 60 mL of 0.05 M citrate buffer. The cells underwent three rounds of disruption using a French press at 10 °C and 20 kPsi. Subsequently, sodium dodecyl sulfate (SDS) was added to get a final concentration of 4%, and the digested cells were boiled at 100 °C for 30 min. The resulting solution was stirred at RT overnight. SDS was used to aid in the separation of LTA from the WTA-PGN-CPS complex through ultracentrifugation (15 min, 4 °C, 30,000 x g). As the result of the ultracentrifugation, the WTA-PGN-CPS complex remained in the pellet, while the supernatant containing the LTA was carefully collected. To ensure effective separation, the pellets were washed three times with a citrate buffer and centrifuged as previously mentioned. Afterward, lyophilization was performed on both combined supernatants and pellets.

To reduce the amount of SDS in the lyophilized supernatants, the material was dissolved in pure ethanol and partially precipitated through centrifugation at 20 °C and 10,650 x g for 15 min. Before each subsequent centrifugation step, the resulting pellet was re-

dissolved with pure ethanol. A small volume from the supernatant after the third washing step was taken and loaded onto a thin-layer chromatography plate to check for the presence of residual SDS. If SDS was still present, further washing and centrifugation steps were performed.

The washed LTA-containing pellet was dried by lyophilization and was then subjected to butanol-water extraction. For this extraction, the pellets were dissolved in 150 mL of butanol and mixed with warmed 0.05 M citrate buffer at 20 °C. The mixture was stirred for 30 min at RT and subsequently centrifuged at 4,000 x g for 15 min at 4 °C. The aqueous phase was removed, and the organic phase (butanol) was subjected to two additional rounds of stirring, each with 100 mL of citrate buffer for 30 min, followed by centrifugation. The combined aqueous phases, which contained the LTA, were lyophilized and to decrease the salt concentration, the resulting lyophilized material was dissolved in Millipore-water (MP) against 10 L of 0.05 M NH_4OAc and transferred to dialysis tubes (MWCO: 3.5 kDa, 11.5 diameter). The dialysis buffer was changed every 24 h for a period of five days. The inner dialysate was lyophilized. The lyophilized dialysate was then suspended in 0.05 M NH_4OAc and 15% 1-propanol, transferred to 1.5 mL eppendorf tubes, and centrifuged for 5 min at 13,000 x g at RT. The resulting pellet was further dissolved as much as possible in 0.05 M NH_4OAc (pH 4.7) with 15% 1-propanol, followed by centrifugation step. The resulting supernatants were transferred to pre-weighed glass vials. This procedure was repeated twice, and the combined supernatants were lyophilized. The subsequent step involved using hydrophobic interaction chromatography (HIC) to purify the LTA. This separation technique was conducted using the following equipment and conditions:

Column: High Prep Octyl FF 16/10 GE Healthcare
Flow rate: 1 mL/min
Mobile phase:
A: 50 mM NH_4OAc, pH 4.7 + 15% 1-propanol
B: 50 mM NH_4OAc, pH 4.7 + 60% 1-propanol
Wavelength: 254 nm
Gradient: The gradient for the HIC run starts with mobile phase A at 100% and mobile phase B at 0% for the first 40 min. From 40 to 120 min, a linear gradient is applied, gradually changing the composition from 100% mobile phase A and 0% mobile phase B to 0% mobile phase A and 100% mobile phase B. From 150 to 180 min, a linear gradient is applied to reach 0% mobile phase B, followed by an isocratic step from 180 to 240 min with 0% mobile phase B.

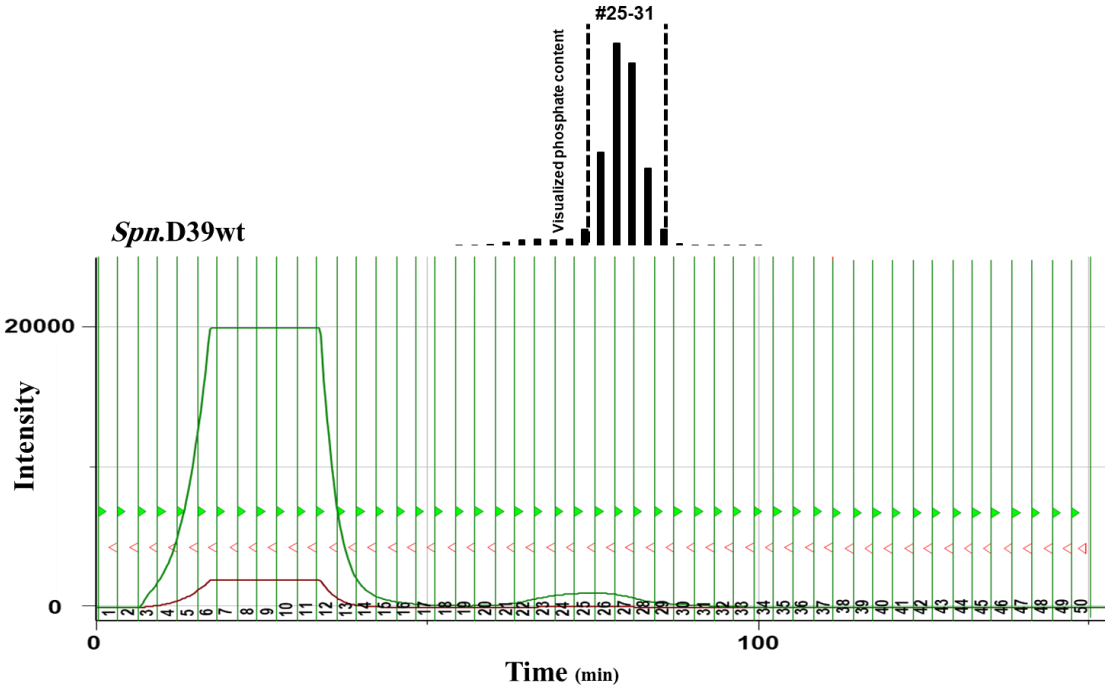

Figure 32: Representative HIC chromatogram including the corresponding phosphate test for *Spn* D39Wt for fractions #20-40.

4.5.2.1.1 Determination of the phosphate content in teichoic acid

The determination of phosphate content was performed based on previously published protocol[36]. Briefly, for the determination of the inorganic phosphate content, 100 µL of each collected fraction (post HIC separation, **Figure 32**) and pairs of the 2, 4, 6, 8, 10 µL of the standard solution (0.05 M Na_2HPO_4) were pipetted into glass tubes. After drying the tubes by placing them in a vacuum overnight, the dried sample were incubated with 100 µL releasing reagent ($HClO_4$) at 100 °C for 1 h and at 165 °C for 2 h. Next, the samples were cooled on ice and 1 mL of the color reagent solution (consisting of 35 mL of MP, 5 mL of 2.5% ammonium molybdate, 1 M sodium acetate, and 10% ascorbic acid) was added to each tube. Later, the solutions were incubated at 37 °C for 90 min, and the total phosphate content was measured at 820 nm.

4.5.2.1.2 Hydrofluoric acid treatment of teichoic acid

During pnTA extraction steps, aliquots were taken at different steps (**Figure 7**) for GC-MS based quantification. These aliquots were subjected to an acidic treatment by adding 50 µL of hydrogen fluoride (HF), followed by incubation for 72 h at 4 °C with stirring. To stop the HF treatment, 100 µL of MP were added to the samples, and the solution was dried using a nitrogen stream. This drying process was repeated twice, with each step involving the addition of 500 µL of MP and subsequent drying under a nitrogen stream. Subsequently, the samples were transferred in 500 µL portions into 1.5 mL glass vials and

dried once again under a nitrogen stream. It is important to be careful when handling with such a highly acidic substance.

4.5.2.1.3 Trifluoroacetic acid treatment of teichoic acid

The HF treated samples were additionally subjected to trifluoroacetic acid (TFA) treatment to breakdown the glycosidic bonds between monosaccharide-LTA components. Each sample received 1 mL of TFA, which was heated at 100 °C for 4 h. Subsequently, the samples were dried using nitrogen gas. All these steps were performed in 1.5 mL glass vials.

4.5.2.1.4 Strong methanolysis of released monosaccharide

Volume of 100 µL of a 3 mM methanolic acid (formic acid) solution was added to each sample (post HF and TFA treatment). The samples were then heated at 85 °C for a duration of 15 min and then dried under nitrogen stream.

4.5.2.1.5 Derivatization of released methylated monosaccharide

Derivatization of the released monosaccharides from pnTA is necessary to make them measurable in GC-MS. To do that, the samples were treated with 250 µL of acetic anhydride followed by 250 µL of pyridine. After adding the reagents, the samples were heated at 85 °C for 15 min. Subsequently, they were dried using a nitrogen stream and washed with methanol three or four times (each time using 200 µL).

4.5.2.1.6 Preparation of matrix matched calibration samples

Matrix-matched calibration samples are used to determine the ratio of LTA and WTA in Wt and Δ*lytR*. The washed WTA-PGN-CPS complex isolated from the Wt has been selected as the matrix sample (**Figure 7**). To prepare the matrix-matched calibration curve, 40 µL of the selected matrix sample (dissolved in MeOH) was poured in seven GC-MS vials, dried under N_2, and enriched with authentic calibrants at various concentrations within the same dynamic range defined earlier. Subsequently, it was dried once more, spiked with the IS (Sorbitol) at a concentration of 2.5 µg/mL (**Figure 10 A**). Blank matrix sample (**Figure 10 B**) was prepared by taking another 40 µL from the selected matrix sample and spiked only with IS (2.5 µg/mL). In this preparation, the size of the used GC-MS vials necessitates three different separated drying steps.

4.5.2.2 Isolation and NMR analysis of the capsule polysaccharide

The obtained WTA-PGN-CPS complex (**Figure 7**) was also utilized for pneumococcal capsule isolation. This complex was dissolved in Tris-HCl buffer (pH 4.7) to get a concentration of 1 mg/mL. The dissolved complex was subsequently treated with LytA (autolysin), followed by centrifugation. This treatment helps in breakdown or destruction process of the bacterial cell wall. The resulting pellet underwent further treatment with Mutanolysin and Lysozyme, followed by another centrifugation step. These treatments

and centrifugation steps were performed following the procedures described in previous published work[36]. Additional details can be found in section 2.2.

4.5.2.2.1 Desalting by size exclusion chromatography

All of the resulted material for capsule isolation was firstly reconstituted in 1 mL of NH_4OAc (0.5 M, pH 4.7) and then purified by P10 or P30 to remove any salt components using 0.05 M NH_4OAc (pH 4.7) as the mobile phase.

4.5.2.2.2 NMR spectroscopy

NMR measurements were conducted together with Dr. Nicolas Gisch on a 700 MHz Bruker Bio-Spin spectrometer equipped with a 5 mm inverse quadruple resonance cryoprobe. Spectra were recorded using TopSpin 3.0/3.1 from Bruker BioSpin. Acetone served as the external calibration standard for ^{1}H NMR (δ_H 2.225 ppm at 300 K). For ^{31}P NMR, 85% phosphoric acid in D_2O (δ_P 0.0 ppm at 300 K) was used as the external reference.

4.6 Isolation of pneumococcal lipids

4.6.1 Preparation of lipidomics samples and study design

Preparation of bacterial samples for lipidomics was carried out by Max Brendel of the group Molecular Genetics and Infection Biology at University of Greifswald, Germany. Briefly, *S. pneumoniae* strains were cultured on Columbia blood agar plates (Thermo Scientific) supplemented with kanamycin (125 µg/mL), erythromycin (2.5 µg/mL), or chloramphenicol (8 µg/mL), if necessary. Liquid cultures were grown in Todd-Hewitt broth (THY; Roth) supplemented with 0.5% yeast extract. Blood agar plates were incubated at 37 °C with 5% CO_2 for 8-10 h. Cultivation in liquid cultures was performed at 37 °C without agitation until reaching the mid-logarithmic phase (OD_{600} 0.35-0.45). Cultures were then harvested at 3,275 x g and washed three times with PBS (pH 7.4). The strains were subsequently resuspended in fresh PBS (pH 7.4) at a volume of 40 mL in a 50 mL Falcon tube. From this, 8 mL were used for CFU determination, and the remaining suspension was equally divided into eight 5 mL Eppendorf tubes (4 mL each). The Eppendorf tubes were then centrifuged, and the supernatant was discarded. The resulting pellets were fixed in methanol containing 0.184% BHT. One aliquot was used for sterility control testing[91]. All samples were stored at –80 °C and sent to Borstel for lipid analysis. Summary of all steps is illustrated in **Figure 19**. The following table lists the preparation date, number of biological replicates, and CFU in a 5 mL tube for all investigated strains.

Table 8: Colony forming units for all used samples in lipidomics study.

Preparation date (batch date)	Sample	Biological replicate	CFU / 5 mL tube
December 2021	D39 Wt	1	$1.32*10^9$
		2	$1.12*10^9$
		3	$1.48*10^9$
	D39 Δ*cps*	1	$2.88*10^9$
		2	$2.12*10^9$
		3	$2.6*10^9$
	D39 Δ*tacL*	1	$1.50*10^9$
		2	$1.56*10^9$
		3	$1.36*10^9$
	D39 Δ*tacL*∇*tacL*	1	$2.08*10^9$
		2	$2.0*10^9$
		3	$1.64*10^9$
April 2022	D39 Wt	1	$1.1*10^9$
		2	$1.2*10^9$
		3	$0.84*10^9$
	D39 Δ*cps*	1	$2.1*10^9$
		2	$1.5*10^9$
		3	$2.4*10^9$
	D39 Δ*tacL*	1	$1.1*10^9$
		2	$1.2*10^9$
		3	$1.2*10^9$
	D39 Δ*tacL*∇*tacL*	1	$0.68*10^9$
		2	$0.52*10^9$
		3	$0.8*10^9$
October 2022	D39 Wt	1	$0.88*10^9$
		2	$1.2*10^9$
		3	$1.7*10^9$
	D39 Δ*cps*	1	$1.1*10^9$
		2	$1.8*10^9$
		3	$2.7*10^9$
	D39 Δ*tacL*	1	$0.56*10^9$
		2	$0.84*10^9$
		3	$0.92*10^9$

	D39 Δ*tacL*∇*tacL*	1	$0.32*10^9$
		2	$1.7*10^9$
		3	$1.6*10^9$
	D39 Δ*lgt*	1	$0.72*10^9$
		2	$0.76*10^9$
		3	$1.4*10^9$
February 2023	D39 Δ*lgt*	1	$0.92*10^9$
		2	$1.48*10^9$
		3	$0.74*10^9$

4.6.2 Lipid extraction

Total lipids were extracted from frozen bacterial aliquots according to the methyl-*tert*-butyl ether (MTBE) method[55]. Briefly, samples were dried in a SpeedVac and solved in 100 µL water. In-house modified internal standard mix based on (SPLASH Lipidomics from Avanti) was first used to determine roughly the proportions of each lipid class. Based on the pilot experiment, a customized *Spn* internal standard was developed. This *Spn* IS contains different, nearly all deuterated, lipid species to avoid any overlap with endogenous species and listed in **Table 1**.

Table 9 describes the components and the calculated concentration of each component for the IS mix used in preliminary tests to adjust the concentrations of individual lipid classes.

Table 9: **In-house modified internal standard mix (based on SPLASH Lipidomics from Avanti) considering expected calculated concentrations for each component when 20 µL were added.** Species marked with stars represent lipid species that have been spiked in-house.

Lipid class	Lipid species	Conc. (pmol/ 20 µL)
PC	15:0-18:1-d7-PC	839.87
PE	15:0-18:1-d7-PE	31.30
PS	15:0-18:1-d7-PS	21.08
P	15:1-18:1-d7-PG	146.77
PI	15:0-18:1-d7-PI	42.14
PA	15:0-18:1-d7-PA	42.00
MAG	18:1-d7 MAG	20.79
TAG	15:0-18:1-d7-TAG	272.97
DAG	15:0-18:1-d7 DAG	62.85
LPC	18:1-d7- LPC	189.06
LPE	18:1-d7- LPE	42.28
CE	18:1-d7- Chol Ester	2100.12
SM	18:1-d9- SM	186.42

ST	Cholesterol(d7)	10497.70
Cer*	C15 Ceramide-d7 (d18:1-d7/15:0)	367.27
HexCer*	C15 Glucosyl (Beta) Ceramide-D7 (D18:1-D7)	144.43
PC-O-P*	C18 (plasm)-18:1-d9- PC	128.00
PE-O-P*	C18 (plasm)-18:1-d9- PE	167.9
ACar*	C26 D, L- Carnitine-d9	460
CL*	18:2/18:2-18:2/18:2-d5-CL	167.9

Following the addition of the internal standard, 540 µL of acidified methanol (containing 3% v/v acetic acid) and 2 mL of MTBE were added to the solution, respectively. The next step was to incubate the mixture for 1 h at RT with continuous shaking at 500 rpm. Afterwards, 500 µL of water were added, and the mixture was centrifuged for 4 min at RT at 16,000 × g. The upper phase was carefully collected in a separate tube. The lower phase underwent a re-extraction process with 800 µL of the re-extraction solution (comprising 20 mL of MTBE, 6 mL of 3% acidified methanol, and 5 mL of water). After vortexing and incubating for 20 min at RT with continuous shaking at 500 rpm, the solution was once again centrifuged as previously described. The resulting upper phases were combined (approximately 2,400 µL) and dried using a SpeedVac. The dried extracts were dissolved in 100 µL of a mixture containing chloroform, methanol, and water (60/30/4.5; v/v/v), then stored at −80 °C and divided into aliquots for lipidomics measurements.

4.6.3 Lipidomics data acquisition

The lipid extracts were dissolved (1:20 v/v) in a solution composed of isopropyl alcohol (IPA), methanol containing 10 mM ammonium acetate, and chloroform. The solvent ratio used for the dissolution was IPA/MeOH with ammonium acetate/$CHCl_3$ in a proportion of 4:2:1 (v/v/v). These dissolved lipid extracts were subsequently added to a 96-well plate for MS analysis. To introduce the lipid samples into the mass spectrometer, a robotic nanoflow ion source (Triversa NanoMate) was used. This advanced system enabled precise and controlled infusion of the lipid samples into the Q-Exactive Plus mass spectrometer. The infusion process utilized chips equipped with spray nozzles, which facilitated the efficient ionization of the lipids.

Following injection, samples underwent both full MS^1 and MS^2 analyses. The first full MS^1 scan covered a broad mass range from *m*/*z* 350 to 2000 and was followed by eight consecutive full MS scans acquired every 100 ms within a narrower *m*/*z* range of 360 to 1000. This strategy allowed for both comprehensive detection of diverse analytes and targeted profiling of specific compounds. The consecutive full MS^1 scans were acquired with five micro scans per scan, a maximum injection time of 100 ms, and a resolving power of 2.8×10^5.

MS^2 acquisitions were performed with several specific parameters set, such as a micro scan count of one, a targeted resolving power of 7×10^4, a MS^2 isolation width of *m*/*z* 1, a

max injection time of 200 ms, an AGC target of 1 x 10^5, and a HCD energy of 30 eV. MS^2 acquisitions targeted parent ions within the range of *m/z* 360 to 1000 using an inclusion list. The lower resulting mass from MS^2 acquisitions was fixed at *m/z* 180 for both modes, while the upper mass limit was set to scale with the parent ion. These settings have been previously optimized in the group to enhance sensitivity, resolution and selectivity of the MS^2 acquisitions.

4.6.4 Lipid identification

To facilitate analysis using LipidXplorer software, all acquired spectra were initially converted to a mzML file format using the Msconvert software. This step is necessary to be able to interpret and analyze the data with lipidXplorer software.

The settings for the MS analysis by LipidXplorer were a selection window of 0.4 Da, a resolution of 1.8 x 10^5 at *m/z* 350, a tolerance of 2 ppm, a relative threshold of 0.001%, and a resolution gradient of −147 for positive mode and −155 for negative mode. The minimum occupation was set to 0.1 and there was no MS^1 offset. The frequency filter was set to 0.6 for positive mode and to 0.4 for negative mode.

In the positive mode, background peaks corresponding to 18:1-d7 MAG (*m/z* 381.3709), Tris(di-*tert*-butylphenyl) phosphate (*m/z* 680.4802), and 15:0-18:1-d7-TAG (*m/z* 829.7985) were utilized as lock masses. Similarly, in the negative mode, Octadecyl (di-*tert*-butyl-hydroxyphenyl)propionate (*m/z* 529.4626), 15:0-18:1-d7-PG (*m/z* 740.5477), and 18:3 GalDAG (*m/z* 833.5437) were employed as lock masses. These lock masses served as reference points to ensure accurate spectra alignment.

For the MS^2 analysis, the resolution was set to 6e4, the tolerance and relative threshold were both set to 2 ppm and 0.001% for positive mode and 2 and 0.005% for negative mode, respectively, with a resolution gradient of −60 for positive mode and −50 for negative mode and a minimum occupation of 0.1. The frequency filter was also set to 0.6 for positive mode and to 0.49 for negative mode. The settings used for lipid identification are summarized in the following in **Figure 33** and **Figure 34**.

In the analysis, lipid species identifications were assigned when the mass accuracy was set at 4 ppm. Using customized MFQL scripts, the following lipid classes were identified in negative ESI mode: CL, PA, PG, GlcDAG and GalGlcDAG. In positive ESI mode, PC and DAG were identified. All used MFQL scripts can be found in section 4.6.9.

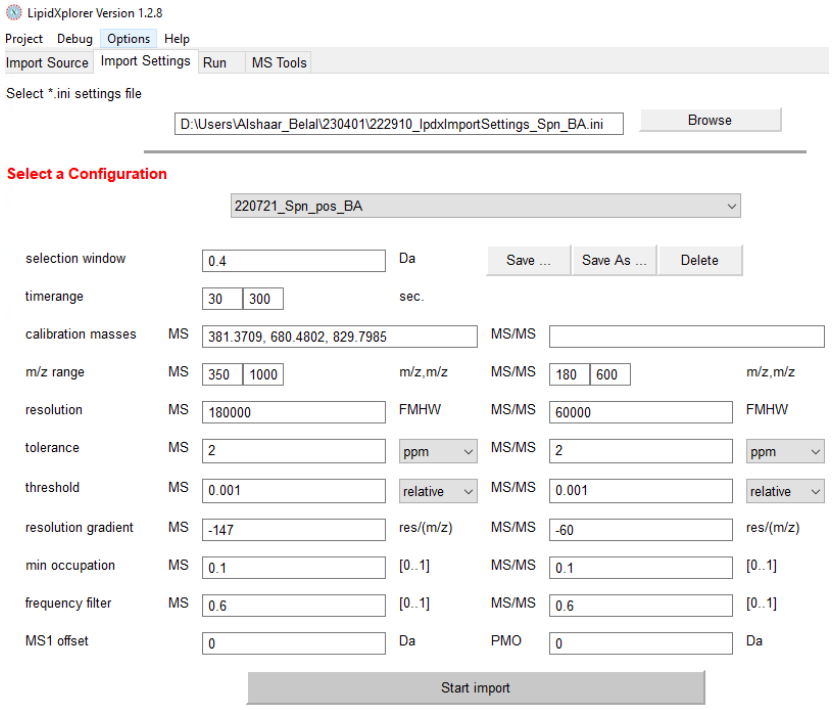

Figure 33: LipidXplorer window displaying the selected settings for lipid annotation in positive mode.

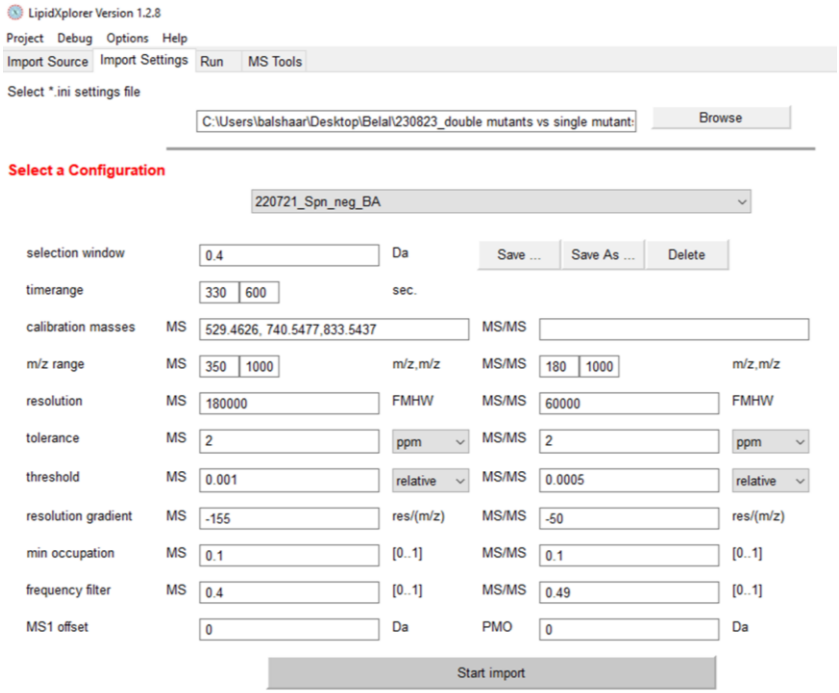

Figure 34: LipidXplorer window displaying the selected settings for lipid annotation in negative mode.

4.6.5 Lipid quantification

The generated data by LipidXplorer is imported into lxPostman, where it is combined and analyzed. To ensure that the results are accurate, a step is taken to eliminate any false-positive signals that may have been introduced during the extraction process. This is done by removing any lipid species that are not at least 10 times more concentrated in the sample compared to the control blank samples. The method for determining the concentration of different lipid species in a set of samples involves identifying specific fragments for each species using MFQL files. The intensity of these fragments is then used to calculate ratios which are used to compute the concentration of each lipid species.
The intensity ratios of precursors were determined for PE, PI, PA, and PG in negative ion mode, and for DAG and PC in positive ion mode. The concentration of different lipid species in a set of samples is determined by comparing the intensity of signals associated with each species to internal standards of known concentration. Lipid species that appear in multiple samples are retained, while those that partially appeared are filtered out by setting a minimum threshold of 50% occupation. A regularly updated version of lxPostman can be accessed at the following location https://apps.lifs.isas.de/ in the tab R shiny Apps.

4.6.6 Determination of protein content by bicinchoninic acid assay

Protein quantification was conducted using a standard Bicinchoninic acid assay (BCA) according to the manufacturer's instructions. In brief, the remaining aqueous phase of the lipid extraction (**Figure 19**) was dried using a SpeedVac and subsequently resuspended in 300 µL of buffer (1% (wt/v) SDS buffered to pH 6.8 with Tris/HCl). The samples were then incubated for 15 min on a shaker (650 rpm) and centrifuged for 2 min at 20,000 x g.
The next step involved preparing calibration solutions by diluting the Thermo BSA stock solution as follows:

Table 10: Serial standard concentrations were used to generate the calibration curve for determining the protein content.

Vial	Volume of Diluent (µL)	Volume and Source of BSA (µL)	Final BCA Concentration µg/mL
A	0	300 of Stock	2000
B	125	375 of Stock	1500
C	325	325 of Stock	1000
D	175	175 of vial B dilution	750
E	325	325 of vial C dilution	500
F	325	325 of vial E dilution	250

G	325	325 of vial F dilution	125
H	400	325 of vial G dilution	25
I	400	0	0=Blank

Next, 50 mL of BCA Reagent A and 1 mL of BCA Reagent B were mixed to prepare the working reagent. Subsequently, 25 µL of each standard or sample were pipetted into a microplate well. To each well, 200 µL of the working reagent were added, and the plate was thoroughly mixed on a plate shaker for 30 sec. The plate was then covered and incubated at 37 °C for 30 min, followed by cooling to room temperature. Absorbance was measured at 562 nm in technical triplicates.

4.6.7 Fatty acid extraction and analysis by GC-MS

At the beginning, aliquots of 300 µL from each studied bacterial strain are transferred into 1.5 mL glass vials and dried using a SpeedVac. As an internal standard, a non-endogenous fatty acid, C19:0 with a concentration of 10 ng/µL, is added. Fatty acid release is accomplished by treating the samples with 100 µL of 4 M HCl and heating them at 100 °C for 4 h on heating plate.

To neutralize the pH of the samples, 100 µL of 5 M NaOH was introduced, and the mixture is heated at 100 °C for 30 min. Subsequently, 500 µL of water was added, followed by three consecutive additions of 500 µL of chloroform. After each addition, the organic phase is carefully collected. The organic phase is then dried under a nitrogen stream and dissolved in 100 µL of chloroform/methanol (1:1, v/v).

Next, to generate fatty acid methyl esters (FAME), 200 µL of diazomethane is added to the samples, which are left at RT for 30 min. Another drying step using a nitrogen stream is carried out and the fatty acid samples are then dissolved in 100 µL of chloroform before GS-MS analysis.

All GC-MS analysis were carried out on an Agilent Technologies 6890N gas chromatograph coupled to a 5975 inert XL Mass Selective Detector. Injection volume was 1 µL in splitless mode. The used GC column was a HP-5ms (5%-phenyl methylpolysiloxane) with the following dimensions: 30 m x 250 µm x 0.25 µm (Agilent, Germany). The initial temperature of GC column was 70 °C (hold 1.5 min), raised linearly with 60 °C/min to 150 °C (hold 3 min), then increased linearly to 320 °C with 5 °C/min. The whole run time was 44.8 min. Identification of each fatty acid was performed based on injecting FAME standard solutions under the same condition and their respective mass spectra. Raw GC/MS dataset were processed by MSD ChemStation, using a threshold of 14.

4.6.8 Separation of lipids on high performance thin layer chromatography

Initially, various GLs and GPs standards were applied to high performance thin layer chromatography (HPTLC) plates. Multiple attempts were made to determine the optimal concentration of standards that would enhance visualization using the staining methods employed. Once the appropriate visible concentration was determined for each tested lipid class, the most suitable amounts of PG, CL, PA, PC, DAG, TAG, GlcDAG, and GalGlcDAG standards were applied to HPTLC plates made of silica gel 60 on glass, measuring 10 x 10 cm with a layer thickness of 0.25 mm. The lipids were separated on the plates using a mobile phase of chloroform/methanol/water (65:25:4, v/v/v). After separation, the HPTLC plates were allowed to air-dry. It's worth mentioning that all HPTLC plates used for lipid separation in this study were initially washed with the same mobile phase mentioned above and then dried in an oven at 120 °C for 1 h. Next, the separated HPTLC spots were stained by immersing them in a solution of 0.03% Coomassie Brilliant Blue G250 in 20% methanol for 15 min. To remove background staining, the plates were put in a solution of 20% methanol for 7-8 min. Finally, the HPTLC plates were air-dried again. The identical procedure described above was employed to analyze different total extracted *Spn* lipids. After the HPTLC plates were stained with Coomassie, the individual lipid spots could be carefully scraped off the plate using a scalpel. The scraped material was subsequently resuspended in 45 µL of MP. Following this, 160 µL of chloroform were added, and the mixture was vigorously vortexed for 2 min. Subsequently, 320 µL of methanol were added, and another round of vortexing was conducted for 20 min. Finally, 320 µL of MP were added, and the mixture was centrifuged at 2,000 x g for 2 min at RT. This step was performed to separate the different classes of the extracted lipids, enabling further analysis using HRMS. Additional information regarding these experiments is described in section 2.3.4.

4.6.9 MFQL scripts

4.6.9.1 MFQL files for customized *Spn* internal standard in positive ion mode

4.6.9.1.1 15:0-18:1-d7 DAG

```
QUERYNAME = DAGSplash;
DEFINE Precursor = 'C[36] H[20..200] D[7] N[1] O[5]' WITH DBR = (0.5,12.5), CHG = +1;
DEFINE FragmentA = 'C[15] H[10..60] N[1] O[2] ' WITH DBR = (0.0,6.0), CHG = 0;
DEFINE FragmentB = 'C[18] H[10..60] D[7] N[1] O[2] ' WITH DBR = (0.0,6.0), CHG = 0;
IDENTIFY
        Precursor IN MS1+ AND
        FragmentA IN MS2+ AND
        FragmentB IN MS2+
SUCHTHAT
        FragmentA.chemsc + FragmentB.chemsc + 'C3 H6 O1' == Precursor.chemsc + 'N1 H4'
REPORT
        LipidSpecies = "IS DAG 15:0-18:1(+[2]H7)";
        LipidClass = "DAG";
        Mass = Precursor.mass;
        IsobaricClass = Precursor.isobaric;
        ChemicalFormula = Precursor.chemsc;
        DerivatizedForm = "None";
        AdductIon = "+NH4+";
        LipidCategory = "Internal standard";
        ScanPolarity = "positive";
        Intensity = FragmentB.intensity;
        IdentificationLevel = "MS2";
        QuantificationIon = "FragmentB";

        PrecursorIdentifier = "[DAG %d:%d_%d:%d(+[2]H7) +NH4]+" % "( (FragmentA.chemsc[C]), (FragmentA.chemsc[db]),
        (FragmentB.chemsc[C]), (FragmentB.chemsc[db]) )";
        FragmentAIdentifier = "-FA %d:%d(-H) -DAG(35)" % "( (FragmentA.chemsc[C]), (FragmentA.chemsc[db]))";
        FragmentBIdentifier = "-FA %d:%d(+[2]H7 -H) -DAG(35)" % "( (FragmentB.chemsc[C]), (FragmentB.chemsc[db]))";
        FragmentCIdentifier = "None";
        PrecursorIntensity = Precursor.intensity;
        FragmentAIntensity = FragmentA.intensity;
        FragmentBIntensity = FragmentB.intensity;
        FragmentCIntensity = "None";
        PrecursorERRppm = "%2.2f" % "(Precursor.errppm)";
        FragmentAERRppm = "%2.2f" % "(FragmentA.errppm)";
        FragmentBERRppm = "%2.2f" % "(FragmentB.errppm)";
```

```
        FragmentCERRppm = "";
        ;
################ end script ##################
```

4.6.9.1.2 15:0-18:1-d7 TAG

```
QUERYNAME= TAGSplash;
DEFINE Precursor = 'C[51] H[93] D[7] N[1] O[6]' WITH DBR = (1.5,19.5), CHG = +1;
DEFINE FragmentA = 'C[18] H[10..76] D[7] N[1] O[2] ' WITH DBR = (0.0,6.0), CHG = 0;
IDENTIFY
        Precursor IN MS1+ AND
        FragmentA IN MS2+
REPORT
        LipidSpecies = "IS TAG 15:0_18:1(+[2]H7)_15:0";
        LipidClass = "TAG";
        Mass = Precursor.mass;
        IsobaricClass = Precursor.isobaric;
        ChemicalFormula = Precursor.chemsc;
        DerivatizedForm = "None";
        AdductIon = "+NH4+";
        LipidCategory = "Internal standard";
        ScanPolarity = "positive";
        Intensity = Precursor.intensity;
        IdentificationLevel = "MS2";
        QuantificationIon = "Precursor";
        PrecursorIdentifier = "[TAG %d:%d(+[2]H7) +NH4]+" % "((Precursor.chemsc[C]-3), (Precursor.chemsc[db]-1.5))";
        FragmentAIdentifier = "-FA %d:%d(+[2]H7 +HO -TAG(17))" % "( (FragmentA.chemsc[C]), (FragmentA.chemsc[db]))";
        FragmentBIdentifier = "None";
        FragmentCIdentifier = "None";
        PrecursorIntensity = Precursor.intensity;
        FragmentAIntensity = FragmentA.intensity;
        FragmentBIntensity = "None";
        FragmentCIntensity = "None";
        PrecursorERRppm = "%2.2f" % "(Precursor.errppm)";
        FragmentAERRppm = "%2.2f" % "(FragmentA.errppm)";
        FragmentBERRppm = "";
        FragmentCERRppm = "";
        ;
################ end script ##################
```

4.6.9.1.3 15:0-18:1-d7 PC

```
QUERYNAME = PCSplash;
DEFINE Precursor = 'C[41] H[74] D[7] O[8] N[1] P[1]' WITH DBR = (1.5,11.5), CHG = +1;
```

```
DEFINE FragmentA = 'C[5] H[15] O[4] N[1] P[1]' WITH DBR = (1.5,3.5), CHG = +1;
IDENTIFY
        Precursor IN MS1+ AND
        FragmentA IN MS2+
REPORT
        LipidSpecies = "IS PC 15:0-18:1(+[2]H7)";
        LipidClass = "PC";
        Mass = Precursor.mass;
        IsobaricClass = Precursor.isobaric;
        ChemicalFormula = Precursor.chemsc;
        DerivatizedForm = "None";
        AdductIon = "+H+";
        LipidCategory = "Internal standard";
        ScanPolarity = "positive";
        Intensity = Precursor.intensity;
        IdentificationLevel = "MS2";
        QuantificationIon = "Precursor";
        PrecursorIdentifier = "[PC %d:%d(+[2]H7) +H]+" % "((Precursor.chemsc)[C] - 8, (Precursor.chemsc)[db] - 1.5)";
        FragmentAIdentifier = "PC(184)";
        FragmentBIdentifier = "None";
        FragmentCIdentifier = "None";
        PrecursorIntensity = Precursor.intensity;
        FragmentAIntensity = FragmentA.intensity;
        FragmentBIntensity = "None";
        FragmentCIntensity = "None";
        PrecursorERRppm = "%2.2f" % "(Precursor.errppm)";
        FragmentAERRppm = "%2.2f" % "(FragmentA.errppm)";
        FragmentBERRppm = "";
        FragmentCERRppm = "";
        ;
################ end script ##################
```

4.6.9.1.4 18:1-d7 MAG

```
 QUERYNAME = MAGSplash;
#DEFINE Precursor = 'C[21] H[34] D[7] O[4]' WITH DBR = (-2.5,5.5), CHG = 1; #M+H+
DEFINE Precursor = 'C[21] H[37] D[7] O[4] N[1]' WITH DBR = (-2.5,5.5), CHG = 1; #M+NH4+
#DEFINE Precursor = 'C[23] H[36] D[7] O[6]' WITH DBR = (-2.5,5.5), CHG = 1; #M+CH3COO+
IDENTIFY
        Precursor IN MS1+
REPORT
        LipidSpecies = "IS MAG 18:1(+[2]H7)";
```

```
        LipidClass = "MAG";
        Mass = Precursor.mass;
        IsobaricClass = Precursor.isobaric;
        ChemicalFormula = Precursor.chemsc;
        DerivatizedForm = "None";
        AdductIon = "+NH4+";
        LipidCategory = "Internal standard";
        ScanPolarity = "positive";
        Intensity = Precursor.intensity;
        IdentificationLevel = "MS1";
        QuantificationIon = "Precursor";
        PrecursorIdentifier = "[MAG %d:%d(+[2]H7) +NH4]+" % "((Precursor.chemsc)[C] - 3, (Precursor.chemsc)[db] + 0.5)";
        FragmentAIdentifier = "None";
        FragmentBIdentifier = "None";
        FragmentCIdentifier = "None";
        PrecursorIntensity = Precursor.intensity;
        FragmentAIntensity = "None";
        FragmentBIntensity = "None";
        FragmentCIntensity = "None";
        PrecursorERRppm = "%2.2f" % "(Precursor.errppm)";
        FragmentAERRppm = "";
        FragmentBERRppm = "";
        FragmentCERRppm = "";
        ;
################ end script ##################
```

4.6.9.2 MFQL files for pneumococcal lipids in positive ion mode

4.6.9.2.1 *Spn*_DAG

```
QUERYNAME = Diacylglycerol;
DEFINE Precursor = 'C[29..49] H[20..150] N[1] O[5]' WITH DBR = (0.5,4.5), CHG = +1;
DEFINE FragmentA = 'C[12..22] H[10..60] N[1] O[2] ' WITH DBR = (0.0,2.0), CHG = 0;
DEFINE FragmentB = 'C[12..22] H[10..60] N[1] O[2] ' WITH DBR = (0.0,2.0), CHG = 0;
IDENTIFY
        Precursor IN MS1+ AND
        FragmentA IN MS2+ AND
        FragmentB IN MS2+
SUCHTHAT
        FragmentA.chemsc + FragmentB.chemsc + 'C3 H6 O1' == Precursor.chemsc + 'N1 H4' AND
        (FragmentA.chemsc[db] == 0 OR FragmentA.chemsc[C]/FragmentA.chemsc[db] >= 3.6) AND
        (FragmentB.chemsc[db] == 0 OR FragmentB.chemsc[C]/FragmentB.chemsc[db] >= 3.6) AND
        FragmentA.chemsc[C] <= FragmentB.chemsc[C]
```

```
REPORT
        LipidSpecies = "DAG %d:%d"  % "((Precursor.chemsc)[C] - 3, (Precursor.chemsc)[db] - 0.5)";
        LipidClass = "DAG";
        Mass = Precursor.mass;
        IsobaricClass = Precursor.isobaric;
        ChemicalFormula = Precursor.chemsc;
        DerivatizedForm = "None";
        AdductIon = "+NH4+";
        LipidCategory = "Glycerolipid";
        ScanPolarity = "positive";
        Intensity = Precursor.intensity;
        IdentificationLevel = "MS2";
        QuantificationIon = "Precursor";
        PrecursorIdentifier = "[DAG %d:%d_%d:%d +NH4]+" % "( (FragmentA.chemsc[C]), (FragmentA.chemsc[db]),
        (FragmentB.chemsc[C]), (FragmentB.chemsc[db]) )";
        FragmentAIdentifier = "-FA %d:%d (-H) -DAG(35)" % "( (FragmentA.chemsc[C]), (FragmentA.chemsc[db]))";
        FragmentBIdentifier = "-FA %d:%d (-H) -DAG(35)" % "( (FragmentB.chemsc[C]), (FragmentB.chemsc[db]))";
        FragmentCIdentifier = "None";
        PrecursorIntensity = Precursor.intensity;
        FragmentAIntensity = FragmentA.intensity;
        FragmentBIntensity = FragmentB.intensity;
        FragmentCIntensity = "None";
        PrecursorERRppm = "%2.2f" % "(Precursor.errppm)";
        FragmentAERRppm = "%2.2f" % "(FragmentA.errppm)";
        FragmentBERRppm = "%2.2f" % "(FragmentB.errppm)";
        FragmentCERRppm = "";
        ;
################# end script ###################
```

4.6.9.2.2 *Spn*_TAG

```
QUERYNAME = TriacylglycerolMSMS;
DEFINE Precursor = 'C[39..69] H[50..200] N[1] O[6]' WITH DBR = (1.5,7.5), CHG = +1;
IDENTIFY
        Precursor IN MS1+
REPORT
        LipidSpecies = "TAG %d:%d" % "((Precursor.chemsc[C]-3), (Precursor.chemsc[db]-1.5))";
        LipidClass = "TAG";
        Mass = Precursor.mass;
        IsobaricClass = Precursor.isobaric;
        ChemicalFormula = Precursor.chemsc;
        DerivatizedForm = "None";
```

```
        AdductIon = "+NH4+";
        LipidCategory = "Glycerolipid";
        ScanPolarity = "positive";
        Intensity = Precursor.intensity;
        IdentificationLevel = "MS1";
        QuantificationIon = "Precursor";
        PrecursorIdentifier = "[TAG %d:%d +NH4]+" % "((Precursor.chemsc[C]-3), (Precursor.chemsc[db]-1.5))";
        FragmentAIdentifier = "None";
        FragmentBIdentifier = "None";
        FragmentCIdentifier = "None";
        PrecursorIntensity = Precursor.intensity;
        FragmentAIntensity = "None";
        FragmentBIntensity = "None";
        FragmentCIntensity = "None";
        PrecursorERRppm = "%2.2f" % "(Precursor.errppm)";
        FragmentAERRppm = "";
        FragmentBERRppm = "";
        FragmentCERRppm = "";
        ;
################ end script ##################
```

4.6.9.2.3 *Spn*_PC

```
QUERYNAME = PhosphatidylcholineMSMS;
DEFINE Precursor = 'C[32..52] H[50..120] O[8] N[1] P[1]' WITH DBR = (1.5,5.5), CHG = +1;
DEFINE FragmentA = 'C[5] H[15] O[4] N[1] P[1]' WITH DBR = (1.5,3.5), CHG = +1;
IDENTIFY
        Precursor IN MS1+ AND
        FragmentA IN MS2+
REPORT
        LipidSpecies = "PC %d:%d" % "((Precursor.chemsc)[C] - 8, (Precursor.chemsc)[db] - 1.5)";
        LipidClass = "PC";
        Mass = Precursor.mass;
        IsobaricClass = Precursor.isobaric;
        ChemicalFormula = Precursor.chemsc;
        DerivatizedForm = "None";
        AdductIon = "+H+";
        LipidCategory = "Glycerolipid";
        ScanPolarity = "positive";
        Intensity = Precursor.intensity;
        IdentificationLevel = "MS2";
        QuantificationIon = "Precursor";
```

```
        PrecursorIdentifier = "[PC %d:%d +H]+" % "((Precursor.chemsc)[C] - 8, (Precursor.chemsc)[db] - 1.5)";
        FragmentAIdentifier = "PC(184)";
        FragmentBIdentifier = "None";
        FragmentCIdentifier = "None";
        PrecursorIntensity = Precursor.intensity;
        FragmentAIntensity = FragmentA.intensity;
        FragmentBIntensity = "None";
        FragmentCIntensity = "None";
        PrecursorERRppm = "%2.2f" % "(Precursor.errppm)";
        FragmentAERRppm = "%2.2f" % "(FragmentA.errppm)";
        FragmentBERRppm = "";
        FragmentCERRppm = "";
        ;
################ end script ##################
```

4.6.9.2.4 *Spn*_MAG

```
QUERYNAME = Monoacylglycerol;
DEFINE Precursor = 'C[15..25] H[10..100] O[4] N[1]' WITH DBR = (-0.5,1.5), CHG = +1;
IDENTIFY
        Precursor IN MS1+
REPORT
        LipidSpecies = "MAG %d:%d" % "((Precursor.chemsc)[C] - 3, (Precursor.chemsc)[db] + 0.5)";
        LipidClass = "MAG";
        Mass = Precursor.mass;
        IsobaricClass = Precursor.isobaric;
        ChemicalFormula = Precursor.chemsc;
        DerivatizedForm = "None";
        AdductIon = "+NH4+";
        LipidCategory = "Glycerolipid";
        ScanPolarity = "positive";
        Intensity = Precursor.intensity;
        IdentificationLevel = "MS1";
        QuantificationIon = "Precursor";
        PrecursorIdentifier = "[MAG %d:%d +NH4+]+" % "((Precursor.chemsc)[C] - 3, (Precursor.chemsc)[db] + 0.5)";
        FragmentAIdentifier = "None";
        FragmentBIdentifier = "None";
        FragmentCIdentifier = "None";
        PrecursorIntensity = Precursor.intensity;
        FragmentAIntensity = "None";
        FragmentBIntensity = "None";
        FragmentCIntensity = "None";
```

```
        PrecursorERRppm = "%2.2f" % "(Precursor.errppm)";
        FragmentAERRppm = "";
        FragmentBERRppm = "";
        FragmentCERRppm = "";
        ;
################ end script ##################
```

4.6.9.3 MFQL files for customized *Spn* internal standard in negative ion mode

4.6.9.3.1 18:2-18:2-18:2-18:2-d5 CL

```
QUERYNAME = CardiolipinStandard;
DEFINE Precursor = 'C[80] Ci[1] H[135] D[5] O[17] P[2]' WITH DBR = (-1.5,24), CHG = -2;
DEFINE FragmentA = 'C[18] H[31] O[2]' WITH DBR = (-1.5,7.5), CHG = -1;
IDENTIFY
        Precursor IN MS1- AND
        FragmentA IN MS2-
REPORT
        LipidSpecies = "IS Cardiolipin(+[2]H5) (18:2/18:2)(18:2/18:2)";
        LipidClass = "CL";
        Mass = Precursor.mass;
        IsobaricClass = Precursor.isobaric;
        ChemicalFormula = Precursor.chemsc;
        DerivatizedForm = "None";
        AdductIon = "-2H+";
        LipidCategory = "Internal standard";
        ScanPolarity = "negative";
        Intensity = FragmentA.intensity;
        IdentificationLevel = "MS2";
        QuantificationIon = "FragmentA";
        PrecursorIdentifier = "[CL(+[2]H5) 72:8 -2H]-";
        FragmentAIdentifier = "FA %d:%d (+O)" % "((FragmentA.chemsc)[C], (FragmentA.chemsc)[db]-1.5)";
        FragmentBIdentifier = "None";
        FragmentCIdentifier = "None";
        PrecursorIntensity = PrecursorIntensity;
        FragmentAIntensity = FragmentA.intensity;
        FragmentBIntensity = "None";
        FragmentCIntensity = "None";
        PrecursorERRppm = "%2.2f" % "(Precursor.errppm)";
        FragmentAERRppm = "%2.2f" % "(FragmentA.errppm)";
        FragmentBERRppm = "";
```

```
        FragmentCERRppm = "";
        ;
################ end script ##################
```

4.6.9.3.2 GlcDAG

```
QUERYNAME = GlycosyldiacylglycerolsStandard;
DEFINE Precursor = 'C[46..48] H[75..79] O[12]' WITH DBR = (9.5,9.5), CHG = -1;
DEFINE FragmentA = 'C[17..19] H[27..31] O[2]' WITH DBR = (4.5,4.5), CHG = -1;
DEFINE FragmentB = 'C[17..19] H[27..31] O[2]' WITH DBR = (4.5,4.5), CHG = -1;
IDENTIFY
        Precursor IN MS1- AND
        FragmentA IN MS2- AND
        FragmentB IN MS2-
REPORT
        LipidSpecies = "IS MGDG %d:%d_%d:%d" % "((FragmentA.chemsc)[C], (FragmentA.chemsc)[db] - 1.5,
        (FragmentB.chemsc)[C], (FragmentB.chemsc)[db] - 1.5)";
        LipidClass = "MGDG";
        Mass = Precursor.mass;
        IsobaricClass = Precursor.isobaric;
        ChemicalFormula = Precursor.chemsc;
        DerivatizedForm = "None";
        AdductIon = "+CH3COO-";
        LipidCategory = "Internal standard";
        ScanPolarity = "negative";
        Intensity = Precursor.intensity;
        IdentificationLevel = "MS2";
        QuantificationIon = "Precursor";
        PrecursorIdentifier = "[MGDG %d:%d_%d:%d +CH3COO]-" % "((FragmentA.chemsc)[C], (FragmentA.chemsc)[db] - 1.5,
        (FragmentB.chemsc)[C], (FragmentB.chemsc)[db] - 1.5)";
        FragmentAIdentifier = "FA %d:%d (+O)" % "((FragmentA.chemsc)[C], (FragmentA.chemsc)[db]     1.5)";
        FragmentBIdentifier = "FA %d:%d (+O)" % "((FragmentB.chemsc)[C], (FragmentB.chemsc)[db] -  1.5)";
        FragmentCIdentifier = "None";
        PrecursorIntensity = Precursor.intensity;
        FragmentAIntensity = FragmentA.intensity;
        FragmentBIntensity = FragmentB.intensity;
        FragmentCIntensity = "None";
        PrecursorERRppm = "%2.2f" % "(Precursor.errppm)";
        FragmentAERRppm = "%2.2f" % "(FragmentA.errppm)";
        FragmentBERRppm = "%2.2f" % "(FragmentB.errppm)";
        FragmentCERRppm = "";
        ;
```

################ end script ##################

4.6.9.3.3 15:1-18:1-d7 PG

```
QUERYNAME = PGSplash;
DEFINE Precursor = 'C[39] H[67] D[7] O[10] P[1]' WITH DBR = (2.5,9.5), CHG = -1;
DEFINE FragmentA = 'C[15] H[20..50] O[2]' WITH DBR = (1.5,7.5), CHG = -1;
DEFINE FragmentB = 'C[18] H[20..49] D[7] O[2]' WITH DBR = (1.5,7.5), CHG = -1;

IDENTIFY
        Precursor IN MS1- AND
        FragmentA IN MS2-  AND
        FragmentB IN MS2-
SUCHTHAT
        FragmentA.chemsc + FragmentB.chemsc + 'C6 H12 P1 O6' == Precursor.chemsc
REPORT
        LipidSpecies = "IS PG 15:0-18:1(+[2]H7)";
        LipidClass = "PG";
        Mass = Precursor.mass;
        IsobaricClass = Precursor.isobaric;
        ChemicalFormula = Precursor.chemsc;
        DerivatizedForm = "None";
        AdductIon = "-H+";
        LipidCategory = "Internal standard";
        ScanPolarity = "negative";
        Intensity = Precursor.intensity;
        IdentificationLevel = "MS2";
        QuantificationIon = "Precursor";
        PrecursorIdentifier = "[PG %d:%d_%d:%d(+[2]H7) -H]-" % "((FragmentA.chemsc)[C], (FragmentA.chemsc)[db] - 1.5,
        (FragmentB.chemsc)[C], (FragmentB.chemsc)[db] - 1.5)";
        FragmentAIdentifier = "FA %d:%d (+O)" % "((FragmentA.chemsc)[C], (FragmentA.chemsc)[db] - 1.5)";
        FragmentBIdentifier = "FA %d:%d(+[2]H7) (+O)" % "((FragmentB.chemsc)[C], (FragmentB.chemsc)[db] - 1.5)";
        FragmentCIdentifier = "None";
        PrecursorIntensity = Precursor.intensity;
        FragmentAIntensity = FragmentA.intensity;
        FragmentBIntensity = FragmentB.intensity;
        FragmentCIntensity = "None";
        PrecursorERRppm = "%2.2f" % "(Precursor.errppm)";
        FragmentAERRppm = "%2.2f" % "(FragmentA.errppm)";
        FragmentBERRppm = "%2.2f" % "(FragmentB.errppm)";
        FragmentCERRppm = "";
        ;
```

################ end script ##################F

4.6.9.3.4 15:0-18:1-d7 PI

```
QUERYNAME = PISplash;
DEFINE Precursor = 'C[42] H[71] D[7] O[13] P[1]' WITH DBR = (3.5,10.5), CHG = -1;
DEFINE FragmentA = 'C[15] H[20..50] O[2]' WITH DBR = (1.5,7.5), CHG = -1;
DEFINE FragmentB = 'C[18] H[20..49] D[7] O[2]' WITH DBR = (1.5,7.5), CHG = -1;
DEFINE FragmentC = 'C[6] H[10] O[8] P[1]' WITH DBR = (1.5,4.5), CHG = -1; #Headgroup-PI
IDENTIFY
        Precursor IN MS1- AND
        FragmentA IN MS2- AND
        FragmentB IN MS2- AND
        FragmentC IN MS2-
SUCHTHAT
        FragmentA.chemsc + FragmentB.chemsc + FragmentC.chemsc + 'C3 H6 O1' == Precursor.chemsc
REPORT
        LipidSpecies = "IS PI 15:0-18:1(+[2]H7)";
        LipidClass = "PI";
        Mass = Precursor.mass;
        IsobaricClass = Precursor.isobaric;
        ChemicalFormula = Precursor.chemsc;
        DerivatizedForm = "None";
        AdductIon = "-H+";
        LipidCategory = "Internal standard";
        ScanPolarity = "negative";
        Intensity = FragmentB.intensity;
        IdentificationLevel = "MS2";
        QuantificationIon = "FragmentB";
        PrecursorIdentifier = "[PI %d:%d_%d:%d(+[2]H7) -H]-" % "((FragmentA.chemsc)[C], (FragmentA.chemsc)[db] - 1.5,
        (FragmentB.chemsc)[C], (FragmentB.chemsc)[db] - 1.5)";
        FragmentAIdentifier = "FA %d:%d (+O)" % "((FragmentA.chemsc)[C], (FragmentA.chemsc)[db] - 1.5)";
        FragmentBIdentifier = "FA %d:%d(+[2]H7) (+O)" % "((FragmentB.chemsc)[C], (FragmentB.chemsc)[db] - 1.5)";
        FragmentCIdentifier = "PI(241)";
        PrecursorIntensity = Precursor.intensity;
        FragmentAIntensity = FragmentA.intensity;
        FragmentBIntensity = FragmentB.intensity;
        FragmentCIntensity = FragmentC.intensity;
        PrecursorERRppm = "%2.2f" % "(Precursor.errppm)";
        FragmentAERRppm = "%2.2f" % "(FragmentA.errppm)";
        FragmentBERRppm = "%2.2f" % "(FragmentB.errppm)";
        FragmentCERRppm = "%2.2f" % "(FragmentC.errppm)";
```

```
;
################ end script ##################
```

4.6.9.3.5 15:0-18:1-d7 PE

```
QUERYNAME = PESplash;
DEFINE Precursor = 'C[38] H[66] D[7] O[8] N[1] P[1]' WITH DBR = (2.5,9.5), CHG = -1;
DEFINE FragmentA = 'C[15] H[20..50] O[2]' WITH DBR = (1.5,7.5), CHG = -1;
DEFINE FragmentB = 'C[18] H[20..49] D[7] O[2]' WITH DBR = (1.5,7.5), CHG = -1;
IDENTIFY
        Precursor IN MS1- AND
        FragmentA IN MS2- AND
        FragmentB IN MS2-
SUCHTHAT
        FragmentA.chemsc + FragmentB.chemsc + 'C5 H11 O4 N1 P1' == Precursor.chemsc
REPORT
        LipidSpecies = "IS PE 15:0-18:1(+[2]H7)";
        LipidClass = "PE";
        Mass = Precursor.mass;
        IsobaricClass = Precursor.isobaric;
        ChemicalFormula = Precursor.chemsc;
        DerivatizedForm = "None";
        AdductIon = "-H+";
        LipidCategory = "Internal standard";
        ScanPolarity = "negative";
        Intensity = FragmentB.intensity;
        IdentificationLevel = "MS2";
        QuantificationIon = "FragmentB";
        PrecursorIdentifier = "[PE %d:%d_%d:%d(+[2]H7) -H]-" % "((FragmentA.chemsc)[C], (FragmentA.chemsc)[db] - 1.5,
        (FragmentB.chemsc)[C], (FragmentB.chemsc)[db] - 1.5)";
        FragmentAIdentifier = "FA %d:%d (+O)" % "((FragmentA.chemsc)[C], (FragmentA.chemsc)[db] - 1.5)";
        FragmentBIdentifier = "FA %d:%d(+[2]H7) (+O)" % "((FragmentB.chemsc)[C], (Fr mentB.chemsc)[db] - 1.5)";
        FragmentCIdentifier = "None";
        PrecursorIntensity = Precursor.intensity;
        FragmentAIntensity = FragmentA.intensity;
        FragmentBIntensity = FragmentB.intensity;
        FragmentCIntensity = "None";
        PrecursorERRppm = "%2.2f" % "(Precursor.errppm)";
        FragmentAERRppm = "%2.2f" % "(FragmentA.errppm)";
        FragmentBERRppm = "%2.2f" % "(FragmentB.errppm)";
        FragmentCERRppm = "";
        ;
```

```
################ end script ##################
```

4.6.9.4 MFQL files for pneumococcal lipids in negative ion mode

4.6.9.4.1 For *Spn*_CL

```
QUERYNAME = CardiolipinIsotope;

DEFINE Precursor = 'Ci[1] C[56..96] H[90..250] O[17] P[2]' WITH DBR = (5,13), CHG = -2;  # Ci is 13C

IDENTIFY

        Precursor IN MS1-

SUCHTHAT

        isEven(Precursor.chemsc[H])

REPORT

        LipidSpecies = "CL %d:%d" % "((Precursor.chemsc)[C] - 8, (Precursor.chemsc)[db] - 5)";

        LipidClass = "CL";

        Mass = Precursor.mass;

        IsobaricClass = Precursor.isobaric;

        ChemicalFormula = Precursor.chemsc;

        DerivatizedForm = "None";

        AdductIon = "-H+";

        LipidCategory = "Glycerophospholipid";

        ScanPolarity = "negative";

        Intensity = Precursor.intensity;

        IdentificationLevel = "MS1";

        QuantificationIon = "Precursor";

        PrecursorIdentifier = "[CL %d:%d -H]-" % "((Precursor.chemsc)[C] - 8, (Precursor.chemsc)[db] - 5)";

        FragmentAIdentifier = "None";

        FragmentBIdentifier = "None";

        FragmentCIdentifier = "None";

        PrecursorIntensity = Precursor.intensity;

        FragmentAIntensity = "None";

        FragmentBIntensity = "None";

        FragmentCIntensity = "None";

        PrecursorERRppm = "%2.2f" % "(Precursor.errppm)";

        FragmentAERRppm = "";

        FragmentBERRppm = "";

        FragmentCERRppm = "";

        ;
```

```
################ end script ##################
```

4.6.9.4.2 *Spn*_LCL

```
QUERYNAME = LysoCardiolipin;

DEFINE Precursor = 'Ci[1] C[44..74] H[50..250] O[16] P[2]' WITH DBR = (4,10), CHG = -2;

IDENTIFY
```

```
        Precursor IN MS1-
SUCHTHAT
        isEven(Precursor.chemsc[H])
REPORT
        LipidSpecies = "LCL %d:%d" % "((Precursor.chemsc)[C] - 8, (Precursor.chemsc)[db] - 4)";
        LipidClass = "LCL";
        Mass = Precursor.mass;
        IsobaricClass = Precursor.isobaric;
        ChemicalFormula = Precursor.chemsc;
        DerivatizedForm = "None";
        AdductIon = "-H+";
        LipidCategory = "Glycerophospholipid";
        ScanPolarity = "negative";
        Intensity = Precursor.intensity;
        IdentificationLevel = "MS1";
        QuantificationIon = "Precursor";
        PrecursorIdentifier = "[LCL %d:%d -H]-" % "((Precursor.chemsc)[C] - 8, (Precursor.chemsc)[db] - 4)";
        FragmentAIdentifier = "None";
        FragmentBIdentifier = "None";
        FragmentCIdentifier = "None";
        PrecursorIntensity = Precursor.intensity;
        FragmentAIntensity = "None";
        FragmentBIntensity = "None";
        FragmentCIntensity = "None";
        PrecursorERRppm = "%2.2f" % "(Precursor.errppm)";
        FragmentAERRppm = "";
        FragmentBERRppm = "";
        FragmentCERRppm = "";
        ;
################ end script ##################
```

4.6.9.4.3 *Spn*_PA

```
QUERYNAME = LysoCardiolipin;
DEFINE Precursor = 'Ci[1] C[44..74] H[50..250] O[16] P[2]' WITH DBR = (4,10), CHG = -2;
IDENTIFY
        Precursor IN MS1-
SUCHTHAT
        isEven(Precursor.chemsc[H])
REPORT
        LipidSpecies = "LCL %d:%d" % "((Precursor.chemsc)[C] - 8, (Precursor.chemsc)[db] - 4)";
        LipidClass = "LCL";
```

```
        Mass = Precursor.mass;
        IsobaricClass = Precursor.isobaric;
        ChemicalFormula = Precursor.chemsc;
        DerivatizedForm = "None";
        AdductIon = "-H+";
        LipidCategory = "Glycerophospholipid";
        ScanPolarity = "negative";
        Intensity = Precursor.intensity;
        IdentificationLevel = "MS1";
        QuantificationIon = "Precursor";
        PrecursorIdentifier = "[LCL %d:%d -H]-" % "((Precursor.chemsc)[C] - 8, (Precursor.chemsc)[db] - 4)";
        FragmentAIdentifier = "None";
        FragmentBIdentifier = "None";
        FragmentCIdentifier = "None";
        PrecursorIntensity = Precursor.intensity;
        FragmentAIntensity = "None";
        FragmentBIntensity = "None";
        FragmentCIntensity = "None";
        PrecursorERRppm = "%2.2f" % "(Precursor.errppm)";
        FragmentAERRppm = "";
        FragmentBERRppm = "";
        FragmentCERRppm = "";
        ;
################ end script ##################
```

4.6.9.4.4 *Spn*_LPA

```
QUERYNAME = LysoPhosphaticAcidMSMS;
DEFINE Precursor = 'C[15..25] H[20..80] O[7]  P[1]' WITH DBR = (1.5,3.5), CHG = -1;
DEFINE FragmentA = 'C[12..22] H[15..50] O[2]' WITH DBR = (1.5,3.5), CHG = -1;
IDENTIFY
        Precursor IN MS1- AND
        FragmentA IN MS2-
SUCHTHAT
        FragmentA.chemsc + 'C3 H7 P1 O5' == Precursor.chemsc AND
        (FragmentA.chemsc[C]/FragmentA.chemsc[db] >= 2.9)
REPORT
        LipidSpecies = "LPA %d:%d" % "((FragmentA.chemsc)[C], (FragmentA.chemsc)[db] - 1.5)";
        LipidClass = "LPA";
        Mass = Precursor.mass;
        IsobaricClass = Precursor.isobaric;
        ChemicalFormula = Precursor.chemsc;
```

```
        DerivatizedForm = "None";
        AdductIon = "-H+";
        LipidCategory = "Glycerophospholipid";
        ScanPolarity = "negative";
        Intensity = FragmentA.intensity;
        IdentificationLevel = "MS2";
        QuantificationIon = "FragmentA";
        PrecursorIdentifier = "[LPA %d:%d -H]-" % "((FragmentA.chemsc)[C], (FragmentA.chemsc)[db] - 1.5)";
        FragmentAIdentifier = "FA %d:%d (+O)" % "((FragmentA.chemsc)[C], (FragmentA.chemsc)[db] - 1.5)";
        FragmentBIdentifier = "None";
        FragmentCIdentifier = "None";
        PrecursorIntensity = Precursor.intensity;
        FragmentAIntensity = FragmentA.intensity;
        FragmentBIntensity = "None";
        FragmentCIntensity = "None";
        PrecursorERRppm = "%2.2f" % "(Precursor.errppm)";
        FragmentAERRppm = "%2.2f" % "(FragmentA.errppm)";
        FragmentBERRppm = "";
        FragmentCERRppm = "";
        ;
################ end script ##################
```

4.6.9.4.5 *Spn*_PE

```
QUERYNAME = Phosphatidylethanolamine;
DEFINE Precursor = 'C[29..49] H[50..120] O[8] N[1] P[1]' WITH DBR = (2.5,6.5), CHG = -1;
DEFINE FragmentA = 'C[12..22] H[15..50] O[2]' WITH DBR = (1.5,3.5), CHG = -1;
DEFINE FragmentB = 'C[12..22] H[15..50] O[2]' WITH DBR = (1.5,3.5), CHG = -1;
IDENTIFY
    Precursor IN MS1- AND
    FragmentA IN MS2- AND
    FragmentB IN MS2-
SUCHTHAT
    FragmentA.chemsc + FragmentB.chemsc + 'C5 H11 O4 N1 P1' == Precursor.chemsc AND
    (FragmentA.chemsc[C]/FragmentA.chemsc[db] >= 2.9) AND
    (FragmentB.chemsc[C]/FragmentB.chemsc[db] >= 2.9)
REPORT
    LipidSpecies = "PE %d:%d_%d:%d" % "((FragmentA.chemsc)[C], (FragmentA.chemsc)[db] - 1.5, (FragmentB.chemsc)[C],
    (FragmentB.chemsc)[db] - 1.5)";
    LipidClass = "PE";
    Mass = Precursor.mass;
    IsobaricClass = Precursor.isobaric;
```

```
        ChemicalFormula = Precursor.chemsc;
        DerivatizedForm = "None";
        AdductIon = "-H+";
        LipidCategory = "Glycerophospholipid";
        ScanPolarity = "negative";
        Intensity = sumIntensity(FragmentA.intensity, FragmentB.intensity)/2;
        IdentificationLevel = "MS2";
        QuantificationIon = "FragmentA and FragmentB";
        PrecursorIdentifier = "[PE %d:%d_%d:%d -H]-" % "((FragmentA.chemsc)[C], (FragmentA.chemsc)[db] - 1.5,
        (FragmentB.chemsc)[C], (FragmentB.chemsc)[db] - 1.5)";
        FragmentAIdentifier = "FA %d:%d (+O)" % "((FragmentA.chemsc)[C], (FragmentA.chemsc)[db] - 1.5)";
        FragmentBIdentifier = "FA %d:%d (+O)" % "((FragmentB.chemsc)[C], (FragmentB.chemsc)[db] - 1.5)";
        FragmentCIdentifier = "None";
        PrecursorIntensity = Precursor.intensity;
        FragmentAIntensity = FragmentA.intensity;
        FragmentBIntensity = FragmentB.intensity;
        FragmentCIntensity = "None";
        PrecursorERRppm = "%2.2f" % "(Precursor.errppm)";
        FragmentAERRppm = "%2.2f" % "(FragmentA.errppm)";
        FragmentBERRppm = "%2.2f" % "(FragmentB.errppm)";
        FragmentCERRppm = "";
        ;
################ end script ##################
```

4.6.9.4.6 *Spn*_LPE

```
QUERYNAME = LysoPhosphatidylethanolamineMSMS;
DEFINE Precursor = 'C[17..27] H[33..57] O[7] N[1] P[1]' WITH DBR = (1.5,3.5), CHG = -1;
DEFINE FragmentA = 'C[12..22] H[15..50] O[2]' WITH DBR = (1.5,3.5), CHG = -1;
IDENTIFY
        Precursor IN MS1- AND
        FragmentA IN MS2-
SUCHTHAT
        FragmentA.chemsc + 'C5 H12 O5 N1 P1' == Precursor.chemsc AND
        (FragmentA.chemsc[C]/FragmentA.chemsc[db] >= 2.9)
REPORT
        LipidSpecies = "LPE %d:%d" % "((FragmentA.chemsc)[C], (FragmentA.chemsc)[db] - 1.5)";
        LipidClass = "LPE";
        Mass = Precursor.mass;
        IsobaricClass = Precursor.isobaric;
        ChemicalFormula = Precursor.chemsc;
        DerivatizedForm = "None";
```

```
        AdductIon = "-H+";
        LipidCategory = "Glycerophospholipid";
        ScanPolarity = "negative";
        Intensity = FragmentA.intensity;
        IdentificationLevel = "MS2";
        QuantificationIon = "FragmentA";
        PrecursorIdentifier = "[LPE %d:%d -H]-" % "((FragmentA.chemsc)[C], (FragmentA.chemsc)[db] - 1.5)";
        FragmentAIdentifier = "FA %d:%d (+O)" % "((FragmentA.chemsc)[C], (FragmentA.chemsc)[db] - 1.5)";
        FragmentBIdentifier = "None";
        FragmentCIdentifier = "None";
        PrecursorIntensity = Precursor.intensity;
        FragmentAIntensity = FragmentA.intensity;
        FragmentBIntensity = "None";
        FragmentCIntensity = "None";
        PrecursorERRppm = "%2.2f" % "(Precursor.errppm)";
        FragmentAERRppm = "%2.2f" % "(FragmentA.errppm)";
        FragmentBERRppm = "";
        FragmentCERRppm = "";
        ;
    ################ end script ##################
```

4.6.9.4.7 *Spn*_PI

```
QUERYNAME = PhosphatidylinositolMSMS;
DEFINE Precursor = 'C[33..53] H[50..120] O[13] P[1]' WITH DBR = (3.5,7.5), CHG = -1;
DEFINE FragmentA = 'C[12..22] H[15..50] O[2]' WITH DBR = (1.5,3.5), CHG = -1;
DEFINE FragmentB = 'C[12..22] H[15..50] O[2]' WITH DBR = (1.5,3.5), CHG = -1;
DEFINE FragmentC = 'C6 H10 O8 P1' WITH CHG = -1;
IDENTIFY
        Precursor IN MS1- AND
        FragmentA IN MS2- AND
        FragmentB IN MS2- AND
        FragmentC IN MS2-
SUCHTHAT
        FragmentA.chemsc + FragmentB.chemsc + FragmentC.chemsc + 'C3 H6 O1' == Precursor.chemsc
REPORT
        LipidSpecies = "PI %d:%d_%d:%d" % "((FragmentA.chemsc)[C], (FragmentA.chemsc)[db] - 1.5, (FragmentB.chemsc)[C],
        (FragmentB.chemsc)[db] - 1.5)";
        LipidClass = "PI";
        Mass = Precursor.mass;
        IsobaricClass = Precursor.isobaric;
        ChemicalFormula = Precursor.chemsc;
```

```
        DerivatizedForm = "None";
        AdductIon = "-H+";
        LipidCategory = "Glycerophospholipid";
        ScanPolarity = "negative";
        Intensity = sumIntensity(FragmentA.intensity, FragmentB.intensity)/2;
        IdentificationLevel = "MS2";
        QuantificationIon = "FragmentA and FragmentB";
        PrecursorIdentifier = "[PI %d:%d_%d:%d -H]-" % "((FragmentA.chemsc)[C], (FragmentA.chemsc)[db] - 1.5,
        (FragmentB.chemsc)[C], (FragmentB.chemsc)[db] - 1.5)";
        FragmentAIdentifier = "FA %d:%d (+O)" % "((FragmentA.chemsc)[C], (FragmentA.chemsc)[db] - 1.5)";
        FragmentBIdentifier = "FA %d:%d (+O)" % "((FragmentB.chemsc)[C], (FragmentB.chemsc)[db] - 1.5)";
        FragmentCIdentifier = "PI(241)";
        PrecursorIntensity = Precursor.intensity;
        FragmentAIntensity = FragmentA.intensity;
        FragmentBIntensity = FragmentB.intensity;
        FragmentCIntensity = FragmentC.intensity;
        PrecursorERRppm = "%2.2f" % "(Precursor.errppm)";
        FragmentAERRppm = "%2.2f" % "(FragmentA.errppm)";
        FragmentBERRppm = "%2.2f" % "(FragmentB.errppm)";
        FragmentCERRppm = "%2.2f" % "(FragmentC.errppm)";
        ;
################ end script ##################
```

4.6.9.4.8 *Spn*_LPI

```
QUERYNAME = LysoPhosphatidylinositol;
DEFINE Precursor = 'C[21..31] H[20..100] O[12] P[1]' WITH DBR = (2.5,4.5), CHG = -1;
DEFINE FragmentA = 'C[12..22] H[15..50] O[2]' WITH DBR = (1.5,3.5), CHG = -1;
DEFINE FragmentB = 'C6 H10 O8 P1' WITH CHG = -1;
IDENTIFY
        Precursor IN MS1- AND
        FragmentA IN MS2- AND
        FragmentB IN MS2-
SUCHTHAT
        FragmentA.chemsc + FragmentB.chemsc + 'C3 H7 O2' == Precursor.chemsc AND
        (FragmentA.chemsc[C]/FragmentA.chemsc[db] >= 2.9)
REPORT
        LipidSpecies = "LPI %d:%d" % "((FragmentA.chemsc)[C], (FragmentA.chemsc)[db] - 1.5)";
        LipidClass = "LPI";
        Mass = Precursor.mass;
        IsobaricClass = Precursor.isobaric;
        ChemicalFormula = Precursor.chemsc;
```

```
        DerivatizedForm = "None";
        AdductIon = "-H+";
        LipidCategory = "Glycerophospholipid";
        ScanPolarity = "negative";
        Intensity = Precursor.intensity;
        IdentificationLevel = "MS2";
        QuantificationIon = "Precursor";
        PrecursorIdentifier = "[LPI %d:%d -H]-" % "((FragmentA.chemsc)[C], (FragmentA.chemsc)[db] - 1.5)";
        FragmentAIdentifier = "None";
        FragmentBIdentifier = "None";
        FragmentCIdentifier = "None";
        PrecursorIntensity = Precursor.intensity;
        FragmentAIntensity = FragmentA.intensity;
        FragmentBIntensity = FragmentB.intensity;
        FragmentCIntensity = "None";
        PrecursorERRppm = "%2.2f" % "(Precursor.errppm)";
        FragmentAERRppm = "%2.2f" % "(FragmentA.errppm)";
        FragmentBERRppm = "%2.2f" % "(FragmentB.errppm)";
        FragmentCERRppm = "";
        ;
################ end script ##################
```

4.6.9.4.9 *Spn*_PS

```
QUERYNAME = PhosphatidylethanolserineMSMS;
DEFINE Precursor = 'C[30..50] H[20..150] O[10] N[1] P[1]' WITH DBR = (3.5,7.5), CHG = -1;
DEFINE FragmentA = 'C[12..22] H[15..50] O[2]' WITH DBR = (1.5,3.5), CHG = -1;
DEFINE FragmentB = 'C[12..22] H[15..50] O[2]' WITH DBR = (1.5,3.5), CHG = -1;
DEFINE FragmentC = 'C3 H5 O2 N1' WITH CHG = 0;
IDENTIFY
        Precursor IN MS1- AND
        FragmentA IN MS2- AND
        FragmentB IN MS2- AND
        FragmentC IN MS2-
SUCHTHAT
        FragmentA.chemsc + FragmentB.chemsc + FragmentC.chemsc + 'C3 H6 P1 O4' == Precursor.chemsc AND
        (FragmentA.chemsc[C]/FragmentA.chemsc[db] >= 2.9) AND
        (FragmentB.chemsc[C]/FragmentB.chemsc[db] >= 2.9) AND
        FragmentA.chemsc[C] <= FragmentB.chemsc[C]
REPORT
        LipidSpecies = "PS %d:%d_%d:%d" % "((FragmentA.chemsc)[C], (FragmentA.chemsc)[db] - 1.5, (FragmentB.chemsc)[C],
        (FragmentB.chemsc)[db] - 1.5)";
```

```
        LipidClass = "PS";
        Mass = Precursor.mass;
        IsobaricClass = Precursor.isobaric;
        ChemicalFormula = Precursor.chemsc;
        DerivatizedForm = "None";
        AdductIon = "-H+";
        LipidCategory = "Glycerophospholipid";
        ScanPolarity = "negative";
        Intensity = sumIntensity(FragmentA.intensity, FragmentB.intensity)/2;
        IdentificationLevel = "MS2";
        QuantificationIon = "FragmentA and FragmentB";
        PrecursorIdentifier = "[PS %d:%d_%d:%d -H]-" % "((FragmentA.chemsc)[C], (FragmentA.chemsc)[db] - 1.5,
        (FragmentB.chemsc)[C], (FragmentB.chemsc)[db] - 1.5)";
        FragmentAIdentifier = "FA %d:%d (+O)" % "((FragmentA.chemsc)[C], (FragmentA.chemsc)[db] - 1.5)";
        FragmentBIdentifier = "FA %d:%d (+O)" % "((FragmentB.chemsc)[C], (FragmentB.chemsc)[db] - 1.5)";
        FragmentCIdentifier = "-PS(87)";
        PrecursorIntensity = Precursor.intensity;
        FragmentAIntensity = FragmentA.intensity;
        FragmentBIntensity = FragmentB.intensity;
        FragmentCIntensity = FragmentC.intensity;
        PrecursorERRppm = "%2.2f" % "(Precursor.errppm)";
        FragmentAERRppm = "%2.2f" % "(FragmentA.errppm)";
        FragmentBERRppm = "%2.2f" % "(FragmentB.errppm)";
        FragmentCERRppm = "%2.2f" % "(FragmentC.errppm)";
        ;
################# end script ##################
```

4.6.9.4.10 *Spn*_PG

```
QUERYNAME = PhosphatidylglycerolMSMS;
DEFINE Precursor = 'C[30..50] H[50..120] O[10] P[1]' WITH DBR = (2.5,6.5), CHG = -1;
DEFINE FragmentA = 'C[12..22] H[15..50] O[2]' WITH DBR = (1.5,3.5), CHG = -1;
DEFINE FragmentB = 'C[12..22] H[15..50] O[2]' WITH DBR = (1.5,3.5), CHG = -1;

IDENTIFY
        Precursor IN MS1- AND
        FragmentA IN MS2-  AND
        FragmentB IN MS2-
SUCHTHAT
        FragmentA.chemsc + FragmentB.chemsc + 'C6 H12 P1 O6' == Precursor.chemsc
REPORT
        LipidSpecies = "PG %d:%d" % "((Precursor.chemsc)[C] - 6, (Precursor.chemsc)[db] - 2.5)";
```

```
        LipidClass = "PG";
        Mass = Precursor.mass;
        IsobaricClass = Precursor.isobaric;
        ChemicalFormula = Precursor.chemsc;
        DerivatizedForm = "None";
        AdductIon = "-H+";
        LipidCategory = "Glycerophospholipid";
        ScanPolarity = "negative";
        Intensity = Precursor.intensity;
        IdentificationLevel = "MS2";
        QuantificationIon = "Precursor";
        PrecursorIdentifier = "[PG %d:%d_%d:%d -H]-" % "((FragmentA.chemsc)[C], (FragmentA.chemsc)[db] - 1.5,
        (FragmentB.chemsc)[C], (FragmentB.chemsc)[db] - 1.5)";
        FragmentAIdentifier = "FA %d:%d (+O)" % "((FragmentA.chemsc)[C], (FragmentA.chemsc)[db] - 1.5)";
        FragmentBIdentifier = "FA %d:%d (+O)" % "((FragmentB.chemsc)[C], (FragmentB.chemsc)[db] - 1.5)";
        FragmentCIdentifier = "None";
        PrecursorIntensity = Precursor.intensity;
        FragmentAIntensity = FragmentA.intensity;
        FragmentBIntensity = FragmentB.intensity;
        FragmentCIntensity = "None";
        PrecursorERRppm = "%2.2f" % "(Precursor.errppm)";
        FragmentAERRppm = "%2.2f" % "(FragmentA.errppm)";
        FragmentBERRppm = "%2.2f" % "(FragmentB.errppm)";
        FragmentCERRppm = "";
        ;
################ end script ##################
```

4.6.9.4.11 *Spn*_LPG

```
QUERYNAME = LysoPhosphatidylglycerol;
DEFINE Precursor = 'C[18..28] H[20..80] O[9] P[1]' WITH DBR = (1.5,3.5), CHG = -1;
DEFINE FragmentA = 'C[12..22] H[15..50] O[2]' WITH DBR = (1.5,3.5), CHG = -1;
IDENTIFY
        Precursor IN MS1- AND
        FragmentA IN MS2-
SUCHTHAT
        FragmentA.chemsc + 'C6 H13 P1 O7' == Precursor.chemsc  AND
        (FragmentA.chemsc[C]/FragmentA.chemsc[db] >= 2.9)
REPORT
        LipidSpecies = "LPG %d:%d" % "((FragmentA.chemsc)[C], (FragmentA.chemsc)[db] - 1.5)";
        LipidClass = "LPG";
        Mass = Precursor.mass;
```

```
        IsobaricClass = Precursor.isobaric;
        ChemicalFormula = Precursor.chemsc;
        DerivatizedForm = "None";
        AdductIon = "-H+";
        LipidCategory = "Glycerophospholipid";
        ScanPolarity = "negative";
        Intensity = FragmentA.intensity;
        IdentificationLevel = "MS2";
        QuantificationIon = "FragmentA";
        PrecursorIdentifier = "[LPG %d:%d -H]-" % "((FragmentA.chemsc)[C], (FragmentA.chemsc)[db] - 1.5)";
        FragmentAIdentifier = "FA %d:%d (+O)" % "((FragmentA.chemsc)[C], (FragmentA.chemsc)[db] - 1.5)";
        FragmentBIdentifier = "None";
        FragmentCIdentifier = "None";
        PrecursorIntensity = Precursor.intensity;
        FragmentAIntensity = FragmentA.intensity;
        FragmentBIntensity = "None";
        FragmentCIntensity = "None";
        PrecursorERRppm = "%2.2f" % "(Precursor.errppm)";
        FragmentAERRppm = "%2.2f" % "(FragmentA.errppm)";
        FragmentBERRppm = "";
        FragmentCERRppm = "";
        ;
################ end script ##################
```

4.6.9.4.12 *Spn*_neg_PC

```
QUERYNAME = Phosphatidylcholine;
DEFINE Precursor = 'C[34..58] H[50..120] O[10] N[1] P[1]' WITH DBR = (2.5,6.5), CHG = -1;
DEFINE FragmentA = 'C[12..22] H[15..50] O[2]' WITH DBR = (1.5,3.5), CHG = -1;
DEFINE FragmentB = 'C[12..22] H[15..50] O[2]' WITH DBR = (1.5,3.5), CHG = -1;
# DEFINE FragmentC = 'C[3] H[6] O[2]' WITH CHG = 0; Loss of -74 is very less intense. For highest sensitifty of ID and quan and application
of higher CE dont use it.
IDENTIFY
        Precursor IN MS1- AND
        FragmentA IN MS2- AND
        FragmentB IN MS2-
#       AND     FragmentC IN MS2-
SUCHTHAT
        FragmentA.chemsc + FragmentB.chemsc + 'C3 H6 O2' + 'C7 H15 P1 O4 N1' == Precursor.chemsc AND
        (FragmentA.chemsc[C]/FragmentA.chemsc[db] >= 2.9) AND
        (FragmentB.chemsc[C]/FragmentB.chemsc[db] >= 2.9) AND
        FragmentA.chemsc[C] <= FragmentB.chemsc[C]
```

```
REPORT
        LipidSpecies = "PC %d:%d_%d:%d" % "((FragmentA.chemsc)[C], (FragmentA.chemsc)[db] - 1.5, (FragmentB.chemsc)[C],
        (FragmentB.chemsc)[db] - 1.5)";
        LipidClass = "PC";
        Mass = Precursor.mass;
        IsobaricClass = Precursor.isobaric;
        ChemicalFormula = Precursor.chemsc;
        DerivatizedForm = "None";
        AdductIon = "+CH3COO-";
        LipidCategory = "Glycerophospholipid";
        ScanPolarity = "negative";
        Intensity = sumIntensity(FragmentA.intensity, FragmentB.intensity)/2;
        IdentificationLevel = "MS2";
        QuantificationIon = "FragmentA and FragmentB";
        PrecursorIdentifier = "[PC %d:%d_%d:%d +CH3COO]-" % "((FragmentA.chemsc)[C], (FragmentA.chemsc)[db] - 1.5,
        (FragmentB.chemsc)[C], (FragmentB.chemsc)[db] - 1.5)";
        FragmentAIdentifier = "FA %d:%d (+O)" % "((FragmentA.chemsc)[C], (FragmentA.chemsc)[db] - 1.5)";
        FragmentBIdentifier = "FA %d:%d (+O)" % "((FragmentB.chemsc)[C], (FragmentB.chemsc)[db] - 1.5)";
        FragmentCIdentifier = "None"; # "-PC(74)";
        PrecursorIntensity = Precursor.intensity;
        FragmentAIntensity = FragmentA.intensity;
        FragmentBIntensity = FragmentB.intensity;
        FragmentCIntensity = "None"; # FragmentC.intensity;
        PrecursorERRppm = "%2.2f" % "(Precursor.errppm)";
        FragmentAERRppm = "%2.2f" % "(FragmentA.errppm)";
        FragmentBERRppm = "%2.2f" % "(FragmentB.errppm)";
        FragmentCERRppm = "None"; # "%2.2f" % "(FragmentC.errppm)";
        ;
################# end script ###################
```

4.6.9.4.13 *Spn*_GlcDAG

```
QUERYNAME = Monohexosyldiacylglycerol;
DEFINE Precursor = 'C[35..55] H[60..110] O[12]' WITH DBR = (3.5,7.5), CHG = -1;
DEFINE FragmentA = 'C[12..22] H[15..50] O[2]' WITH DBR = (1.5,3.5), CHG = -1;
DEFINE FragmentB = 'C[12..22] H[15..50] O[2]' WITH DBR = (1.5,3.5), CHG = -1;
DEFINE FragmentC = 'C[9] H[17] O[8]' WITH CHG = -1;
IDENTIFY
        Precursor IN MS1- AND
        FragmentC IN MS2- AND
        FragmentA IN MS2- AND
        FragmentB IN MS2-
```

```
SUCHTHAT
        FragmentA.chemsc + FragmentB.chemsc + FragmentC.chemsc + 'C2 H2' == Precursor.chemsc
REPORT
        LipidSpecies = "monoHexDAG %d:%d" % "((Precursor.chemsc)[C] - 11, (Precursor.chemsc)[db] - 3.5)";
        LipidClass = "monoHexDAG";
        Mass = Precursor.mass;
        IsobaricClass = Precursor.isobaric;
        ChemicalFormula = Precursor.chemsc;
        DerivatizedForm = "None";
        AdductIon = "+CH3COO-";
        LipidCategory = "Monoglycosylglycerolipid";
        ScanPolarity = "negative";
        Intensity = Precursor.intensity;
        IdentificationLevel = "MS2";
        QuantificationIon = "Precursor";
        PrecursorIdentifier = "[monoHexDAG %d:%d_%d:%d +CH3COO]-" % "((FragmentA.chemsc)[C], (FragmentA.chemsc)[db] -
        1.5, (FragmentB.chemsc)[C], (FragmentB.chemsc)[db] - 1.5)";
        FragmentAIdentifier = "FA %d:%d (+O)" % "((FragmentA.chemsc)[C], (FragmentA.chemsc)[db] - 1.5)";
        FragmentBIdentifier = "FA %d:%d (+O)" % "((FragmentB.chemsc)[C], (FragmentB.chemsc)[db] - 1.5)";
        FragmentCIdentifier = "HexGro(253)";
        PrecursorIntensity = Precursor.intensity;
        FragmentAIntensity = FragmentA.intensity;
        FragmentBIntensity = FragmentB.intensity;
        FragmentCIntensity = FragmentC.intensity;
        PrecursorERRppm = "%2.2f" % "(Precursor.errppm)";
        FragmentAERRppm = "%2.2f" % "(FragmentA.errppm)";
        FragmentBERRppm = "%2.2f" % "(FragmentB.errppm)";
        FragmentCERRppm = "%2.2f" % "(FragmentC.errppm)";
        ;
################ end script ##################
```

4.6.9.4.14 *Spn*_GalGlcDAG

```
QUERYNAME = Dihexosyldiacylglycerol;
DEFINE Precursor = 'C[41..61] H[50..120] O[17]' WITH DBR = (4.5,8.5), CHG = -1;
DEFINE FragmentA = 'C[12..22] H[15..50] O[2]' WITH DBR = (1.5,3.5), CHG = -1;
DEFINE FragmentB = 'C[12..22] H[15..50] O[2]' WITH DBR = (1.5,3.5), CHG = -1;
DEFINE FragmentC = 'C[15] H[25] O[12]' WITH CHG = -1;
IDENTIFY
        Precursor IN MS1- AND
        FragmentC IN MS2- AND
        FragmentA IN MS2- AND
```

```
        FragmentB IN MS2-
SUCHTHAT
        FragmentA.chemsc + FragmentB.chemsc + FragmentC.chemsc + 'C2 H4 O' == Precursor.chemsc
REPORT
        LipidSpecies = "diHexDAG %d:%d" % "((Precursor.chemsc)[C] - 17, (Precursor.chemsc)[db] - 4.5)";
        LipidClass = "diHexDAG";
        Mass = Precursor.mass;
        IsobaricClass = Precursor.isobaric;
        ChemicalFormula = Precursor.chemsc;
        DerivatizedForm = "None";
        AdductIon = "+CH3COO-";
        LipidCategory = "Diglycosylglycerolipid";
        ScanPolarity = "negative";
        Intensity = Precursor.intensity;
        IdentificationLevel = "MS2";
        QuantificationIon = "Precursor";
        PrecursorIdentifier = "[diHexDAG %d:%d_%d:%d +CH3COO]-" % "((FragmentA.chemsc)[C], (FragmentA.chemsc)[db] - 1.5,
        (FragmentB.chemsc)[C], (FragmentB.chemsc)[db] - 1.5)";
        FragmentAIdentifier = "FA %d:%d (+O)" % "((FragmentA.chemsc)[C], (FragmentA.chemsc)[db] - 1.5)";
        FragmentBIdentifier = "FA %d:%d (+O)" % "((FragmentB.chemsc)[C], (FragmentB.chemsc)[db] - 1.5)";
        FragmentCIdentifier = "diHexGroanh(397)";
        PrecursorIntensity = Precursor.intensity;
        FragmentAIntensity = FragmentA.intensity;
        FragmentBIntensity = FragmentB.intensity;
        FragmentCIntensity = FragmentC.intensity;
        PrecursorERRppm = "%2.2f" % "(Precursor.errppm)";
        FragmentAERRppm = "%2.2f" % "(FragmentA.errppm)";
        FragmentBERRppm = "%2.2f" % "(FragmentB.errppm)";
        FragmentCERRppm = "%2.2f" % "(FragmentC.errppm)";
        ;
################ end script ##################
```

5) List of Figures

List of figures in supplementary data

6) Reference

1. Wilhelm MJ, Sheffield JB, Sharifian Gh M, et al. Gram's stain does not cross the bacterial cytoplasmic membrane. *ACS Chem Biol*. 2015, 10(7):1711–7. doi:10.1021/acschembio.5b00042
2. Vollmer W, Blanot D, De Pedro MA. Peptidoglycan structure and architecture. *FEMS Microbiol Rev*. 2008, 32(2):149–167. doi:10.1111/j.1574-6976.2007.00094.x
3. Zhang Y, Rock CO. Membrane lipid homeostasis in bacteria. *Nat Rev Microbiol*. 2008, 6(3):222–233. doi:10.1038/nrmicro1839
4. Rohde M. The Gram-positive bacterial cell wall. *Microbiol Spectr*. 2019, 7(3):GPP3–0044–2018. doi:10.1128/microbiolspec.GPP3-0044-2018
5. Watson DA, Musher DM, Jacobson JW, et al. A Brief history of the pneumococcus in biomedical research: a panoply of scientific discovery. *Clin Infect Dis*. 1993, 17(5):913–24. doi:10.1093/clinids/17.5.913
6. Henriques-Normark B, Tuomanen EI. The pneumococcus: epidemiology, microbiology, and pathogenesis. *Cold Spring Harb Perspect Med*. 2013, 3(7):a010215. doi:10.1101/cshperspect.a010215
7. Paton JC, Trappetti C. *Streptococcus pneumoniae* capsular polysaccharide. *Microbiol Spectr*. 2019, 7(2):microbiolspec.GPP3–0019–2018. doi:10.1128/microbiolspec.GPP3-0019-2018.
8. Ganaie FA, Saad JS, Lo SW, et al. Novel pneumococcal capsule type 33E results from the inactivation of glycosyltransferase WciE in vaccine type 33F. *J Biol Chem*. 2023, 299(9):105085. doi:10.1016/j.jbc.2023.105085
9. Ganaie FA, Saad JS, Lo SW, et al. Discovery and characterization of pneumococcal serogroup 36 capsule subtypes, serotypes 36A and 36B. *J Clin Microbiol*. 2023, 61(4):e0002423. doi:10.1128/jcm.00024-23
10. Weinberger DM, Malley R, Lipsitch M. Serotype replacement in disease after pneumococcal vaccination. *Lancet*. 2011, 378(9807):1962–73. doi:10.1016/S0140-6736(10)62225-8
11. Manika K, Kioumis I. The clinical significance of *Streptococcus pneumoniae* resistance in community-acquired pneumonia. *Pneumon*. 2011, 24(4):376–388.
12. Kohler S, Voß F, Mejia AG, et al. Pneumococcal lipoproteins involved in bacterial fitness, virulence, and immune evasion. *FEBS Lett*. 2016, 590(21):3820–3839. doi:10.1002/1873-3468.12352
13. Dochez L, Avery O T. The elaboration of specific soluble substance by pneumococcus during growth. *J Exp Med*. 1917, 26(4):477–93. doi:10.1084/jem.26.4.477
14. Austrian R. Pneumococcus: The first one hundred years. *Rev Infect Dis*. 1981, 3(2):183–189. doi:10.1093/clinids/3.2.183
15. Bentley SD, Aanensen DM, Mavroidi A, et al. Genetic analysis of the capsular biosynthetic locus from all 90 pneumococcal serotypes. *PLoS Genet*. 2006, 2(3):e31. doi:org/10.1371/journal.pgen.0020031

16. Yother J. Capsules of *Streptococcus pneumoniae* and other bacteria: paradigms for polysaccharide biosynthesis and regulation. *Annu Rev Microbiol*. 2011, 65:563–81. doi:10.1146/annurev.micro.62.081307.162944
17. Geno KA, Gilbert GL, Song JY, et al. Pneumococcal capsules and their types: past, present, and future. *Clin Microbiol Rev*. 2015, 28(3):871–99. doi:10.1128/CMR.00024-15
18. Larson TR, Yother J. *Streptococcus pneumoniae* capsular polysaccharide is linked to peptidoglycan via a direct glycosidic bond to β-D-*N*-acetylglucosamine. *Proc Natl Acad Sci U S A*. 2017, 114(22):5695–5700. doi:10.1073/pnas.1620431114
19. Vollmer W, Massidda O, Tomasz A. The Cell wall of *Streptococcus pneumoniae*. *Microbiol Spectr*. 2019, 7(3):10.1128/microbiolspec.GPP3–0018–2018. doi:10.1128/microbiolspec.gpp3-0018-2018
20. Goebel WF, Adams MH. The immunological properties of the heterophile antigen and somatic polysaccharide of pneumococcus. *Exp Med*. 1943, 77(5):435–49. doi:10.1084/jem.77.5.435
21. Brown S, Meredith T, Swoboda J, et al. *Staphylococcus aureus* and *Bacillus subtilis* W23 make polyribitol wall teichoic acids using different enzymatic pathways. *Chem Biol*. 2010, 17(10):1101–10. doi:10.1016/j.chembiol.2010.07.017
22. Swoboda J, Campbell J, C. Meredith TC, et al. Wall teichoic acid function, biosynthesis, and inhibition. *Chembiochem*. 2010, 11(1):35–45. doi:10.1002/cbic.200900557
23. Weidenmaier C, Peschel A. Teichoic acids and related cell-wall glycopolymers in Gram-positive physiology and host interactions. *Nat Rev Microbiol*. 2008, 6(4):276–287. doi:10.1038/nrmicro1861
24. Fischer W. Pneumococcal lipoteichoic and teichoic acid. *Microb Drug Resist*. 1997, 3(4):309–25. doi:10.1089/mdr.1997.3.309
25. Knaack W, Hölzl G, Gisch N. Structural analysis of glycosylglycerolipids using NMR spectroscopy. *Methods Mol Biol* 2295, 249–272 (2021). doi:10.1007/978-1-0716-1362-7_14
26. Denapaite D, Bruckner R, Hakenbeck R, et al. Biosynthesis of teichoic acids in *Streptococcus pneumoniae* and closely related species: Lessons from genomes. *Microb Drug Resist*. 2012, 18(3):344–58. doi:10.1089/mdr.2012.0026
27. Draing C, Pfitzenmaier M, Zummo S, et al. Comparison of lipoteichoic acid from different serotypes of *Streptococcus pneumoniae*. *J Biol Chem*. 2006, 281(45):33849–59. doi:10.1074/jbc.M602676200
28. Seo HS, Cartee RT, Pritchard DG, et al. A new model of pneumococcal lipoteichoic acid structure resolves biochemical, biosynthetic, and serologic inconsistencies of the current model. *J Bacteriol*. 2008, 190(7):2379–87. doi:10.1128/JB.01795-07
29. Gisch N, Kohler T, Ulmer AJ, et al. Structural reevaluation of *Streptococcus pneumoniae* lipoteichoic acid and new insights into its immunostimulatory potency. *J Biol Chem*. 2013, 288(22):15654–67. doi:10.1074/jbc.M112.446963
30. Kawai Y, Marles-Wright J, Cleverley RM J, et al. A widespread family of bacterial cell wall assembly proteins. *EMBO J*. 2011, 30(24):4931–41. doi:10.1038/emboj.2011.358

31. Hübscher J, Lüthy L, Berger-Bächi B, et al. Phylogenetic distribution and membrane topology of the LytR-CpsA-Psr protein family. *BMC Genomics*. 2008, 9(617). doi:10.1186/1471-2164-9-617
32. Hübscher J, Mccallum N, Sifri CD, et al. MsrR contributes to cell surface characteristics and virulence in *Staphylococcus aureus*. *FEMS Microbiol Lett*. 2009, 295(2):251–261. doi:10.1111/j.1574-6968.2009.01603.x
33. Chan YG, Frankel MB, Dengler V, et al. *Staphylococcus aureus* mutants lacking the LytR-CpsA-Psr family of enzymes release cell wall teichoic acids into the extracellular medium. *J Bacteriol*. 2013, 195(20):4650–4659. doi:10.1128/JB.00544-13
34. Schaefer K, Matano LM, Qiao Y, et al. In vitro reconstitution demonstrates the cell wall ligase activity of LCP proteins. *Nat Chem Biol*. 2017, 13(4):396–401. doi:10.1038/nchembio.2302
35. Eberhardt A, Hoyland CN, Vollmer D, et al. Attachment of capsular polysaccharide to the cell wall in *Streptococcus pneumoniae*. *Microb Drug Resist*. 2012, 18(3):240–255. doi:10.1089/mdr.2011.0232
36. Heß N, Waldow F, Kohler TP, et al. Lipoteichoic acid deficiency permits normal growth but impairs virulence of *Streptococcus pneumoniae*. *Nat Commun*. 2017, 8(1):2093. doi:10.1038/s41467-017-01720-z
37. Larrouy-Maumus G. Lipids as biomarkers of cancer and bacterial infections. *Curr Med Chem*. 2019, 26(11):1924–1932. doi:10.2174/0929867325666180904120029
38. Lee TH, Hoffererk V; Separovic F, et al. The role of bacterial lipid diversity and membrane properties in modulating antimicrobial peptide activity and drug resistance. *Curr Opin Chem Biol*. 2019, (52):85–92. doi:10.1016/j.cbpa.2019.05.025
39. Jorasch P, Wolter FP, Zalhringer U, et al. A UDP glucosyltransferase from *Bacillus subtilis* successively transfers up to four glucose residues to 1,2-diacylglycerol: expression of ypfP in *Escherichia coil* and structural analysis of its reaction products. *Mol Microbiol*. 1998, 29(2):419–430. doi:10.1046/j.1365-2958.1998.00930.x
40. Edman M, Berg S, Storm P, et al. Structural features of glycosyltransferases synthesizing major bilayer and nonbilayer-prone membrane lipids in *Acholeplasma laidlawii* and *Streptococcus pneumoniae*. *J Biol Chem*. 2003, 278(10):8420–8428. doi:10.1074/jbc.M211492200
41. Hu Y & Walker S. Remarkable structural similarities between diverse glycosyltransferases. *Chem Biol*. 2002, 9(12):1287–1296. doi:https://doi.org/10.1016/S1074-5521(02)00295-8
42. Sohlenkamp C & Geiger O. Bacterial membrane lipids: diversity in structures and pathways. *FEMS Microbiol Rev*. 2016, 40(1):133–159. doi:10.1093/femsre/fuv008
43. López-Lara IM & Geiger O. Bacterial lipid diversity. *Biochim Biophys Acta Mol Cell Biol Lipids*. 2017, 1862(11):1287–1299. doi:10.1016/j.bbalip.2016.10.007
44. Meiers M, Volz C, Eise J, et al. Altered lipid composition in *Streptococcus pneumoniae cpoA* mutants. BMC Microbiol. 2014, 12(14). doi:10.1186/1471-2180-14-12
45. Joyce LR, Guan Z, Palmer KL. *Streptococcus pneumoniae*, S. *pyogenes* and *S*. *agalactiae* membrane phospholipid remodelling in response to human serum. *Microbiology*. 2021, 167(5):001048. doi:10.1099/mic.0.001048

46. Kiriukhin MY, Debabov D V., Shinabarger DL, et al. Biosynthesis of the glycolipid anchor in lipoteichoic acid of *Staphylococcus aureus* RN4220: Role of YpfP, the diglucosyldiacylglycerol synthase. *J Bacteriol*. 2001, 183(11):3506–3514. doi:10.1128/JB.183.11.3506-3514.2001
47. Diercks H, Semeniuk A, Gisch N, et al. Accumulation of novel glycolipids and ornithine lipids in *Mesorhizobium loti* under phosphate deprivation. *J Bacteriol*. 2015, 197(3):497–509. doi:10.1128/JB.02004-14
48. Zajonc DM & Girardi E. Recognition of microbial glycolipids by natural killer T cells. *Front Immunol*. 2015, 6(400). doi:10.3389/fimmu.2015.00400
49. Kinjo Y, Illarionov P, Vela J, et al. Invariant natural killer T cells recognize glycolipids from pathogenic Gram-positive bacteria. *Nat Immunol*. 2011, 12(10):966–974. doi:10.1038/ni.2096
50. Kishimoto K, Urade R, Ogawa T, et al. Nondestructive quantification of neutral lipids by thin-layer chromatography and laser-fluorescent scanning: Suitable methods for "lipidome" analysis. *Biochem Biophys Res Commun*. 2001, 281(3):657–662. doi:10.1006/bbrc.2001.4404
51. Wenk MR. Lipidomics: New tools and applications. *Cell*. 2010, 143(6):888–895. doi:10.1016/j.cell.2010.11.033
52. Liebisch G, Vizcaino JA, Köfeler H, et al. Shorthand notation for lipid structures derived from mass spectrometry. *J Lipid Res*. 2013, 54(6):1523–1530. doi:10.1194/jlr.M033506
53. Cajka T & Fiehn O. Toward merging untargeted and targeted methods in mass spectrometry-based metabolomics and lipidomics. *Anal Chem*. 2016, 88(1):524–545. doi:10.1021/acs.analchem.5b04491
54. Tumanov S & Kamphorst JJ. Recent advances in expanding the coverage of the lipidome. *Curr Opin Biotechnol*. 2017, (43):127–133. doi:10.1016/j.copbio.2016.11.008
55. Matyash V, Liebisch G, Kurzchalia TV, et al. Lipid extraction by methyl-*tert*-butyl ether for high-throughput lipidomics. *J Lipid Res*. 2008, 49(5):1137–1149. doi:10.1194/jlr.D700041-JLR200
56. Holčapek M, Liebisch G, Kim Ekroos. Lipidomic analysis. *Anal Chem*. 2018, 90(7):4249–4257. doi:10.1021/acs.analchem.7b05395
57. Cajka T & Fiehn O. Comprehensive analysis of lipids in biological systems by liquid chromatography-mass spectrometry. *Trends Anal Chem*. 2014, 61:192–206. doi:10.1016/j.trac.2014.04.017
58. Schwudke D, Liebisch G, Herzog R, et al. Shotgun lipidomics by tandem mass spectrometry under data-dependent acquisition control. *Methods Enzym*. 2007, 433:175–11. doi:10.1016/S0076-6879(07)33010-3
59. Köfeler HC, Ahrends R, Baker ES, et al. Recommendations for good practice in MS-based lipidomics. *J Lipid Res*. 2021, 62:100138. doi:10.1016/j.jlr.2021.100138
60. Hu C, Duan Q, Han X. Strategies to improve/eliminate the limitations in shotgun lipidomics. *Proteomics*. 2020, 20(11):e1900070. doi:10.1002/pmic.201900070
61. Han X & Gross RW. Global analyses of cellular lipidomes directly from crude extracts of biological samples by ESI mass spectrometry: a bridge to lipidomics. *J Lipid Res*. 2003, 44(6):1071–1079. doi:10.1194/jlr.R300004-JLR200

62. Schwudke D, Hannich JT, Surendranath V, et al. Top-down lipidomic screens by multivariate analysis of high-resolution survey mass spectra. *Anal Chem*. 2007, 79(11):4083–4093. doi:10.1021/ac062455y
63. Schwudke D, Schuhmann K, Herzog R. Shotgun lipidomics on high resolution mass spectrometers. *Cold Spring Harb Perspect Biol*. 2011, 3(9):a004614. doi:10.1101/cshperspect.a004614
64. Herzog R, Schwudke D, Schuhmann K, et al. A novel informatics concept for high-throughput shotgun lipidomics based on the molecular fragmentation query language. *Genome Biol*. 2011, 12(1):R8. doi:10.1186/gb-2011-12-1-r8
65. Herzog R, Schwudke D, Shevchenko A. LipidXplorer: Software for quantitative shotgun lipidomics compatible with multiple mass spectrometry platforms. *Curr Protoc Bioinformatics*. 2013:14.12.1–14.12.30. doi:10.1002/0471250953.bi1412s43
66. Schwudke D, Shevchenko A, Hoffmann N, et al. Lipidomics informatics for life-science. *J Biotechnol*. 2017, 261:131-136. doi:10.1016/j.jbiotec.2017.08.010
67. Husen P, Tarasov K, Katafiasz M, et al. Analysis of lipid experiments (ALEX): A software framework for analysis of high-resolution shotgun lipidomics data. *PLoS One*. 2013, 8(11):e79736. doi:10.1371/journal.pone.0079736
68. Rustam YH & Reid GE. Analytical challenges and recent advances in mass spectrometry based lipidomics. *Anal Chem*. 2018, 90(1):374–397. doi:10.1021/acs.analchem.7b04836
69. Brügger B, Erben G, Sandhoff R, et al. Quantitative analysis of biological membrane lipids at the low picomole level by nano-electrospray ionization tandem mass spectrometry. *Proc Natl Acad Sci U S A*. 1997, 94(6):2339–2344. doi:10.1073/pnas.94.6.2339
70. Khoury S, Canlet C, Lacroix MZ, et al. Quantification of lipids: model, reality, and compromise. *Biomolecules*. 2018, 8(4):1–16. doi:10.3390/biom8040174
71. Liebisch G, Ahrends R, Arita M, et al. Lipidomics needs more standardization. *Nat Metab*. 2019, 1(8):745–747. doi:10.1038/s42255-019-0094-z
72. Kopczynski D, Krause D, Al Machot F, et al. The past and future of lipidomics bioinformatics. *Mass Spectrom Lipidomics*. 2023, 1:271–290. doi:10.1002/9783527836512.ch10
73. Briles EB & Tomasz A. Membrane lipoteichoic acid is not a precursor to wall teichoic acid in pneumococci. *J Bacteriol*. 1975, 122(1):335–337. doi:10.1128/JB.122.1.335-337.1975
74. Horne DS & Tomasz A. Possible role of a choline-containing teichoic acid in the maintenance of normal cell shape and physiology in *Streptococcus oralis*. *J Bacteriol*. 1993, 175(6):1717–1722. doi:10.1128/jb.175.6.1717-1722.1993
75. Minhas V, Domenech A, Synefiaridou D, et al. Competence remodels the pneumococcal cell wall exposing key surface virulence factors that mediate increased host adherence. *PLoS Biol*. 2023, 21(1):e3001990. doi:10.1371/journal.pbio.3001990
76. Vollmer W, Massidda O, Tomasz A. The cell wall of *Streptococcus pneumoniae*. *Microbiol Spectr*. 2019, 7(3):10.1128/microbiolspec.GPP3–0018–2018. doi:10.1128/microbiolspec.GPP3-0018-2018

77. Briles EB & Tomasz A. Pneumococcal forssman antigen a choline containing lipoteichoic acid. *J Biol Chem*. 1973, 248(18):6394–6397. doi:10.1016/s0021-9258(19)43459-5

78. Waldow F. Strukturanalytische Untersuchungen zur Biosynthese, Modifikation und Quantifizierung von Teichonsäuren in *Streptococcus pneumoniae*. Dissertation. 2018, University of Lubeck.

79. Abdullah MR, Gutiérrez-Fernández J, Pribyl T, et al. Structure of the pneumococcal l,d-carboxypeptidase DacB and pathophysiological effects of disabled cell wall hydrolases DacA and DacB. *Mol Microbiol*. 2014, 93(6):1183–1206. doi:10.1111/mmi.12729

80. Nahm MH, Brissac T, Kilian M, et al. Pneumococci can become virulent by acquiring a new capsule from oral streptococci. *J Infect Dis*. 2020, 222(3):372–380. doi:10.1093/infdis/jiz456

81. Bender MH, Robert T. Cartee, Yother J. Positive correlation between tyrosine phosphorylation of CpsD and capsular polysaccharide production in *Streptococcus pneumoniae*. *J Bacteriol*. 2003, 185(20):6057–6066. doi:10.1128/JB.185.20.6057-6066.2003

82. Lannes-Costa PS, De Oliveira JSS, Da silva Santos G, et al. A current review of pathogenicity determinants of *Streptococcus* sp. *J Appl Microbiol*. 2020, 131(4):1600–1620. doi:10.1111/jam.15090

83. Trombe MC, Lanéelle MA, Lanéelle G. Lipid composition of aminopterin-resistant and sensitive strains of *Streptococcus pneumoniae*. Effect of aminopterin inhibition. *Biochim Biophys Acta*. 1979, 574(2):290–300. doi:10.1016/0005-2760(79)90010-9

84. Joyce LR, Guan Z, Palmer KL. Phosphatidylcholine biosynthesis in Mitis group streptococci via host metabolite scavenging. *J Bacteriol*. 2019, 202(22):e00495–19. doi:10.1128/JB.00495-19

85. Calvez P, Jouhet J, Vié V, et al. Lipid phases and cell geometry during the cell cycle of streptococcus pneumoniae. *Front Microbiol*. 2019, 10:351. doi:10.3389/fmicb.2019.00351

86. Schuhmann K, Shevchenko A. Shotgun lipidomics on a LTQ Orbitrap mass spectrometer by successive switching between acquisition polarity modes. *J Mass Spectrom*. 2012, 47(1):96–104. doi:10.1002/jms.2031

87. de Jonckheere B, Kollotzek F, Münzer P, et al. Critical shifts in lipid metabolism promote megakaryocyte differentiation and proplatelet formation. *Nat Cardiovasc Res*. 2023, 2(9):835–852. doi:10.1038/s44161-023-00325-8

88. Surma MA, Herzog R, Vasilj A, et al. An automated shotgun lipidomics platform for high throughput, comprehensive, and quantitative analysis of blood plasma intact lipids. *Eur J Lipid Sci Technol*. 2015, 117(10):1540–1549. doi:10.1002/ejlt.201500145

89. Grimard V, Massier J, Richter D, et al. SiRNA screening reveals JNK2 as an evolutionary conserved regulator of triglyceride homeostasis. *J Lipid Res*. 2008, 49(11):2427-2440. doi:10.1194/jlr.M800168-JLR200

90. Hofmann T & Schmidt C. Thin-layer chromatography and coomassie staining of phospholipids for fast and simple lipidomics sample preparation. *Anal Sens*. 2021, 1(4):171–179. doi:10.1002/anse.202100029

91. Brendel M. Charakterisierung der Enzyme für die Teichonsäureverankerung an der Bakteriellen Zellwand Und deren Einfluss Auf die Pathophysiologie von *Streptococcus pneumoniae*. Dissertation. 2024, University of Greifswald.

92. Pribyl T, Moche M, Dreisbach A, et al. Influence of impaired lipoprotein biogenesis on surface and exoproteome of *Streptococcus pneumoniae*. *J Proteome Res*. 2014;13(2):650–667. doi:10.1021/pr400768v

93. Rennemeier C, Hammerschmidt S, Niemann S, et al.Thrombospondin-1 promotes cellular adherence of gram-positive pathogens via recognition of peptidoglycan. *FASEB J*. 2007;21(12):3118–3132. doi:10.1096/fj.06-7992

94. Entchev EV, Schwudke D, Zagoriy V, et al. LET-767 is required for the production of branched chain and long chain fatty acids in *Caenorhabditis elegans*. *J Biol Chem*. 2008;283(25):17550–17560. doi:10.1074/jbc.M80096520

95. Reich A, Schwudke D, Meurer M, Lehmann B, Shevchenko A. Lipidome of narrow-band ultraviolet B irradiated keratinocytes shows apoptotic hallmarks. *Exp Dermatol*. 2010;19(8):e103–e110. doi:10.1111/j.1600-0625.2009.01000.x

96. Visconti G, Boccard J, Feinberg M, et al. From fundamentals in calibration to modern methodologies: A tutorial for small molecules quantification in liquid chromatography-mass spectrometry bioanalysis. *Anal Chim Acta*. 2023;1240:340–711. doi:10.1016/j.aca.2022.34071

Acknowledgements

I wish to express my sincere gratitude to my supervisor, PD Dr. Dominik Schwudke, and co-supervisor, Dr. Nicolas Gisch, for granting me the opportunity to pursue my doctoral research in your laboratories:

To PD Dr. Dominik Schwudke: Your expertise in mass spectrometry has been invaluable throughout my journey. Whenever I faced experimental challenges and felt discouraged, your insightful solutions not only recharged my enthusiasm but also guided me out of the most intricate situations. I appreciate your patience in addressing my numerous inquiries, providing constructive feedback, and introducing me to the attractive area of lipidomics. Your mentorship has left a permanent mark on my PhD journey and my future career. It has been an honor to collaborate with and learn from you.

To Dr. Nicolas Gisch: I extend my heartfelt thanks for your solid support, mentorship, and for entrusting me to develop my own research ideas. Your exceptional patience, steadfast encouragement, and extensive discussions on our exciting projects have been instrumental in my academic growth. Beyond your role as a supervisor, you have revealed life lessons that have contributed to my personal development. Working with you over the past three years has been a truly enriching experience.

I am grateful to PD Dr Norbert Reiling for being second BBRS supervisor and for very fruitful discussion.

I would also like to express my appreciation to Prof. Dr. Lars Redecke for graciously agreeing to review my thesis.

I am immensely grateful to all my colleagues in the Department of Bioanalytical Chemistry at the Research Center Borstel for their support and the friendships we have formed.

Finally, I want to extend my deepest gratitude to my family in Syria for their continuous support and encouragement. This journey would not have been possible without your love and the resilience you instilled in me. I offer special thanks to my wonderful wife, Aseel, and my beloved son, Rafi, for their patience, support and understanding, especially during these recent months when I was consumed with the manuscript and our pursuit of a new life.